bioRxiv preprint doi: https://doi.org/10.1101/014241; this version posted January 23, 2015. The copyright holder for this preprint (which was not certified by peer review) is the author/funder, who has granted bioRxiv a license to display the preprint in perpetuity. It is made available under aCC-BY-ND 4.0 International license.

Partitioning heritability by functional category using GWAS summary statistics

Hilary K. Finucane*†[1,2], Brendan Bulik-Sullivan*[3,4], Alexander Gusev[2], Gosia Trynka[5,6,7,8], Yakir Reshef[9], Po-Ru Loh[2], Verneri Anttila[3,4,8], Han Xu[10], Chongzhi Zang[10], Kyle Farh[3,11], Stephan Ripke[3,4], Felix R. Day[12], ReproGen Consortium, Schizophrenia Working Group of the Psychiatric Genomics Consortium, The RACI Consortium, Shaun Purcell[5,6,13], Eli Stahl[13], Sara Lindstrom[2], John R. B. Perry[12], Yukinori Okada[14,15], Soumya Raychaudhuri[5,6,7,8,16], Mark Daly[3,4], Nick Patterson[8], Benjamin M. Neale**[3,4], and Alkes L. Price**†[2,8]

[1]Department of Mathematics, Massachusetts Institute of Technology, Cambridge, Massachusetts, USA.

[2]Department of Epidemiology, Harvard T.H. Chan School of Public Health, Boston, Massachusetts, USA.

[3]Analytic and Translational Genetics Unit, Massachusetts General Hospital and Harvard Medical School, Boston, Massachusetts, USA.

[4]Stanley Center for Psychiatric Research, Broad Institute of MIT and Harvard, Cambridge, Massachusetts, USA.

[5]Division of Genetics, Brigham and Women's Hospital, Harvard Medical School, Boston, Massachusetts, USA.

[6]Division of Rheumatology, Brigham and Women's Hospital, Harvard Medical School, Boston, Massachusetts, USA.

[7]Partners Center for Personalized Genetic Medicine, Boston, Massachusetts, USA.

[8]Program in Medical and Population Genetics, Broad Institute of MIT and Harvard, Cambridge, Massachusetts, USA.

[9]Department of Computer Science, Harvard University, Massachusetts,USA.

[10]Department of Biostatistics and Computational Biology, Dana-Farber Cancer Institute and Harvard T.H. Chan School of Public Health, Boston, Massachusetts, USA.

[11]Epigenomics Program, Broad Institute of MIT and Harvard, Cambridge, Massachusetts, USA.

[12]MRC Epidemiology Unit, University of Cambridge School of Clinical Medicine, Institute of Metabolic Science, Cambridge Biomedical Campus, Cambridge, CB2 0QQ, UK

[13]The Department of Psychiatry at Mount Sinai School of Medicine, New York, New York, USA.

[14]Department of Human Genetics and Disease Diversity, Graduate School of Medical and Dental Sciences, Tokyo Medical and Dental University, Tokyo 113-8510, Japan.

[15]Laboratory for Statistical Analysis, RIKEN Center for Integrative Medical Sciences, Yokohama 230-0045, Japan.

[16]Faculty of Medical and Human Sciences, University of Manchester, Manchester, UK.

*Co-first authors

**Co-last authors

†Correspondence should be addressed to H.K.F. (hilaryf@mit.edu) or A.L.P. (aprice@hsph.harvard.edu)

bioRxiv preprint doi: https://doi.org/10.1101/014241; this version posted January 23, 2015. The copyright holder for this preprint (which was not certified by peer review) is the author/funder, who has granted bioRxiv a license to display the preprint in perpetuity. It is made available under aCC-BY-ND 4.0 International license.

Abstract

Recent work has demonstrated that some functional categories of the genome contribute disproportionately to the heritability of complex diseases. Here, we analyze a broad set of functional elements, including cell-type-specific elements, to estimate their polygenic contributions to heritability in genome-wide association studies (GWAS) of 17 complex diseases and traits spanning a total of 1.3 million phenotype measurements. To enable this analysis, we introduce a new method for partitioning heritability from GWAS summary statistics while controlling for linked markers. This new method is computationally tractable at very large sample sizes, and leverages genome-wide information. Our results include a large enrichment of heritability in conserved regions across many traits; a very large immunological disease-specific enrichment of heritability in FANTOM5 enhancers; and many cell-type-specific enrichments including significant enrichment of central nervous system cell types in body mass index, age at menarche, educational attainment, and smoking behavior. These results demonstrate that GWAS can aid in understanding the biological basis of disease and provide direction for functional follow-up.

Introduction

In GWAS of complex traits, much of the heritability lies in single-nucleotide polymorphisms (SNPs) that do not reach genome-wide significance at current sample sizes.[1,2] However, many current approaches that leverage functional information[3,4] and GWAS data to inform disease biology use only SNPs in genome-wide significant loci,[5–7] assume only one causal SNP per locus,[8] or do not account for LD.[9] We can improve power by estimating the proportion of SNP heritability[1] attributable to various functional categories, using information from all SNPs and explicitly modeling LD.

Previous work on partitioning SNP heritability has used restricted maximum likelihood (REML) as implemented in GCTA.[10–13] REML requires individual genotypes, but many of the largest GWAS analyses are conducted through meta-analysis of study-specific results, and so typically only summary statistics, not individual genotypes, are available for these studies. Even when individual genotypes are available, using REML to analyze multiple functional categories becomes computationally intractable at sample sizes in the tens of thousands. Here, we introduce a method for partitioning heritability, stratified LD score regression, that requires only GWAS summary statistics and LD information from an external reference panel that matches the population studied in the GWAS.

We apply our novel approach to 17 complex diseases and traits spanning 1,263,072 phenotype measurements. We first analyze non-cell-type-specific annotations and identify heritability enrichment in

bioRxiv preprint doi: https://doi.org/10.1101/014241; this version posted January 23, 2015. The copyright holder for this preprint (which was not certified by peer review) is the author/funder, who has granted bioRxiv a license to display the preprint in perpetuity. It is made available under aCC-BY-ND 4.0 International license.

many of these functional annotations, including a large enrichment in conserved regions across many traits and a very large immunological disease-specific enrichment in FANTOM5 enhancers. We then analyze cell-type-specific annotations and identify many cell-type-specific heritability enrichments, including enrichment of central nervous system (CNS) cell types in body mass index, age at menarche, educational attainment, and smoking behavior.

Results

Overview of methods

Our method for partitioning heritability from summary statistics, called stratified LD score regression, relies on the fact that the χ^2 association statistic for a given SNP includes the effects of all SNPs that it tags.[14,15] Thus, for a polygenic trait, SNPs with high linkage disequilibrium (LD) will have higher χ^2 statistics on average than SNPs with low LD.[15] This might be driven either by the higher likelihood of these SNPs to tag an individual large effect, or their ability to tag multiple weak effects. If we partition SNPs into functional categories with different contributions to heritability, then LD to a category that is enriched for heritability will increase the χ^2 statistic of a SNP more than LD to a category that does not contribute to heritability. Thus, our method determines that a category of SNPs is enriched for heritability if SNPs with high LD to that category have higher χ^2 statistics than SNPs with low LD to that category.

More precisely, under a polygenic model,[1] the expected χ^2 statistic of SNP j is

$$\mathrm{E}[\chi_j^2] = N \sum_C \tau_C \ell(j, C) + Na + 1, \tag{1}$$

where N is sample size, C indexes disjoint categories, $\ell(j, C)$ is the LD Score of SNP j with respect to category C (defined as $\ell(j, C) := \sum_{k \in C} r^2(j, k)$), a is a term that measures the contribution of confounding biases,[15] and τ_C is the per-SNP heritability in category C (Methods). Equation (1) allows us to estimate τ_C via a (computationally simple) multiple regression of χ_j^2 against $\ell(j, C)$. The method easily generalizes to overlapping categories and case-control studies[16] (Methods). We define the enrichment of a category to be the proportion of SNP heritability explained divided by the proportion of SNPs. We estimate standard errors with a block jackknife,[15] and use these standard errors to calculate z-scores, P-values, and FDRs (Methods). We have released open-source software implementing the method (Web Resources).

bioRxiv preprint doi: https://doi.org/10.1101/014241; this version posted January 23, 2015. The copyright holder for this preprint (which was not certified by peer review) is the author/funder, who has granted bioRxiv a license to display the preprint in perpetuity. It is made available under aCC-BY-ND 4.0 International license.

To apply LD score regression (or REML) we must first specify which categories we include in our model. We created a "full baseline model" from 24 main annotations that are not specific to any cell type (Table S1; see Methods and Web Resources). Below, we show that including many categories in our model leads to more accurate estimates of enrichment. The 24 main annotations include: coding, UTR, promoter, and intron;[17] histone marks H3K4me1, H3K4me3, H3K9ac[5] and two versions of H3K27ac;[18,19] open chromatin reflected by DNase I hypersensitivity Site (DHS) regions;[5] combined chromHMM/Segway predictions,[20] which are a computational combination of many ENCODE annotations into a single partition of the genome into seven underlying "chromatin states,"; regions that are conserved in mammals;[21] super-enhancers, which are large clusters of highly active enhancers;[19] and active enhancers from the FANTOM5 panel of samples, which we call FANTOM5 enhancers.[22] For the histone marks and other annotations that differ among cell types, we combined the different cell types into a single annotation for the baseline model by taking a union. To prevent our estimates from being biased upwards by enrichment in nearby regions,[13] we also included 500bp windows around each functional category as separate functional categories in the baseline model, as well as 100bp windows around ChIP-seq peaks when appropriate (see Methods). This yielded a total of 53 (overlapping) functional categories in the baseline model, including a category containing all SNPs.

To prevent our estimates from being biased upwards by enrichment in nearby regions,[13] we also included 500bp windows around each functional category as separate categories in the full baseline model, as well as 100bp windows around ChIP-seq peaks when appropriate (Methods). The 24 main annotations plus additional windows and a category containing all SNPs yielded a total of 53 (overlapping) functional categories in the full baseline model.

Simulation results

In order to assess the robustness of the method, we performed a variety of simulations. We used chromosome 1 genotypes of controls from the Wellcome Trust Case Control Consortium,[23] imputed using a 1000 Genomes reference panel.[24] After quality control, we had 2,680 individuals and 360,106 SNPs (Methods). We simulated quantitative phenotypes with a heritability of 0.5 using an additive model. For each simulation, SNP effect sizes were drawn from a normal distribution with mean zero and variance (i.e., average per-SNP heritability) determined by functional categories. We estimated the enrichment of the DHS category, i.e., $(\%h^2)/(\%\text{SNPs})$, using three methods:(1) REML with two categories (DHS/Other), (2) LD score regression with two categories (DHS/Other), and (3) LD score

bioRxiv preprint doi: https://doi.org/10.1101/014241; this version posted January 23, 2015. The copyright holder for this preprint (which was not certified by peer review) is the author/funder, who has granted bioRxiv a license to display the preprint in perpetuity. It is made available under aCC-BY-ND 4.0 International license.

regression with the full baseline model (53 categories, described above). Since REML with 53 categories did not converge at this sample size and would be computationally intractable at sample sizes in the tens of thousands, we did not include it in our comparison; an advantage of LD score regression is that it is possible to include a large number of categories in the underlying model. We report means and standard errors of the mean over 100 independent simulations.

We first performed three sets of simulations where the causal pattern of enrichment was well modeled by the two-category (DHS/Other) model; for these, all three methods performed well, although LD score regression with the full baseline model had larger standard errors around the mean (Figure 1a). For example, the standard errors around the mean in simulations with no DHS enrichment were 0.08 for REML, 0.11 for two-category LD score regression and 0.19 for LD score regression with the full baseline model. For the first set of simulations, all SNPs were causal and SNP effect sizes were drawn i.i.d. from a normal distribution. For the second set of simulations, all SNPs were causal and SNP effect sizes were drawn independently from a normal distribution, but the variance of the normal distribution depended on whether the SNP was in a DHS region, and two variances (DHS and Other) were chosen so that the proportion of heritability of DHS would be 3x more than the proportion of SNPs. For the third set of simulations, only SNPs in DHS regions were causal, and effect sizes of DHS SNPs were drawn i.i.d. from a normal distribution.

Next, to explore the realistic scenario where the model used to estimate enrichment does not match the (unknown) causal model, we performed three sets of simulations where all causal SNPs were in a particular category, but the model used to estimate heritability did not include this causal category. The three sets of simulations were (1) all causal SNPs in coding regions, yielding 1.6x DHS enrichment due to coding/DHS overlap, (2) all causal SNPs in FANTOM5 enhancers, yielding 4.0x DHS enrichment due to FANTOM5 enhancer/DHS overlap, and (3) all causal SNPs in 200bp DHS flanking regions, yielding 0x DHS enrichment. For the coding and FANTOM5 enhancer causal simulations, we made the full baseline model into a misspecified model by removing the causal category (and windows around the causal category). Results from these simulations are displayed in Figure 1b).

The two-category estimators were not robust to model misspecification and consistently over-estimated DHS enrichment by a wide margin. LD score regression with the full baseline model gave more accurate mean estimates of enrichment. Specifically, for the simulations with coding and FANTOM5 Enhancers causal, LD score regression with the full baseline model gave unbiased mean enrichment estimates of 1.8x (s.e. 0.22) and 4.2x (s.e. 0.22), respectively, while the mean enrichment estimates of REML and two-category LD score regression were nearly double these. The full baseline model includes a 500bp

bioRxiv preprint doi: https://doi.org/10.1101/014241; this version posted January 23, 2015. The copyright holder for this preprint (which was not certified by peer review) is the author/funder, who has granted bioRxiv a license to display the preprint in perpetuity. It is made available under aCC-BY-ND 4.0 International license.

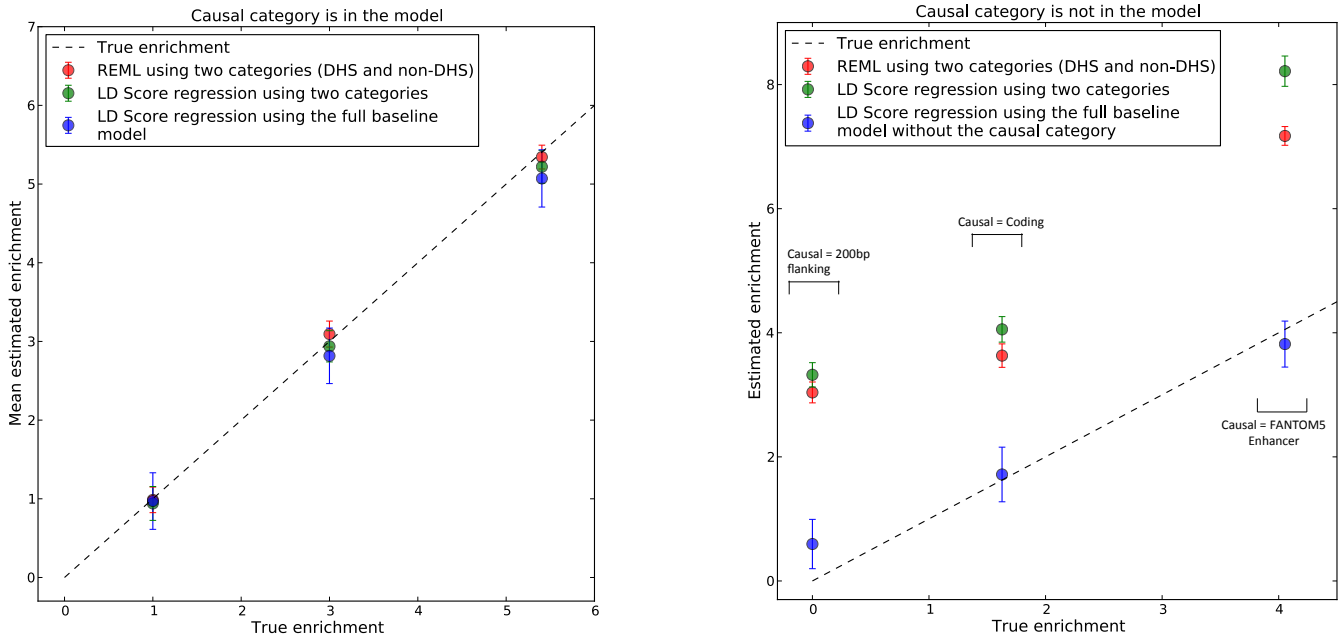

(a) No model misspecification.

(b) Model is misspecified.

Figure 1: Simulation results. Enrichment is the proportion of heritability in DHS regions divided by the proportion of SNPs in DHS regions. Bars show 95% confidence intervals around the mean of 100 trials. (a) From left to right, the simulated genetic architectures are 1x DHS enrichment, 3x DHS enrichment, and 5.5x DHS enrichment (100% of heritability in DHS SNPs). (b) From left to right, the simulated genetic architectures are 200bp flanking regions causal, coding regions causal, and FANTOM5 Enhancer regions causal. For simulations with coding or FANTOM5 Enhancer as the causal category, we removed the causal category and the window around that category from the full baseline model in order to simulate enrichment in an unknown functional category.

window around DHS but not a 200bp window, and gave a mean estimated DHS enrichment of 0.65x (s.e. 0.22) when the 200bp flanking regions were causal, which is inflated relative to the true enrichment of 0x but much less inflated than $>$ 3x mean enrichment estimates given by the two-category methods.

In summary, while these simulations include exaggerated patterns of enrichment (e.g., 100% of heritability in DHS flanking regions), the results highlight the possibility that two-category estimators of enrichment can yield incorrect conclusions. Although we cannot entirely rule out model misspecification as a source of bias for LD score regression with the full baseline model, we have shown here that it is robust to a wide variety of patterns of enrichment, because including many categories gives it the flexibility to adapt to the unknown causal model.

bioRxiv preprint doi: https://doi.org/10.1101/014241; this version posted January 23, 2015. The copyright holder for this preprint (which was not certified by peer review) is the author/funder, who has granted bioRxiv a license to display the preprint in perpetuity. It is made available under aCC-BY-ND 4.0 International license.

Application to real data

We applied LD score regression with the full baseline model to 17 diseases and quantitative traits: height, BMI, age at menarche, LDL levels, HDL levels, triglyceride levels, coronary artery disease, type 2 diabetes, fasting glucose levels, schizophrenia, bipolar disorder, anorexia, educational attainment, smoking behavior, rheumatoid arthritis, Crohn's disease, and ulcerative colitis (Table S2, Web resources). This includes all traits with publicly available summary statistics with sufficient sample size and SNP heritability, measured by the z-score of total SNP-heritability (Methods), spanning a total of of 1,263,072 unique phenotype measurements. We removed the MHC region from all analyses, due to its unusual LD and genetic architecture. Figure 2 shows results for the 24 main functional annotations, averaged across nine independent traits (Methods). Figure 3 shows trait-specific results for selected annotations and traits (Methods). Tables S3 and S4 show meta-analysis and trait-specific results for all traits and all 53 categories in the full baseline model.

We observed large and statistically significant enrichments for many functional categories. A few categories stood out in particular. First, regions conserved in mammals[21] showed the largest enrichment of any category, with 2.6% of SNPs explaining an estimated 35% of SNP heritability on average across traits ($P < 10^{-15}$ for enrichment). This is a significantly higher average enrichment than for coding regions, and provides evidence for the biological importance of conserved regions, even though the biochemical function of many conserved regions remains uncharacterized.[25] Second, FANTOM5 Enhancers[22] were extremely enriched in the three immunological diseases, with 0.4% of SNPs explaining an estimated 15% of SNP heritability on average across these three diseases ($P < 10^{-5}$), but showed no evidence of enrichment for non-immunological traits (Figure 3). Third, repressed regions were depleted: 46% of SNPs explain only 29% of heritability on average ($P < 0.006$), consistent with the hypothesis that these are regions of low activity.[20] We did not see a large enrichment of H3K27ac regions marked as super-enhancers over all H3K27ac regions; the estimates for enrichment were 1.8x (s.e. 0.2) and 1.6x (s.e. 0.1), respectively. This lack of enrichment supports the argument that super-enhancers may not play a much more important role in regulating transcription than regular enhancers.[26] For many annotations, there was also enrichment in the 500bp flanking regions (Table S3). Analyses stratified by minor allele frequency produced broadly similar results for all of these enrichments (Table S5; see Methods).

We performed two different cell-type-specific analyses: an analysis of 220 individual cell-type-specific annotations, and an analysis of 10 cell-type groups. The 220 individual cell-type-specific annotations are a combination of cell-type-specific annotations from four histone marks: 77 from H3K4me1,[5] 81 from

bioRxiv preprint doi: https://doi.org/10.1101/014241; this version posted January 23, 2015. The copyright holder for this preprint (which was not certified by peer review) is the author/funder, who has granted bioRxiv a license to display the preprint in perpetuity. It is made available under aCC-BY-ND 4.0 International license.

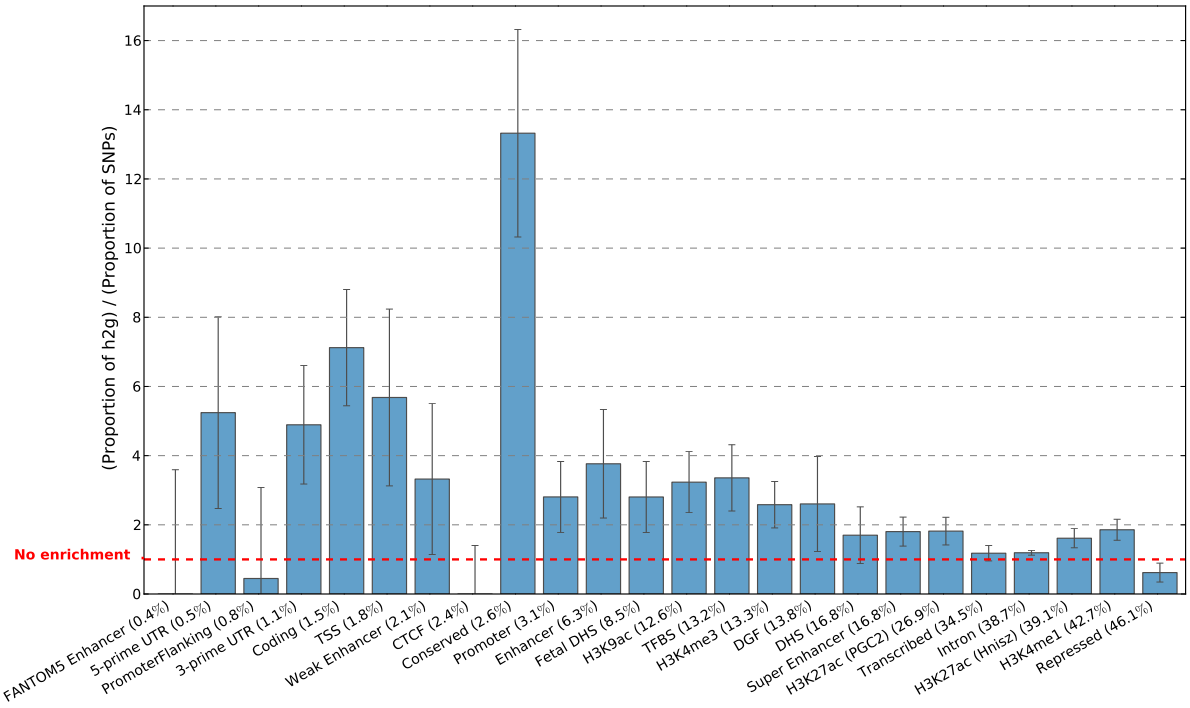

Figure 2: Enrichment estimates for the 24 main annotations, averaged over nine independent traits. Error bars represent 95% confidence intervals around the estimate.

H3K4me3,[5] 27 from H3K9ac,[5] and 35 from H3K27ac[18] (Table S6, Methods). When ranking these 220 cell-type-specific annotations, we wanted to control for overlap with the functional categories in the full baseline model, but not for overlap with the 219 other cell-type-specific annotations. Thus, we added the 220 cell-type-specific annotations individually, one at a time, to the full baseline model, and ranked these 220 annotations by the P-value for the coefficient corresponding to the annotation. This P-value tests whether the annotation contributes significantly to per-SNP heritability after controlling for the effects of the annotations in the full baseline model. We assessed statistical significance at the 0.05 level after Bonferroni correction for $220 \times 17 = 3,740$ hypotheses tested. (This is conservative, since the 220 annotations are not independent.) We also report results with false discovery rate (FDR) < 0.05 (computed over 220 cell types for each trait). For 15 of the 17 traits, the top cell type passed an FDR threshold of 0.05. The top cell type for each trait is displayed in Table 1, with additional top cell types reported in Table S7.

bioRxiv preprint doi: https://doi.org/10.1101/014241; this version posted January 23, 2015. The copyright holder for this preprint (which was not certified by peer review) is the author/funder, who has granted bioRxiv a license to display the preprint in perpetuity. It is made available under aCC-BY-ND 4.0 International license.

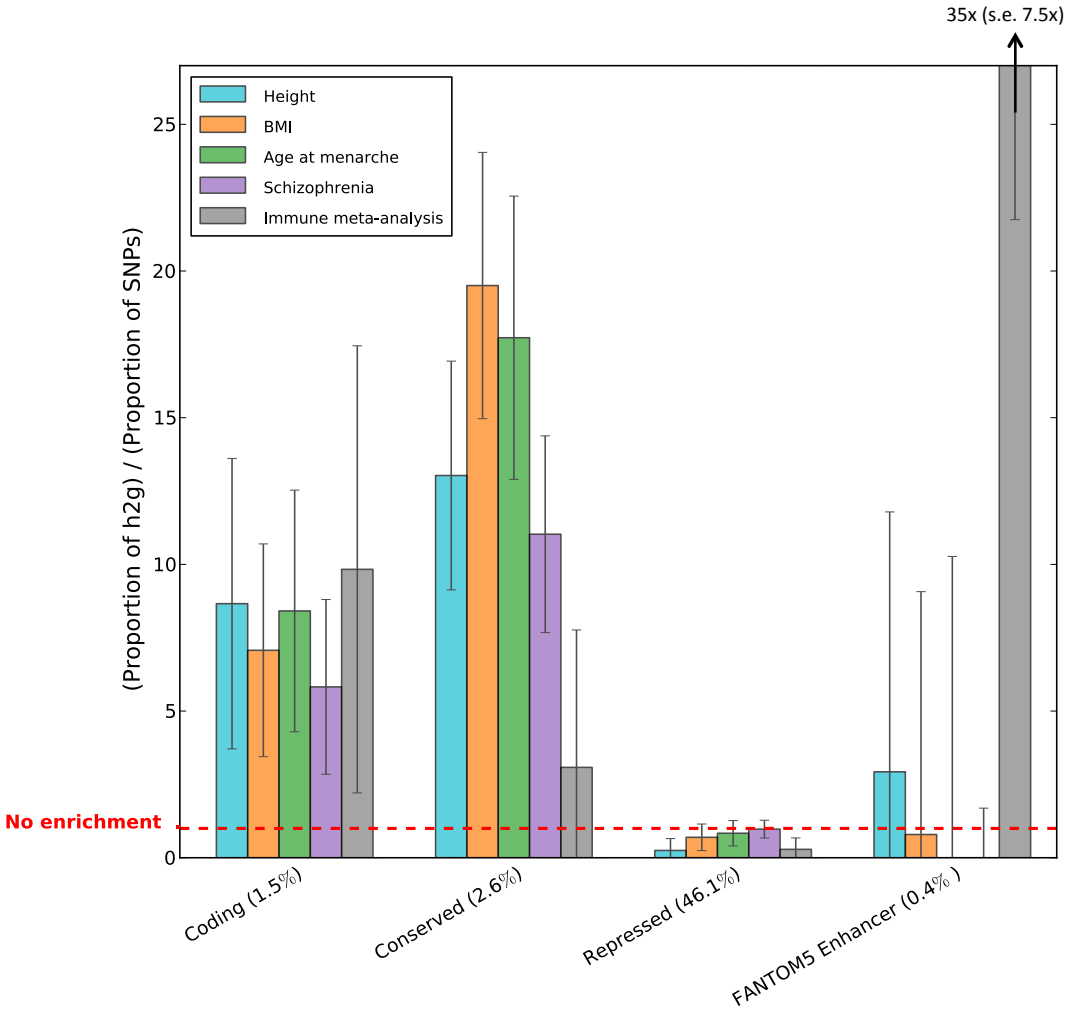

Figure 3: Enrichment estimates for selected annotations and traits. Error bars represent 95% confidence intervals around the estimate.

We combined information from related cell types by aggregating the 220 cell-type-specific annotations into 10 groups (Figure 4 legend and Table S6; see Methods). For each trait, we performed the same analysis on the 10 group-specific annotations as with the 220 cell-type-specific annotations. We assessed statistical significance at the 0.05 level after Bonferroni correction for $10 \times 17 = 170$ hypotheses tested, and we again also report results with false discovery rate (FDR) < 0.05 (now computed over all cell-type groups and traits). For 16 of the 17 traits (all traits except anorexia), the top cell type group passed an FDR threshold of 0.05. Results for the 11 traits with the most significant enrichments (after pruning closely related traits) are shown in Figure 4, with remaining traits in Figure S1.

These two analyses are generally concordant, and show highly trait-specific patterns of cell-type

bioRxiv preprint doi: https://doi.org/10.1101/014241; this version posted January 23, 2015. The copyright holder for this preprint (which was not certified by peer review) is the author/funder, who has granted bioRxiv a license to display the preprint in perpetuity. It is made available under aCC-BY-ND 4.0 International license.

Phenotype	Cell type	Tissue	Mark	$-log_{10}(p)$
Height	Chondrogenic dif**	Bone	H3K27ac	6.81
BMI	Fetal brain*	Fetal brain	H3K4me3	4.48
Age at menarche	Fetal brain**	Fetal brain	H3K4me3	12.25
LDL	Liver (BI)*	Liver	H3K4me1	4.76
HDL	Liver (BI)*	Liver	H3K4me1	4.51
Triglycerides	Liver (BI)*	Liver	H3K4me1	3.99
Coronary artery disease	Adipose nuclei*	Adipose	H3K4me1	4.21
Type 2 Diabetes	Pancreatic islets	Pancreas	H3K4me3	2.87
Fasting Glucose	Pancreatic islets*	Pancreas	H3K27ac	3.93
Schizophrenia	Fetal brain**	Fetal brain	H3K4me3	18.51
Bipolar disorder	Mid frontal lobe*	Brain	H3K27ac	4.42
Anorexia	Angular gyrus	Brain	H3K9ac	2.61
Years of education	Angular gyrus**	Brain	H3K4me3	6.63
Ever smoked	Inferior temporal lobe*	Brain	H3K4me3	3.21
Rheumatoid arthritis	CD4+ CD25- IL17+ stim Th17**	Immune	H3K4me1	6.76
Crohn's disease	CD4+ CD25- IL17+ stim Th17**	Immune	H3K4me1	7.59
Ulcerative colitis	CD4+ CD25- IL17+ stim Th17**	Immune	H3K4me1	6.37

Table 1: Enrichment of individual cell types. We report the cell type with the lowest P-value for each trait analyzed. * denotes FDR < 0.05. ** denotes significant at $p < 0.05$ after Bonferroni correction for multiple hypotheses. Sample sizes are in Table S2.

enrichment. They also recapitulate several well-known findings. For example, the top cell type for each of the three lipid traits is liver (FDR < 0.05 for all three traits). For both type 2 diabetes and fasting glucose, the top cell type is pancreatic islets (FDR < 0.05 for fasting glucose but not type 2 diabetes). For the three psychiatric traits, the top cell type is a brain cell type (FDR < 0.05 for schizophrenia and bipolar disorder but not for anorexia) and the top cell-type group is CNS (significant after multiple testing for schizophrenia and bipolar disorder but not for anorexia).

There are also several new insights among these results. For example, the three immunological disorders show patterns of enrichment that reflect biological differences among the three disorders. Crohn's disease has 40 cell types with FDR < 0.05, of which 39 are immune cell types and one (colonic mucosa) is a GI cell type. On the other hand, the 39 cell types with FDR < 0.05 for ulcerative colitis include nine GI cell types in addition to 30 immune cell types, whereas all 39 cell types with FDR < 0.05 for rheumatoid arthritis are immune cell types. The top cell type for all three traits is CD4+ CD25- IL17+ PMA Ionomycin simulated Th17 primary. Th17 cells are thought to act in opposition to Treg cells, which have been shown to suppress immune activity and whose malfunction has been associated with immunological disorders.[27]

We also identified several non-psychiatric phenotypes with enrichments in brain cell types. For both BMI and age at menarche, cell types in the central nervous system (CNS) ranked highest among

bioRxiv preprint doi: https://doi.org/10.1101/014241; this version posted January 23, 2015. The copyright holder for this preprint (which was not certified by peer review) is the author/funder, who has granted bioRxiv a license to display the preprint in perpetuity. It is made available under aCC-BY-ND 4.0 International license.

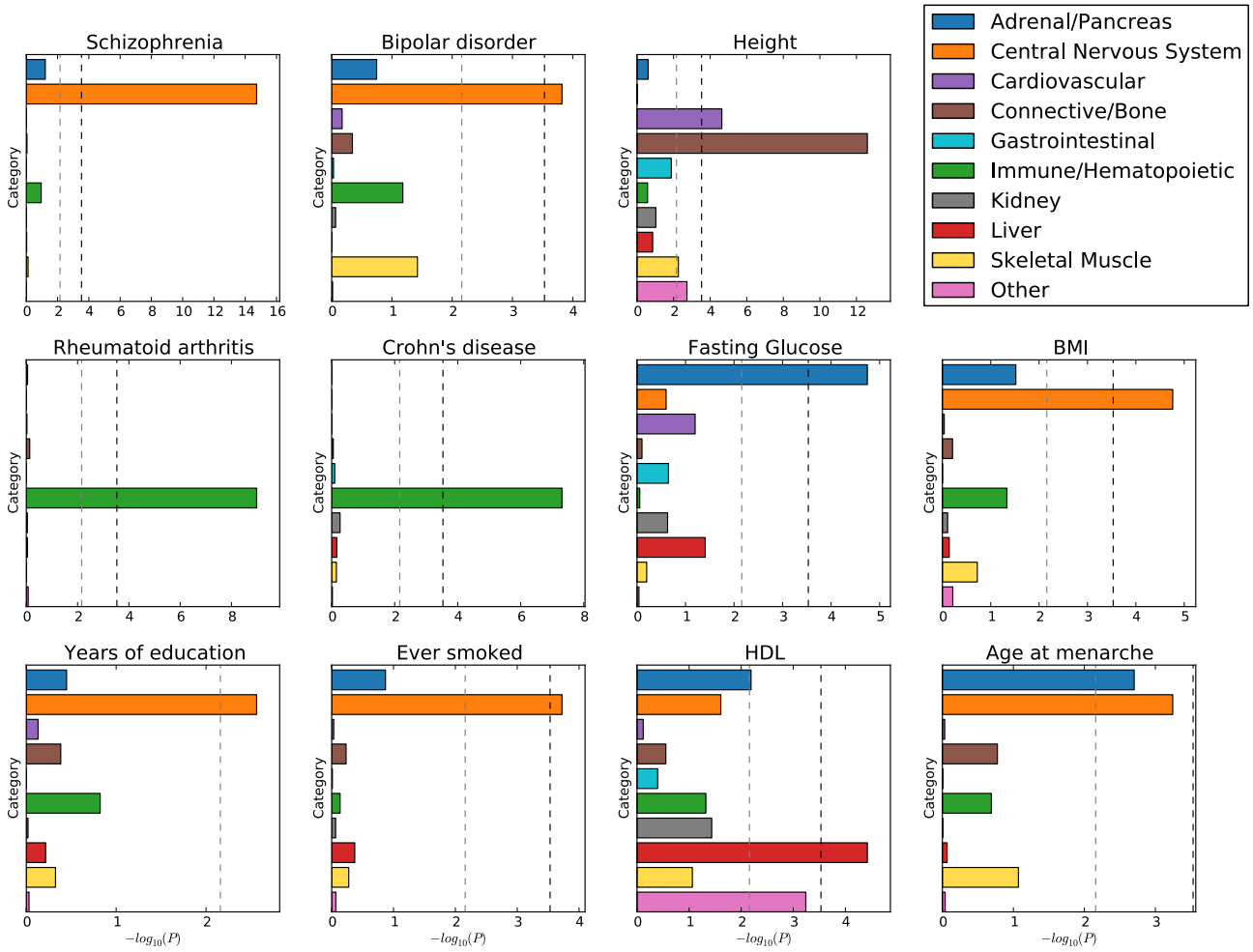

Figure 4: Enrichment of cell type groups. We report significance of enrichment for each of 10 cell-type groups, for each of 11 traits. The black dotted line at $-\log_{10}(P) = 3.5$ is the cutoff for Bonferroni significance. The grey dotted line at $-\log_{10}(P) = 2.1$ is the cutoff for FDR < 0.05. For HDL, three of the top individual cell types are adipose nuclei, which explains the enrichment of the "Other" category.

individual cell types, and the top cell-type group was CNS, all with FDR < 0.05. These enrichments support previous human and animal studies that propose a strong neural basis for the regulation of energy homeostasis.[28] For educational attainment, the top cell-type group is CNS (FDR < 0.05) and of the ten cell types that are significant after multiple testing, nine are CNS cell types. This is consistent with our understanding that the genetic component of educational attainment, which excludes environmental factors and population structure, is highly correlated with IQ.[29] Finally, for smoking behavior, the CNS cell-type group is significant after multiple testing correction, and the top cell type is again a brain cell type, likely reflecting CNS involvement in nicotine processing.

bioRxiv preprint doi: https://doi.org/10.1101/014241; this version posted January 23, 2015. The copyright holder for this preprint (which was not certified by peer review) is the author/funder, who has granted bioRxiv a license to display the preprint in perpetuity. It is made available under aCC-BY-ND 4.0 International license.

Discussion

We developed a new statistical method, stratified LD score regression, for identifying functional enrichment from GWAS data that uses information from all SNPs and explicitly models LD. We applied this method to GWAS data spanning 17 traits and 1.3 million phenotype measurements. Our method identified strong enrichment for conserved regions across all traits, and immunological disease-specific enrichment for FANTOM5 enhancers. Our cell-type-specific enrichment results confirmed previously known enrichments, such as liver enrichment for HDL levels and pancreatic islet enrichment for fasting glucose. In addition, we identified enrichments that would have been challenging to detect using existing methods, such as CNS enrichment for smoking behavior and educational attainment—traits with one and three genome-wide significant loci, respectively.[29,30] Stratified LD score regression represents a significant departure from previous methods that require raw genotypes,[10] use only SNPs in genome-wide significant loci,[5–7] assume only one causal SNP per locus,[8] or do not account for LD[9] (see Methods for a discussion of other methods). Our method is also computationally efficient, despite the 53 overlapping functional categories analyzed.

Although our polygenic approach has enabled a powerful analysis of genome-wide summary statistics, it has several limitations. First, the method requires a very large sample size and/or large SNP heritability, and the trait analyzed must be polygenic. Second, it requires an LD reference panel matched to the population studied; all results in this paper are from European datasets and use 1000G Europeans as a reference panel. Third, our method is currently not applicable to studies using custom genotyping arrays (e.g., Metabochip; see Methods). Fourth, our method is based on an additive model and does not consider the contribution of epistatic or other non-additive effects, nor does it model causal contributions of SNPs not in the reference panel; in particular, it is possible that patterns of enrichment may be different at extremely rare variants. Fifth, the method is limited by available functional data: if a trait is enriched in a cell type for which we have no data, we cannot detect the enrichment. Last, though we have shown our method to be robust in a wide range of scenarios, we cannot rule out model misspecification caused by enrichment in an unidentified functional category as a possible source of bias.

The polygenic approach described here is a powerful and efficient way to learn about functional enrichments from summary statistics, and it will become increasingly useful as functional data continues to grow and improve, and as GWAS studies of larger sample size are conducted.

bioRxiv preprint doi: https://doi.org/10.1101/014241; this version posted January 23, 2015. The copyright holder for this preprint (which was not certified by peer review) is the author/funder, who has granted bioRxiv a license to display the preprint in perpetuity. It is made available under aCC-BY-ND 4.0 International license.

Web Resources

- `ldsc` software:

  `github.com/bulik/ldsc`

- DNaseI Digital Genomic Footprinting (DGF) annotations:[3,13]

  `http://hgdownload.cse.ucsc.edu/goldenPath/hg19/encodeDCC/wgEncodeUwDgf/`

- Transcription factor binding sites:[3,13]

  `http://hgdownload.cse.ucsc.edu/goldenPath/hg19/encodeDCC/wgEncodeAwgTfbsUniform/`

- Segway-chromHMM combined enhancer annotations:[20]

  `ftp://ftp.ebi.ac.uk/pub/databases/ensembl/encode/integration_data_jan2011/`

  `byDataType/segmentations/jan2011`

- Super-enhancers and H3K27ac: Available as a supplementary table to Hnisz et al 2014.[19]

- Conserved regions:[21,31]

  `http://compbio.mit.edu/human-constraint/data/gff/`

- FANTOM5 Enhancers:[22]

  `http://enhancer.binf.ku.dk/presets/`

- Post-processed H3K4me1, H3K4me3, and H3K9ac:[5]

  `https://www.broadinstitute.org/mpg/goshifter/`

- Height[32] and BMI[33] summary statistics:

  `www.broadinstitute.org/collaboration/giant/index.php/GIANT_consortium_data_files`

- Menarche summary statistics:[34]

  `www.reprogen.org`

- LDL, HDL, and Triglycerides summary statistics:[35]

  `www.broadinstitute.org/mpg/pubs/lipids2010/`

- Coronary artery disease summary statistics:[36]

  `www.cardiogramplusc4d.org`

- Type 2 diabetes summary statistics:[37]

  `www.diagram-consortium.org`

- Fasting glucose summary statistics:[38]

  `www.magicinvestigators.org/downloads/`

bioRxiv preprint doi: https://doi.org/10.1101/014241; this version posted January 23, 2015. The copyright holder for this preprint (which was not certified by peer review) is the author/funder, who has granted bioRxiv a license to display the preprint in perpetuity. It is made available under aCC-BY-ND 4.0 International license.

- Schizophrenia,[18] Bipolar Disorder,[39] Anorexia,[40] and Smoking behavior[30] summary statistics:
  `www.med.unc.edu/pgc/downloads`
- Education attainment summary statistics:[29]
  `www.ssgac.org`
- Rheumatoid arthritis summary statistics:[41]
  `http://plaza.umin.ac.jp/ yokada/datasource/software.htm`
- Crohn's disease and ulcerative colitis summary statistics:[42]
  `www.ibdgenetics.org/downloads.html`
  We used a newer version of these data with 1000 Genomes imputation.

Acknowledgements

We thank Brad Bernstein, Mariel Finucane, Eran Hodis, Dylan Kotliar, X. Shirley Liu, Manolis Kellis, Michael O'Donovan, Bogdan Pasaniuc, Abhishek Sarkar, Patrick Sullivan, Bjarni Vilhjalmsson, and Adrian Veres for helpful discussions. This research was funded by NIH grants R01 MH101244, R03 CA173785, and 1U01HG0070033. H.K.F. was supported by the Fannie and John Hertz Foundation. S.R. is supported by funding from the Arthritis Foundation and by a Doris Duke Clinical Scientisit Development Award. This study made use of data generated by the Wellcome Trust Case Control Consortium (WTCCC) and the Wellcome Trust Sanger Institute. A full list of the investigators who contributed to the generation of the WTCCC data is available at www.wtccc.org.uk. Funding for the WTCCC project was provided by the Wellcome Trust under award 076113. The members of the Schizophrenia Working Group of the Psychiatric Genetics Consortium are listed in the Supplementary Information.

References

[1] Jian Yang, Beben Benyamin, Brian P McEvoy, Scott Gordon, Anjali K Henders, Dale R Nyholt, Pamela A Madden, Andrew C Heath, Nicholas G Martin, Grant W Montgomery, et al. Common snps explain a large proportion of the heritability for human height. *Nature Genetics*, 42(7):565–569, 2010.

[2] Eli A. Stahl, Daniel Wegmann, Gosia Trynka, Javier Gutierrez-Achury, Ron Do, et al. Bayesian inference analyses of the polygenic architecture of rheumatoid arthritis. *Nature Genetics*, 44(5):483–489, 2012.

bioRxiv preprint doi: https://doi.org/10.1101/014241; this version posted January 23, 2015. The copyright holder for this preprint (which was not certified by peer review) is the author/funder, who has granted bioRxiv a license to display the preprint in perpetuity. It is made available under aCC-BY-ND 4.0 International license.

[3] ENCODE Project Consortium. An integrated encyclopedia of DNA elements in the human genome. *Nature*, 489:57–74, 2012.

[4] Bradley E. Bernstein, John A. Stamatoyannopoulos, Joseph F. Costello, Bing Ren, and Aleksandar Milosavljevic. The NIH Roadmap Epigenomics Mapping Consortium. *Nature Biotechnology*, 28:1045–1048, 2010.

[5] Gosia Trynka, Cynthia Sandor, Buhm Han, Han Xu, Barbara E. Stranger, X. Shirley Liu, and Soumya Raychaudhuri. Chromatin marks identify critical cell types for fine mapping complex trait variants. *Nature Genetics*, 45(2), 2013.

[6] Kyle Kai-How Farh, Alexander Marson, Jiang Zhu, Markus Kleinewietfeld, William J. Housley, et al. Genetic and epigenetic fine mapping of causal autoimmune disease variants. *Nature*, 2014.

[7] Gleb Kichaev, Wen-Yun Yang, Sara Lindstrom, Farhad Hormozdiari, Eleazar Eskin, et al. Integrating functional data to prioritize causal variants in statistical fine-mapping studies. *PLOS Genetics*, 2014.

[8] Joseph K. Pickrell. Joint analysis of functional genomic data and genome-wide association studies of 18 human traits. *American Journal of Human Genetics*, 94:559–573, 2014.

[9] Matthew T. Maurano, Richard Humbert, Eric Rynes, Robert E. Thurman, Eric Haugen, et al. Systematic localization of common disease-associated variation in regulatory DNA. *Science*, 337(6099):1190–1195, 2012.

[10] Jian Yang, S Hong Lee, Michael E Goddard, and Peter M Visscher. GCTA: a tool for genome-wide complex trait analysis. *The American Journal of Human Genetics*, 88(1):76–82, 2011.

[11] S. Hong Lee, Teresa R. DeCandia, Stephan Ripke, Jian Yang, The Schizophrenia Psychiatric Genome-Wide Association Study Consortium, et al. Estimating the proportion of variation in susceptibility to schizophrenia captured by common SNPs. *Nature Genetics*, 44(3):247–250, 2012.

[12] Lea K. Davis, Dongmei Yu, Clare L. Keenan, Eric R. Gamazon, Anua I. Konkashbaev, et al. Partitioning the heritability of Tourette syndrome and obsessive compulsive disorder reveals differences in genetic architecture. *PLOS Genetics*, 2013.

[13] Alexander Gusev, S. Hong Lee, Gosia Trynka, Hilary Finucane, Bjarni J. Vilhjalmsson, et al. Partitioning heritability of regulatory and cell-type-specific variants across 11 common diseases. *American Journal of Human Genetics*, 95:535–552, 2014.

[14] Jian Yang, Michael Weedon, Shaun Purcell, Guillaume Lettre, Karol Estrada, et al. Genomic inflation factors under polygenic inheritance. *European Journal of Human Genetics*, 19:807–812, 2011.

bioRxiv preprint doi: https://doi.org/10.1101/014241; this version posted January 23, 2015. The copyright holder for this preprint (which was not certified by peer review) is the author/funder, who has granted bioRxiv a license to display the preprint in perpetuity. It is made available under aCC-BY-ND 4.0 International license.

[15] Brendan Bulik-Sullivan, Po-Ru Loh, Hilary Finucane, Stephan Ripke, Jian Yang, Nick Patterson, Mark J Daly, Alkes L Price, and Benjamin M Neale. LD Score regression distinguishes confounding from polygenicity in genome-wide association studies. *Nature Genetics*, In press.

[16] Brendan Bulik-Sullivan, Hilary Finucane, et al. Estimating genetic correlations between traits from GWAS summary statistics. *arxiv*.

[17] UCSC Genome Browser: http://genome.ucsc.edu.

[18] Schizophrenia Working Group of the Psychiatric Genomics Consortium. Biological insights from 108 schizophrenia-associated genetic loci. *Nature*, 511:421–427, 2014.

[19] Denes Hnisz, Brian J. Abraham, Tong Ihn Lee, Ashley Lau, Violaine Saint-Andre, Alla A. Sigova, Heather A. Hoke, and Richard A. Young. Super-enhancers in the control of cell identity and disease. *Cell*, 155(4):934–947, 2013.

[20] Michael M. Hoffman, Jason Ernst, Steven P. Wilder, Anshul Kundaje, Robert S. Harris, et al. Integrative annotation of chromatin elements from ENCODE data. *Nucleic Acids Research*, 41:827–841, 2013.

[21] Kerstin Lindblad-Toh, Manuel Garber, Or Zuk, Michael Lin, Brian Parker, Stefan Washietl, et al. A high-resolution map of human evolutionary constraint using 29 mammals. *Nature*, 478:476–482, 2011.

[22] Robin Andersson, Claudia Gebhard, Irene Miguel-Escalada, Ilka Hoof, Jette Bornholdt, et al. An atlas of active enhancers across human cell types and tissues. *Nature*, 507:455–461, 2014.

[23] Wellcome Trust Case Control Consortium. Genome-wide association study of 14,000 cases of seven common diseases and 3,000 shared controls. *Nature*, 446:661–678, 2007.

[24] 1000 Genomes Project Consortium. An integrated map of genetic variation from 1,092 human genomes. *Nature*, 491:56–65, 2012.

[25] John A. Stamatoyannopoulos. What does our genome encode? *Genome Research*, 22:1602–1611, 2012.

[26] Sebastian Pott and Jason D. Lieb. What are super-enhancers? *Nature Genetics*, 47(1), 2015.

[27] Wenhong Wang, Shihe Shao, Zhijun Jiao, Mingquan Guo, Huaxi Xu, and Shengjun Wang. The th17/treg imbalance and cytokine environment in peripheral blood of patients with rheumatoid arthritis. *Rheumatology International*, 32:887–893, 2012.

[28] Farooqi I. Sadaf. Defining the neural basis of appetite and obesity: from genes to behaviour. *Clinical Medicine*, 14(3):286–289, 2014.

bioRxiv preprint doi: https://doi.org/10.1101/014241; this version posted January 23, 2015. The copyright holder for this preprint (which was not certified by peer review) is the author/funder, who has granted bioRxiv a license to display the preprint in perpetuity. It is made available under aCC-BY-ND 4.0 International license.

[29] Cornelius A Rietveld, Sarah E Medland, Jaime Derringer, Jian Yang, Tõnu Esko, Nicolas W Martin, Harm-Jan Westra, Konstantin Shakhbazov, Abdel Abdellaoui, Arpana Agrawal, et al. GWAS of 126,559 individuals identifies genetic variants associated with educational attainment. *Science*, 340(6139):1467–1471, 2013.

[30] Tobacco and Genetics Consortium et al. Genome-wide meta-analyses identify multiple loci associated with smoking behavior. *Nature Genetics*, 42(5):441–447, 2010.

[31] Lucas D. Ward and Manolis Kellis. Evidence of abundant purifying selection in humans for recently-acquired regulatory functions. *Science*, 337(6102):1675–1678, 2012.

[32] Hana Lango Allen, Karol Estrada, Guillaume Lettre, Sonja I. Berndt, Mihcale N. Weedon, et al. Hundreds of variants clustered in genomic loci and biological pathways affect human height. *Nature*, 467:832–838, 2010.

[33] Elizabeth K Speliotes, Cristen J Willer, Sonja I Berndt, Keri L Monda, Gudmar Thorleifsson, Anne U Jackson, Hana Lango Allen, Cecilia M Lindgren, Jian'an Luan, Reedik Mägi, et al. Association analyses of 249,796 individuals reveal 18 new loci associated with body mass index. *Nature genetics*, 42(11):937–948, 2010.

[34] John R. Perry, Felix Day, Cathy E. Elks, Patrick Sulem, Deborah Thompson, et al. Parent-of-origin-specific allelic associations among 106 genomic loci for age at menarche. *Nature*, 514:92–97, 2014.

[35] Tanya M Teslovich, Kiran Musunuru, Albert V Smith, Andrew C Edmondson, Ioannis M Stylianou, Masahiro Koseki, James P Pirruccello, Samuli Ripatti, Daniel I Chasman, Cristen J Willer, et al. Biological, clinical and population relevance of 95 loci for blood lipids. *Nature*, 466(7307):707–713, 2010.

[36] Heribert Schunkert, Inke R König, Sekar Kathiresan, Muredach P Reilly, Themistocles L Assimes, Hilma Holm, Michael Preuss, Alexandre FR Stewart, Maja Barbalic, Christian Gieger, et al. Large-scale association analysis identifies 13 new susceptibility loci for coronary artery disease. *Nature genetics*, 43(4):333–338, 2011.

[37] Andrew P Morris, Benjamin F Voight, Tanya M Teslovich, Teresa Ferreira, Ayellet V Segre, Valgerdur Steinthorsdottir, Rona J Strawbridge, Hassan Khan, Harald Grallert, Anubha Mahajan, et al. Large-scale association analysis provides insights into the genetic architecture and pathophysiology of type 2 diabetes. *Nature genetics*, 44(9):981, 2012.

[38] Alisa K Manning, Marie-France Hivert, Robert A Scott, Jonna L Grimsby, Nabila Bouatia-Naji, Han Chen, Denis Rybin, Ching-Ti Liu, Lawrence F Bielak, Inga Prokopenko, et al. A genome-wide

bioRxiv preprint doi: https://doi.org/10.1101/014241; this version posted January 23, 2015. The copyright holder for this preprint (which was not certified by peer review) is the author/funder, who has granted bioRxiv a license to display the preprint in perpetuity. It is made available under aCC-BY-ND 4.0 International license.

approach accounting for body mass index identifies genetic variants influencing fasting glycemic traits and insulin resistance. *Nature genetics*, 44(6):659–669, 2012.

[39] Pamela Sklar, Stephan Ripke, Laura J Scott, Ole A Andreassen, Sven Cichon, Nick Craddock, Howard J Edenberg, John I Nurnberger, Marcella Rietschel, Douglas Blackwood, et al. Large-scale genome-wide association analysis of bipolar disorder identifies a new susceptibility locus near odz4. *Nature Genetics*, 43(10):977, 2011.

[40] Vesna Boraska, Christopher S Franklin, James AB Floyd, Laura M Thornton, Laura M Huckins, Lorraine Southam, N William Rayner, Ioanna Tachmazidou, Kelly L Klump, Janet Treasure, et al. A genome-wide association study of anorexia nervosa. *Molecular psychiatry*, 2014.

[41] Yukinori Okada, Di Wu, Gosia Trynka, Towfique Raj, Chikashi Terao, et al. Genetics of rheumatoid arthritis contributes to biology and drug discovery. *Nature*, 506:376–381, 2014.

[42] Luke Jostins, Stephan Ripke, Rinse K Weersma, Richard H Duerr, Dermot P McGovern, Ken Y Hui, James C Lee, L Philip Schumm, Yashoda Sharma, Carl A Anderson, et al. Host-microbe interactions have shaped the genetic architecture of inflammatory bowel disease. *Nature*, 491(7422):119–124, 2012.

[43] International HapMap 3 Consortium. Integrating common and rare genetic variation in diverse human populations. *Nature*, 467:52–58, 2010.

[44] Gosia Trynka, Harm-Jan Westra, Kamil Slowikowski, Xinli Hu, and Han Xu. Disentangling effects of colocalizing genomic annotations to functionally prioritize non-coding variants within complex trait loci, 2014. bioRxivdoi: http://dx.doi.org/10.1101/004309.

bioRxiv preprint doi: https://doi.org/10.1101/014241; this version posted January 23, 2015. The copyright holder for this preprint (which was not certified by peer review) is the author/funder, who has granted bioRxiv a license to display the preprint in perpetuity. It is made available under aCC-BY-ND 4.0 International license.

Methods

Stratified LD score regression

We begin with a derivation of Equation (1) for overlapping categories in a sample with no population structure or other confounding. The derivation of the intercept term in the presence of confounding is identical to the derivation in previous work.[15]

Let y_i be a quantitative phenotype in individual i, standardized to mean 0 and variance 1 in the population, and let X_{ij} be the genotype of individual i at the j-th SNP, standardized so that for each SNP j, X_{ij} has mean 0 and variance 1 in the population. We will assume a linear model:

$$y_i = \sum_{j \in G} X_{ij} \beta_j(G) + \epsilon_i,$$

where G is some fixed set of SNPs, $\beta_j(G)$ is the effect size of SNP j, and ϵ_i is mean-0 noise.

We define $\beta(G) = (\beta_1(G), \ldots, \beta_M(G))$ as the hypothetical result of multiple linear regression of y on X at infinite sample size. Thus, $\beta(G)$ depends on the set G; for example, if G is the set of genotyped SNPs then $\beta_j(G)$ includes the causal effects of non-typed SNPs that are tagged by SNP j, whereas if G contains all SNPs, then $\beta_j(G)$ will reflect only the true effect at SNP j.

We will define the heritability of the set G of SNPs to be

$$h^2_G = \sum_{j \in G} \beta_j(G)^2$$

and the heritability of a category $\mathcal{C} \subset G$ to be

$$h^2_G(\mathcal{C}) = \sum_{j \in \mathcal{C}} \beta_j(G)^2.$$

The definition of $h^2_G(\mathcal{C})$ depends on both G and $\mathcal{C}$; for example, if $\mathcal{C}$ is the set of SNPs with minor allele frequency (MAF) greater than 5%, $h^2_G(\mathcal{C})$ will be larger if $G = \mathcal{C}$ than if G contains SNPs with lower MAF since in the first case $h^2_G(\mathcal{C})$ includes tagged effects of low-frequency SNPs, whereas in the second case the low-frequency effects are included in $h^2_G(G \setminus \mathcal{C})$.

Suppose that we have a sample of N individuals. Let $y = (y_1, \ldots, y_N)$, and let X be the $N \times M$ matrix of standardized genotypes, where $M = |G|$. (We will assume that our sample is large enough that normalizing each SNP within our sample is roughly equivalent to normalizing each SNP in the

bioRxiv preprint doi: https://doi.org/10.1101/014241; this version posted January 23, 2015. The copyright holder for this preprint (which was not certified by peer review) is the author/funder, who has granted bioRxiv a license to display the preprint in perpetuity. It is made available under aCC-BY-ND 4.0 International license.

population.) Let $\epsilon = (\epsilon_1, \ldots, \epsilon_N)$ be a vector of residuals. Then we can write

$$y = X\beta(G) + \epsilon.$$

Let $\hat{\beta}_j$ be the estimate of the marginal effect of SNP j in our sample, given by

$$\hat{\beta}_j := \frac{1}{N} X_j^T y,$$

where X_j is the j-th column of X. Define χ^2 statistics $\chi_j^2 := N\hat{\beta}_j^2$.

Our goal here is to estimate $h_G^2(\mathcal{C})$, where G is the set of 1000G SNPs that have minor allele count greater than five in Europeans, and $\mathcal{C}$ is a functional category, such as coding SNPs or SNPs that are in H3K4me3 regions in fetal brain tissue. From now on, we will omit the dependence on G, understanding G to be the set of 1000G SNPs with minor allele count greater than five in Europeans. We would like to estimate this quantity from summary statistics; i.e., the input to our method will be $\{\chi_j^2\}_{j \in R}$, where R is the set of SNPs that were tested in a GWAS. We will also need LD information from a reference panel.

Substituting $y = X\beta + \epsilon$ into the the definition of $\hat{\beta}_j$, we get

$$\hat{\beta}_j = \frac{1}{N} X_j^T X\beta + \frac{1}{N} X_j^T \epsilon = \hat{D}_j \beta + \epsilon_j',$$

where $\hat{D}_j$ is the j-th row of the in-sample LD matrix $\hat{D} = X^T X/N$ and $\epsilon_j' = X_j^T \epsilon/N$. For a single entry β_j, this means that

$$\hat{\beta}_j = \sum_k \hat{r}_{jk} \beta_k + \epsilon_j',$$

where $\hat{r}_{jk} := \hat{D}(j,k)$ and ϵ_j' has mean 0 and variance σ_e^2/N.

To estimate $h_G^2(\mathcal{C})$, we will model β as a mean-0 random vector with independent entries. We will allow the variance of β_j to depend on certain functional properties of SNP j; for example, we will allow coding and non-coding SNPs to have different variances. More precisely, we will assume we have C functional categories $\mathcal{C}_1, \ldots, \mathcal{C}_C \subset \{1, \ldots, M\}$. One of the categories must always contain all SNPs to allow for baseline heritability. We will model the variance of β_j as

$$\mathrm{Var}(\beta_j) = \sum_{c: j \in \mathcal{C}_c} \tau_c. \tag{2}$$

bioRxiv preprint doi: https://doi.org/10.1101/014241; this version posted January 23, 2015. The copyright holder for this preprint (which was not certified by peer review) is the author/funder, who has granted bioRxiv a license to display the preprint in perpetuity. It is made available under aCC-BY-ND 4.0 International license.

In the case that the $\mathcal{C}_c$ are disjoint, we will have $\tau_c = h^2(\mathcal{C}_c)/M(\mathcal{C}_c)$, where $M(\mathcal{C}_c)$ is the number of SNPs in $\mathcal{C}_c$.

Consider the expectation of $\chi_j^2 = N\hat{\beta}_j^2$.

$$\begin{aligned}
\mathrm{E}[\chi_j^2] &= N\mathrm{E}\left(\sum_k \hat{r}_{jk}\beta_k + \epsilon'_j\right)^2 \\
&= N\sum_k \hat{r}_{jk}^2 \mathrm{E}[\beta_k^2] + N\mathrm{E}[{\epsilon'}_j^2] \\
&= N\sum_k \hat{r}_{jk}^2 \left(\sum_{c:k\in\mathcal{C}_c} \tau_c\right) + N\sigma_e^2 \\
&= N\sum_c \tau_c \sum_{k\in\mathcal{C}_c} \hat{r}_{jk}^2 + N\sigma_e^2,
\end{aligned}$$

where the second equality follows because the random variables are all independent with mean 0.

Let r_{jk} denote the true correlation between SNPs j and k in the underlying population. In an unstructured sample, $\mathrm{E}[\hat{r}_{jk}^2] \approx r_{jk}^2 + 1/N$.

We now have

$$\begin{aligned}
\mathrm{E}[\chi_j^2] &= N\sum_c \tau_c \sum_{c:k\in\mathcal{C}_c} \hat{r}_{jk}^2 + N\sigma_e^2 \\
&= N\sum_c \tau_c \sum_{c:k\in\mathcal{C}_c} (\hat{r}_{jk}^2 - 1/N) + N\sum_c \tau_c \sum_{k\in\mathcal{C})c} (1/N) + N\sigma_e^2 \\
&\approx N\sum_c \tau_c \sum_{k\in\mathcal{C}_c} r_{jk}^2 \\
&= N\sum_c \tau_c \ell(j,c) + \sum_k \mathrm{Var}(\beta_k) + N\sigma_e^2,
\end{aligned}$$

where $\ell(j,c) := \sum_{k\in\mathcal{C}_c} r_{jk}^2$. The variance of y_j is $\sum_j \mathrm{Var}(\beta_j) + \sigma_e^2$. Since our phenotype has variance one, we can replace $\sum_j \mathrm{Var}(\beta_j) + \sigma_e^2$ with 1, giving us our main equation:

$$\mathrm{E}[\chi_j^2] = N\sum_c \tau_c \ell(j,c) + 1 \tag{3}$$

Our goal is to estimate $h^2(\mathcal{C}_c) := \sum_{j\in\mathcal{C}_c} \beta_j^2 \approx \sum_{j\in\mathcal{C}_c} \mathrm{Var}(\beta_j)$, given a vector of χ^2 statistics and LD information either from the sample or from a reference panel. To estimate $\mathrm{Var}(\beta_j)$, we need to estimate each of the coefficients τ_c, and then we apply Equation (2). To estimate τ_c, we first compute $\ell(j,c)$, then

bioRxiv preprint doi: https://doi.org/10.1101/014241; this version posted January 23, 2015. The copyright holder for this preprint (which was not certified by peer review) is the author/funder, who has granted bioRxiv a license to display the preprint in perpetuity. It is made available under aCC-BY-ND 4.0 International license.

we regress χ_j^2 on $\ell(j,c)$. This is called stratified LD score regression.

We estimate standard errors using a block jackknife over SNPs with 200 equally-sized blocks of adjacent SNPs,[15] and use these standard errors to calculate z-scores, P-values, and FDRs. To minimize standard error, we remove outliers by excluding SNPs j with $\chi_j^2 > \max\{80, 0.001N\}$, where N is the maximum sample size in the study, and we also weight the regression in a way that takes into account both over-counting and heteroskedasticity due to LD (see below). We remove the MHC region from all analyses.

Proportion of heritability and GC correction. As described above, stratified LD score regression is a method for estimating $h^2(\mathcal{C})$ for a given category $\mathcal{C}$. However, we are often more interested in estimating the proportion of heritability $h^2(\mathcal{C})/h^2$. For this, we estimate $h^2(\mathcal{C})$ and h^2 separately and divide the estimates. For inference, we jackknife the proportion, rather than jackknifing the numerator and denominator separately.

Estimating the proportion of heritability is possible for summary statistics with GC correction, even though GC correction makes estimating the category specific heritability and total heritability impossible. This is because GC correction introduces a multiplicative error into estimates of both $h^2(\mathcal{C})$ and h^2,[15] but the two multiplicative errors are equal, and cancel out in the ratio.

Choice of regression SNPs and reference SNPs. The derivation above does not incorporate imperfect imputation. Ideally, we would prune our χ^2 statistics to a set of "regression SNPs" with imputation accuracy above 0.9, but since imputation accuracy is not always available, we instead use HapMap Project Phase 3 (HapMap3[43]) SNPs as a proxy for well-imputed SNPs. So for the purposes of this paper, our regression SNPs are always the HapMap3 SNPs.

However, we do not assume that only HapMap3 SNPs are causal. It is important that our model allow as many SNPs as possible to contribute causally, since if we use a model with, for example, only HapMap3 SNPs causal then we are assigning causality of any SNP that is tagged by HapMap3 but not included in HapMap3 to the HapMap3 SNPs that tag it. This is problematic specifically for functional partitioning because the functional categories containing the causal SNP may not be the same as the functional categories of the HapMap3 SNPs that tag it.

Recall that $h_A^2(B)$ is the heritability of set B defined using a model that allows any SNP in set A to be causal. Another way to restate our above point is that we are interested in $h_{1000G}^2(\mathcal{C})$ rather than $h_{HapMap3}^2(\mathcal{C})$ because a model that only allows HapMap3 SNPs to be causal is allowing non-HapMap3

bioRxiv preprint doi: https://doi.org/10.1101/014241; this version posted January 23, 2015. The copyright holder for this preprint (which was not certified by peer review) is the author/funder, who has granted bioRxiv a license to display the preprint in perpetuity. It is made available under aCC-BY-ND 4.0 International license.

heritability to be tagged by HapMap3 SNPs and therefore potentially assigning heritability to the wrong functional category. For this reason, our set of potentially causal SNPs—i.e., the set of SNPs in our reference panel—is the set of 1000G SNPs[24] with minor allele count greater than five in Europeans.

However, there is a problem introduced by having many reference panel SNPs that are not tagged by regression SNPs: it leads us to extrapolate the enrichments at well-tagged SNPs to the rare SNPs on our reference panel that are not well-tagged. In other words, we estimate τ_c using summary statistics at HapMap3 SNPs, and then we multiply these coefficients by the number of SNPs in the relevant categories in 1000G, extrapolating the enrichments observed at HapMap3 SNPs to all 1000G SNPs.

To prevent ourselves from this extrapolation, we only estimate enrichments of categories containing common SNPs—i.e., SNPs with MAF > 0.05, all of which we assume to be well-tagged by HapMap3. Let $\mathcal{G}$ denote the set of SNPs with $MAF > 0.05$. Then for any category $\mathcal{C}$, we can estimate $\mathcal{C} \cap \mathcal{G}$ without potentially inaccurate extrapolation. For this reason, the proportions of heritability that we report throughout this manuscript are $h^2_{1000G}(\mathcal{C} \cap \mathcal{G})/h^2_{1000G}(\mathcal{G})$.

Out-of-bounds estimates. Stratified LD score regression can give heritability estimates that are not between 0 and 1. When an unbiasedness is important—for example, when we are averaging estimates over several simulation replicates—we do not adjust these out-of-bounds estimates. However when mean squared error is more important than unbiasedness—for example, when reporting the results of a single analysis—we truncate these estimates to be between 0 and 1. To get a confidence interval around the truncated estimate, we intersect the original confidence interval with the interval $[0, 1]$.

Custom genotyping arrays. LD score regression is not currently applicable to studies using a custom genotyping arrays. For these arrays, SNPs that are more likely to have a large effect size also have a larger sample size, and this dependency is not modeled in the above derivation.

Regression weights. To minimize standard error, we weight the regression in a way that takes into account both over-counting and heteroskedasticity due to LD. For over-counting, we compute LD Scores within HapMap3 SNPs; call these $\ell_{hm3}(j)$. We also compute $\ell_{1000G}(j, c)$ for all categories c in our model. The variance of χ^2_j is proportional to $(1 + N \sum_c \tau_c \ell_{1000G}(j, c))^2$, but we do not have τ_c. We use a rough approximation of τ_c obtained by taking the mean over regression SNPs of both sides of Equation (3) and assuming that all the τ_c are equal. This gives us $\hat{\tau} = \left(\bar{\chi}^2 - 1\right) / \left(N \cdot \bar{\ell}(j)\right)$, where $\bar{\chi}^2$ is the mean of χ^2_j and $\bar{\ell}(j)$ is the mean of $\sum_c \ell_{1000G}(j, c)$, both taken over regression SNPs. We then

bioRxiv preprint doi: https://doi.org/10.1101/014241; this version posted January 23, 2015. The copyright holder for this preprint (which was not certified by peer review) is the author/funder, who has granted bioRxiv a license to display the preprint in perpetuity. It is made available under aCC-BY-ND 4.0 International license.

weight SNP j by the inverse product of the over counting weights and heteroskedasticity weights:

$$w_j := \frac{1}{\ell_{hm3}(j)(1 + N\hat{\tau}\sum_c \ell_{1000G}(j,c))^2}.$$

Baseline model. The 53 functional categories, derived from 24 main annotations, were obtained as follows:

- Coding, 3'-UTR, 5'-UTR promoter, and intron annotations from the RefSeq gene model were obtained from UCSC[17] and post-processed by Gusev et al.[13]
- Digital genomic footprint and transcription factor binding site annotations were obtained from ENCODE[3] and post-processed by Gusev et al.[13]
- The combined chromHMM/Segway annotations for six cell lines were obtained from Hoffman et al.[20] CTCF, promoter flanking, transcribed, transcription start site, strong enhancer, and weak enhancers are a union the six cell lines; repressed is an intersection over the six cell lines.
- DNase I hypersensitive sites (DHSs) are a combination of ENCODE and Roadmap data, post-processed by Trynka et al.[5] We combined the cell-type-specific annotations into two annotations for inclusion in the full baseline model: a union of all cell types, and a union of only fetal cell types. DHS and fetal DHS.
- H3K4me1, H3K4me, and H3K9ac were all obtained from Roadmap and post-processed by Trynka et al.[5] For each, we took a union over cell types for the full baseline model, and used the individual cell types for our cell-type-specific analysis.
- One version of H3K27ac was obtained from Roadmap, post-processed,[18] and a second version of H3K27ac was obtained from the data of Hnisz et al.[19] For each, we took a union over cell types for the full baseline model, and used the individual cell types for our cell-type-specific analysis.
- Super enhancers were also obtained from Hnisz et al,[19] and comprise a subset of the H3K27ac annotation from that paper. We took a union over cell types for the full baseline model
- Regions conserved in mammals were obtained from Lindblad-Toh et al.,[21] post-processed by Ward and Kellis.[31]
- FANTOM5 enhancers were obtained from Andersson et al.[22]
- For each of these 24 categories, we added a 500bp window around the category as an additional category to keep our heritability estimates from being inflated by heritability in flanking regions.[13]

bioRxiv preprint doi: https://doi.org/10.1101/014241; this version posted January 23, 2015. The copyright holder for this preprint (which was not certified by peer review) is the author/funder, who has granted bioRxiv a license to display the preprint in perpetuity. It is made available under aCC-BY-ND 4.0 International license.

- For each of DHS, H3K4me1, H3K4me3, and H3K9ac, we added a 100bp window around the ChIP-seq peak as an additional category.
- We added an additional category containing all SNPs.

WTCCC1 genotypes. We used chromosome 1 genotypes from the NBS and 1966BC control cohorts from the Wellcome Trust Case-Control Consortium.[23] Imputation of the genotypes to integrated phase1 v3 1000 Genomes and QC were done as in Gusev et al.;[13] we removed any SNPs that were below a MAF of 0.01, were above 0.002 missingness, or deviated from Hardy-Weinberg equilibrium at a $P < 0.01$.

Choice of phenotypes. We quantified the combination of sample size and heritability by the z-score of total SNP-heritability in the baseline analysis. We applied our method to all traits with available summary statistics, and removed all traits with a heritability z-score less than six. We then removed one of each pair of traits with a large genetic correlation (> 0.95): college attendance, which has a very high genetic correlation with years of education, and total cholesterol, which has a very high genetic correlation with LDL.[16]

Meta-analysis over traits. For our meta-analysis over traits, we identified pairs of traits with substantial sample overlap and trait correlation by using the intercept of LD score regression for genetic covariance. Specifically, we identified pairs of traits for which the intercept on N1N2 scale, which is an unbiased estimator of phenotypic correlation times sample overlap, was at least 10% of the sample size of either of the traits, and we excluded one of each such pair. The remaining set of traits was: Height, BMI, menarche, LDL levels, coronary artery disease, schizophrenia, educational attainment, smoking behavior, and rheumatoid arthritis. We then performed a random-effects meta-analysis of proportion of heritability over these phenotypes for each functional category. The results are in Figure 2 and Table S3.

Choice of traits to include in Figure 3. Height, BMI, age at menarche, and schizophrenia are the four traits with the highest combination of SNP heritability and sample size, which we quantify by the z-score of total heritability in the baseline analysis. We also included a meta-analysis of immunological diseases, since they have a different pattern of enrichment from other traits; for example FANTOM5 enhancers are very enriched for immunological diseases but not for other traits. This meta-analysis included only rheumatoid arthritis and Crohn's disease; we excluded ulcerative colitis because that dataset shares controls with the Crohn's disease dataset.

bioRxiv preprint doi: https://doi.org/10.1101/014241; this version posted January 23, 2015. The copyright holder for this preprint (which was not certified by peer review) is the author/funder, who has granted bioRxiv a license to display the preprint in perpetuity. It is made available under aCC-BY-ND 4.0 International license.

Robustness to derived allele frequency. To check that our results are not affected by a derived-allele-frequency-dependent genetic architecture, we repeated the meta-analysis over traits with a model that contained all of the categories of the full baseline model as well as seven derived allele frequency bins to the model as extra annotations: 0-0.1, 0.1-0.2, 0.2-0.3, 0.3-0.4, 0.4-0.6, 0.6-0.8, and 0.8-1. This allowed for effect size to depend on derived allele frequency, independently of functional annotation. These results are very similar to our results without derived allele frequency bins, and are displayed in Table S5.

Cell-type specific analysis. We used all available cell types from the four histone marks, excluding cell lines and cells labeled as cultured cells to limit ourselves to data with the clearest biological interpretation. The resulting cell-type-specific annotations are listed in Table S6. We then added each annotation individually to the baseline model and evaluated the significance of the coefficient τ_c of the cell-type-specific annofarh2014naturetation. Next, we combined the 220 cell-type-specific annotations into 10 cell-type groups and repeated the same analysis.

Discussion of other methods. There are no other methods designed to estimate genome-wide components of heritability from summary statistics. However, there are existing methods that identify enriched functional categories and cell types from summary statistics; here, we discuss a few of these methods.

A paper by Pickrell[8] combines GWAS data with functional data to identify enriched and depleted functional categories, and leverages the resulting model to increase GWAS power. While the method is effective at increasing power and identifies many interesting enrichments, it is unclear whether the method is effective at ranking cell types; for example, fetal fibroblasts are the top cell type for Crohn's disease. This could be because the model only allows for one causal SNP per locus, or could be a result of including all cell types simultaneously, thereby penalizing redundant cell types.

Kichaev et al.[7] introduce a new method that leverages functional data for improved fine-mapping. Their method also outputs annotations associated with disease. While their method is effective in increasing fine-mapping resolution, it is again unclear whether the method is effective at ranking cell types; for example, the cell types they identify as contributing the most to HDL, LDL, and Triglycerides are muscle, kidney, and fetal small intestine, respectively, whereas the top cell types for those three phenotypes identified using our method are liver, liver, and liver. The lower power of this method in ranking cell types is likely because it considers only genome-wide significant loci. Similarly, a recent

bioRxiv preprint doi: https://doi.org/10.1101/014241; this version posted January 23, 2015. The copyright holder for this preprint (which was not certified by peer review) is the author/funder, who has granted bioRxiv a license to display the preprint in perpetuity. It is made available under aCC-BY-ND 4.0 International license.

method from Farh et al.[6] focuses on fine-mapping and considers only genome-wide significant loci, although their cell-type-specific results are more concordant with known biology.

Maurano et al. use enrichment of SNPs passing P-value thresholds of increasing stringency to identify important cell types. However, they are implicitly assuming that the functional annotation at a GWAS SNP matches the functional annotation at the causal SNP. While this could be true for functional annotations composed of very wide regions, it is not likely to be true for functional annotations composed of smaller regions, such as conserved regions. Moreover, their method does not account for total LD, and so could give biased results if used to compare functional annotations with different average amounts of total LD.

The method of Trynka et al.[5] (also see a more recent manuscript[44]) is conservative in its identification of enrichment, comparing to a null obtained by local shifting rather than a genome-wide null, and leverages only genome-wide significant SNPs. As a result, they have very low power not only in traits such as bipolar disorder which have few genome-wide significant loci, but even for traits such as rheumatoid arthritis that have many significant loci. (Lowest P-value 10^{-4} much larger than the lowest P-value given by LD Score regression, 2×10^{-7}.)

bioRxiv preprint doi: https://doi.org/10.1101/014241; this version posted January 23, 2015. The copyright holder for this preprint (which was not certified by peer review) is the author/funder, who has granted bioRxiv a license to display the preprint in perpetuity. It is made available under aCC-BY-ND 4.0 International license.

Supplementary Information

Members of the Schizophrenia Working Group of the Psychiatric Genetics Consortium. The members of the Schizophrenia Working Group of the Psychiatric Genetics Consortium are Stephan Ripke, Benjamin M. Neale, Aiden Corvin, James T.R. Walters, Kai-How Farh, Peter A. Holmans, Phil Lee, Brendan Bulik-Sullivan, David A. Collier, Hailiang Huang, Tune H. Pers, Ingrid Agartz, Esben Agerbo, Margot Albus, Madeline Alexander, Farooq Amin, Silviu A. Bacanu, Martin Begemann, Richard A. Belliveau, Jr., Judit Bene, Sarah E. Bergen, Elizabeth Bevilacqua, Tim B. Bigdeli, Donald W. Black, Anders D. Brglum, Richard Bruggeman, Nancy G. Buccola, Randy L. Buckner, William Byerley, Wiepke Cahn, Guiqing Cai, Dominique Campion, Rita M. Cantor, Vaughan J. Carr, Noa Carrera, Stanley V. Catts, Kimberly D. Chambert, Raymond C.K. Chan, Ronald Y.L. Chen, Eric Y.H. Chen, Wei Cheng, Eric F.C. Cheung, Siow Ann Chong, C. Robert Cloninger, David Cohen, Nadine Cohen, Paul Cormican, Nick Craddock, James J. Crowley, David Curtis, Michael Davidson, Kenneth L. Davis, Franziska Degenhardt, Jurgen Del Favero, Lynn E. DeLisi, Ditte Demontis, Dimitris Dikeos, Timothy Dinan, Srdjan Djurovic, Gary Donohoe, Elodie Drapeau, Jubao Duan, Frank Dudbridge, Naser Durmishi, Peter Eichhammer, Johan Eriksson, Valentina Escott-Price, Laurent Essioux, Ayman H. Fanous, Martilias S. Farrell, Josef Frank, Lude Franke, Robert Freedman, Nelson B. Freimer, Marion Friedl, Joseph I. Friedman, Menachem Fromer, Giulio Genovese, Lyudmila Georgieva, Elliot S. Gershon, Ina Giegling, Paola Giusti-Rodrguez, Stephanie Godard, Jacqueline I. Goldstein, Vera Golimbet, Srihari Gopal, Jacob Gratten, Jakob Grove, Lieuwe de Haan, Christian Hammer, Marian L. Hamshere, Mark Hansen, Thomas Hansen, Vahram Haroutunian, Annette M. Hartmann, Frans A. Henskens, Stefan Herms, Joel N. Hirschhorn, Per Hoffmann, Andrea Hofman, Mads V. Hollegaard, David M. Hougaard, Masashi Ikeda, Inge Joa, Antonio Julia, Rene S. Kahn, Luba Kalaydjieva, Sena Karachanak-Yankova, Juha Karjalainen, David Kavanagh, Matthew C. Keller, Brian J. Kelly, James L. Kennedy, Andrey Khrunin, Yunjung Kim, Janis Klovins, James A. Knowles, Bettina Konte, Vaidutis Kucinskas, Zita Ausrele Kucinskiene, Hana Kuzelova-Ptackova, Anna K. Kahler, Claudine Laurent, Jimmy Lee Chee Keong, S. Hong Lee, Sophie E. Legge, Bernard Lerer, Miaoxin Li, Tao Li, Kung-Yee Liang, Jeffrey Lieberman, Svetlana Limborska, Carmel M. Loughland, Jan Lubinski, Jouko Lnnqvist, Milan Macek, Jr., Patrik K.E. Magnusson, Brion S. Maher, Wolfgang Maier, Jacques Mallet, Sara Marsal, Manuel Mattheisen, Morten Mattingsdal, Robert W. McCarley, Colm McDonald, Andrew M. McIntosh, Sandra Meier, Carin J. Meijer, Bela Melegh, Ingrid Melle, Raquelle I. Mesholam-Gately, Andres Metspalu, Patricia T. Michie, Lili Milani, Vihra Milanova, Younes Mokrab, Derek W. Morris, Ole Mors, Preben

bioRxiv preprint doi: https://doi.org/10.1101/014241; this version posted January 23, 2015. The copyright holder for this preprint (which was not certified by peer review) is the author/funder, who has granted bioRxiv a license to display the preprint in perpetuity. It is made available under aCC-BY-ND 4.0 International license.

B. Mortensen, Kieran C. Murphy, Robin M. Murray, Inez Myin-Germeys, Bertram Mller-Myhsok, Mari Nelis, Igor Nenadic, Deborah A. Nertney, Gerald Nestadt, Kristin K. Nicodemus, Liene Nikitina-Zake, Laura Nisenbaum, Annelie Nordin, Eadbhard O'Callaghan, Colm O'Dushlaine, F. Anthony O'Neill, Sang-Yun Oh, Ann Olincy, Line Olsen, Jim Van Os, Psychosis Endophenotypes International Consortium, Christos Pantelis, George N. Papadimitriou, Sergi Papiol, Elena Parkhomenko, Michele T. Pato, Tiina Paunio, Milica Pejovic-Milovancevic, Diana O. Perkins, Olli Pietilinen, Jonathan Pimm, Andrew J. Pocklington, John Powell, Alkes Price, Ann E. Pulver, Shaun M. Purcell, Digby Quested, Henrik B. Rasmussen, Abraham Reichenberg, Mark A. Reimers, Alexander L. Richards, Joshua L. Roffman, Panos Roussos, Douglas M. Ruderfer, Veikko Salomaa, Alan R. Sanders, Ulrich Schall, Christian R. Schubert, Thomas G. Schulze, Sibylle G. Schwab, Edward M. Scolnick, Rodney J. Scott, Larry J. Seidman, Jianxin Shi, Engilbert Sigurdsson, Teimuraz Silagadze, Jeremy M. Silverman, Kang Sim, Petr Slominsky, Jordan W. Smoller, Hon-Cheong So, Chris C.A. Spencer, Eli A. Stahl, Hreinn Stefansson, Stacy Steinberg, Elisabeth Stogmann, Richard E. Straub, Eric Strengman, Jana Strohmaier, T. Scott Stroup, Mythily Subramaniam, Jaana Suvisaari, Dragan M. Svrakic, Jin P. Szatkiewicz, Erik Sderman, Srinivas Thirumalai, Draga Toncheva, Paul A. Tooney, Sarah Tosato, Juha Veijola, John Waddington, Dermot Walsh, Dai Wang, Qiang Wang, Bradley T. Webb, Mark Weiser, Dieter B. Wildenauer, Nigel M. Williams, Stephanie Williams, Stephanie H. Witt, Aaron R. Wolen, Emily H.M. Wong, Brandon K. Wormley, Jing Qin Wu, Hualin Simon Xi, Clement C. Zai, Xuebin Zheng, Fritz Zimprich, Naomi R. Wray, Kari Stefansson, Peter M. Visscher, Wellcome Trust Case Control Consortium, Rolf Adolfsson, Ole A. Andreassen, Douglas H.R. Blackwood, Elvira Bramon, Joseph D. Buxbaum, Anders D. Brglum, Sven Cichon, Ariel Darvasi, Enrico Domenici, Hannelore Ehrenreich, Tonu Esko, Pablo V. Gejman, Michael Gill, Hugh Gurling, Christina M. Hultman, Nakao Iwata, Assen V. Jablensky, Erik G. Jonsson, Kenneth S. Kendler, George Kirov, Jo Knight, Todd Lencz, Douglas F. Levinson, Qingqin S. Li, Jianjun Liu, Anil K. Malhotra, Steven A. McCarroll, Andrew McQuillin, Jennifer L. Moran, Preben B. Mortensen, Bryan J. Mowry, Markus M. Nthen, Roel A. Ophoff, Michael J. Owen, Aarno Palotie, Carlos N. Pato, Tracey L. Petryshen, Danielle Posthuma, Marcella Rietschel, Brien P. Riley, Dan Rujescu, Pak C. Sham, Pamela Sklar, David St. Clair, Daniel R. Weinberger, Jens R. Wendland, Thomas Werge, Mark J. Daly, Patrick F. Sullivan, and Michael C. O'Donovan.

bioRxiv preprint doi: https://doi.org/10.1101/014241; this version posted January 23, 2015. The copyright holder for this preprint (which was not certified by peer review) is the author/funder, who has granted bioRxiv a license to display the preprint in perpetuity. It is made available under aCC-BY-ND 4.0 International license.

Annotation	Prop. SNPs	Mean segment length (bp)
Coding	0.015	315
Conserved	0.026	34
CTCF	0.024	490
DGF	0.138	208
DHS	0.168	358
FANTOM5 Enhancer	0.004	289
Enhancer	0.063	678
Fetal DHS	0.085	339
H3K27ac[19]	0.391	12411
H3K27ac[18]	0.269	1051
H3K4me1	0.427	1676
H3K4me3	0.133	941
H3K9ac	0.126	964
Intron	0.387	6537
PromoterFlanking	0.008	266
Promoter	0.031	4192
Repressed	0.461	572
Super Enhancer	0.168	54744
TFBS	0.132	509
Transcribed	0.345	484
TSS	0.018	813
3-prime UTR	0.011	844
5-prime UTR	0.005	197
Weak Enhancer	0.021	249

Table S1: *Annotations used. For DHS, H3K4me1, H3K4me3, and H3K9ac, we include peaks and regions as two annotations. For the annotations from the Hoffman segmentation,[20] we union over six cell lines for each category except Repressed, where we take an intersection instead. We also include a 500bp window around each annotation as a separate annotation in the model.*

bioRxiv preprint doi: https://doi.org/10.1101/014241; this version posted January 23, 2015. The copyright holder for this preprint (which was not certified by peer review) is the author/funder, who has granted bioRxiv a license to display the preprint in perpetuity. It is made available under aCC-BY-ND 4.0 International license.

Phenotype	Reference/consortium	N
Height	Lango Allen et al., 2010 Nature	133,858
BMI	Speliotes et al., 2010 Nat Genet	123,912
Age at menarche	Perry et al., 2014 Nature	132,989
LDL	Teslovich et al., 2010 Nature	95,454
HDL	Teslovich et al., 2010 Nature	99,900
Triglycerides	Teslovich et al., 2010 Nature	96,598
Coronary Artery Disease	Schunkert et al., Nat Genet 2011	86,995
Type-2 Diabetes	Morris et al., 2012 Nat Genet	69,033
Fasting glucose	Manning et. al., Nat Genet, 2012	58,074
Schizophrenia	SCZ Working Group of the PGC, 2014 Nature	70,100
Bipolar Disorder	Bip Working Group of the PGC, 2011 Nat Genet	16,731
Anorexia	Boraska et al., 2014 Mol Psych	17,767
Educational attainment	Rietveld et al., Science 2013	101,069
Ever smoked	TAG Consortium, 2010 Nat Genet	74,035
Rheumatoid Arthritis	Okada et al., 2014 Nature	38,242
Crohn's Disease	Jostins et al., 2012 Nature	20,883
Ulcerative Colitis	Jostins et al., 2012 Nature	27,432

Table S2: *Phenotypes used in the main analyses. The total number of phenotype measurements is 1,263,072. There is sample overlap among the studies, so the number of unique individuals is lower.*

bioRxiv preprint doi: https://doi.org/10.1101/014241; this version posted January 23, 2015. The copyright holder for this preprint (which was not certified by peer review) is the author/funder, who has granted bioRxiv a license to display the preprint in perpetuity. It is made available under aCC-BY-ND 4.0 International license.

Annotation	Prop. SNPs	Prop. h^2	Enrichment
Coding	0.015	0.104 (0.012)	7.122 (0.840)
Coding + 500bp	0.065	0.190 (0.030)	2.938 (0.467)
Conserved	0.026	0.347 (0.039)	13.322 (1.500)
Conserved + 500bp	0.333	0.654 (0.026)	1.966 (0.078)
CTCF	0.024	-0.004 (0.019)	-0.176 (0.789)
CTCF + 500bp	0.071	0.059 (0.019)	0.825 (0.272)
DGF	0.138	0.358 (0.094)	2.604 (0.686)
DGF + 500bp	0.542	0.761 (0.069)	1.405 (0.128)
DHS peaks	0.112	0.224 (0.063)	2.005 (0.566)
DHS	0.168	0.285 (0.069)	1.699 (0.410)
DHS + 500bp	0.499	0.788 (0.041)	1.580 (0.082)
FANTOM5 Enhancer	0.004	-0.003 (0.009)	-0.727 (2.160)
FANTOM5 Enhancer + 500bp	0.019	0.017 (0.017)	0.878 (0.896)
Enhancer	0.063	0.238 (0.050)	3.764 (0.784)
Enhancer + 500bp	0.154	0.359 (0.042)	2.334 (0.272)
Fetal DHS	0.085	0.238 (0.043)	2.805 (0.512)
Fetal DHS + 500bp	0.285	0.591 (0.058)	2.073 (0.204)
H3K27ac[19]	0.391	0.631 (0.054)	1.612 (0.138)
H3K27ac[19] + 500bp	0.423	0.664 (0.059)	1.572 (0.140)
H3K27ac[18]	0.269	0.490 (0.054)	1.818 (0.200)
H3K27ac[18] + 500bp	0.336	0.611 (0.040)	1.817 (0.118)
H3K4me1 peaks	0.171	0.447 (0.040)	2.611 (0.235)
H3K4me1	0.427	0.792 (0.065)	1.857 (0.152)
H3K4me1 + 500bp	0.609	0.910 (0.039)	1.494 (0.064)
H3K4me3 peaks	0.042	0.158 (0.025)	3.780 (0.599)
H3K4me3	0.133	0.344 (0.045)	2.582 (0.336)
H3K4me3 + 500bp	0.255	0.487 (0.056)	1.905 (0.220)
H3K9ac peaks	0.039	0.248 (0.024)	6.399 (0.618)
H3K9ac	0.126	0.408 (0.056)	3.233 (0.441)
H3K9ac + 500bp	0.231	0.504 (0.040)	2.184 (0.172)
Intron	0.387	0.462 (0.014)	1.192 (0.035)
Intron + 500bp	0.397	0.521 (0.015)	1.313 (0.037)
PromoterFlanking	0.008	0.004 (0.011)	0.448 (1.314)
PromoterFlanking + 500bp	0.033	0.081 (0.018)	2.433 (0.531)
Promoter	0.031	0.087 (0.016)	2.806 (0.512)
Promoter + 500bp	0.039	0.080 (0.016)	2.063 (0.424)
Repressed	0.461	0.286 (0.063)	0.619 (0.137)
Repressed + 500bp	0.719	0.446 (0.049)	0.620 (0.068)
Super Enhancer	0.168	0.304 (0.035)	1.804 (0.210)
Super Enhancer + 500bp	0.172	0.319 (0.037)	1.857 (0.216)
TFBS	0.132	0.445 (0.063)	3.357 (0.479)
TFBS + 500bp	0.343	0.503 (0.052)	1.464 (0.152)
Transcribed	0.345	0.407 (0.038)	1.179 (0.111)
Transcribed + 500bp	0.763	0.721 (0.028)	0.945 (0.036)
TSS	0.018	0.104 (0.023)	5.682 (1.278)
TSS + 500bp	0.035	0.172 (0.029)	4.940 (0.827)
3-prime UTR	0.011	0.054 (0.009)	4.892 (0.856)
3-prime UTR + 500bp	0.027	0.074 (0.011)	2.730 (0.412)
5-prime UTR	0.005	0.028 (0.008)	5.243 (1.385)
5-prime UTR + 500bp	0.028	0.065 (0.010)	2.340 (0.374)
Weak Enhancer	0.021	0.070 (0.023)	3.323 (1.090)
Weak Enhancer + 500bp	0.089	0.199 (0.030)	2.238 (0.335)

Table S3: Proportion of SNP-heritability and enrichment for different functional categories. We display results meta-analyzed across nine traits for each of the 53 annotations, including two distinct H3K27ac annotations (Methods). Although true SNP-heritability is non-negative, we report here unbiased estimates, we can be negative (Methods).

bioRxiv preprint doi: https://doi.org/10.1101/014241; this version posted January 23, 2015. The copyright holder for this preprint (which was not certified by peer review) is the author/funder, who has granted bioRxiv a license to display the preprint in perpetuity. It is made available under aCC-BY-ND 4.0 International license.

Annotation	Prop. SNPs	Prop. h^2	Enrichment
Coding	0.015	0.127 (0.036)	8.661 (2.475)
Coding + 500bp	0.065	0.192 (0.034)	2.979 (0.521)
Conserved	0.026	0.340 (0.051)	13.029 (1.950)
Conserved + 500bp	0.333	0.636 (0.053)	1.913 (0.159)
CTCF	0.024	0.050 (0.045)	2.118 (1.909)
CTCF + 500bp	0.071	0.089 (0.048)	1.249 (0.669)
DGF	0.138	0.585 (0.085)	4.253 (0.621)
DGF + 500bp	0.542	0.983 (0.066)	1.815 (0.122)
DHS peaks	0.112	0.429 (0.107)	3.837 (0.958)
DHS	0.168	0.512 (0.120)	3.050 (0.717)
DHS + 500bp	0.499	0.787 (0.062)	1.579 (0.124)
FANTOM5 Enhancer	0.004	0.013 (0.019)	2.930 (4.429)
FANTOM5 Enhancer + 500bp	0.019	0.014 (0.023)	0.711 (1.224)
Enhancer	0.063	0.184 (0.064)	2.906 (1.018)
Enhancer + 500bp	0.154	0.396 (0.054)	2.573 (0.353)
Fetal DHS	0.085	0.281 (0.089)	3.311 (1.050)
Fetal DHS + 500bp	0.285	0.504 (0.080)	1.770 (0.280)
H3K27ac[19]	0.391	0.782 (0.035)	1.999 (0.089)
H3K27ac[19] + 500bp	0.423	0.780 (0.043)	1.846 (0.101)
H3K27ac[18]	0.269	0.533 (0.065)	1.978 (0.243)
H3K27ac[18] + 500bp	0.336	0.674 (0.061)	2.005 (0.181)
H3K4me1 peaks	0.171	0.422 (0.091)	2.465 (0.530)
H3K4me1	0.427	0.965 (0.074)	2.261 (0.173)
H3K4me1 + 500bp	0.609	0.946 (0.036)	1.553 (0.060)
H3K4me3 peaks	0.042	0.075 (0.053)	1.791 (1.263)
H3K4me3	0.133	0.429 (0.071)	3.215 (0.535)
H3K4me3 + 500bp	0.255	0.584 (0.054)	2.286 (0.211)
H3K9ac peaks	0.039	0.266 (0.060)	6.851 (1.539)
H3K9ac	0.126	0.558 (0.066)	4.428 (0.520)
H3K9ac + 500bp	0.231	0.602 (0.055)	2.612 (0.237)
Intron	0.387	0.448 (0.031)	1.156 (0.081)
Intron + 500bp	0.397	0.532 (0.025)	1.340 (0.064)
PromoterFlanking	0.008	-0.046 (0.025)	-5.400 (3.021)
PromoterFlanking + 500bp	0.033	0.116 (0.034)	3.453 (1.029)
Promoter	0.031	0.089 (0.033)	2.848 (1.057)
Promoter + 500bp	0.039	0.101 (0.020)	2.603 (0.528)
Repressed	0.461	0.115 (0.093)	0.248 (0.203)
Repressed + 500bp	0.719	0.369 (0.039)	0.513 (0.054)
Super Enhancer	0.168	0.384 (0.026)	2.280 (0.155)
Super Enhancer + 500bp	0.172	0.398 (0.023)	2.317 (0.137)
TFBS	0.132	0.455 (0.083)	3.438 (0.628)
TFBS + 500bp	0.343	0.682 (0.065)	1.984 (0.190)
Transcribed	0.345	0.572 (0.094)	1.657 (0.272)
Transcribed + 500bp	0.763	0.652 (0.052)	0.854 (0.068)
TSS	0.018	0.107 (0.038)	5.853 (2.103)
TSS + 500bp	0.035	0.174 (0.032)	4.991 (0.905)
3-prime UTR	0.011	0.102 (0.032)	9.240 (2.857)
3-prime UTR + 500bp	0.027	0.118 (0.032)	4.380 (1.176)
5-prime UTR	0.005	0.045 (0.022)	8.310 (4.056)
5-prime UTR + 500bp	0.028	0.069 (0.023)	2.470 (0.840)
Weak Enhancer	0.021	0.018 (0.043)	0.853 (2.025)
Weak Enhancer + 500bp	0.089	0.109 (0.048)	1.229 (0.539)

(S4.A) Proportion of heritability and enrichment for different functional categories for Height.

bioRxiv preprint doi: https://doi.org/10.1101/014241; this version posted January 23, 2015. The copyright holder for this preprint (which was not certified by peer review) is the author/funder, who has granted bioRxiv a license to display the preprint in perpetuity. It is made available under aCC-BY-ND 4.0 International license.

Annotation	Prop. SNPs	Prop. h^2	Enrichment
Coding	0.015	0.104 (0.027)	7.071 (1.813)
Coding + 500bp	0.065	0.129 (0.032)	1.992 (0.500)
Conserved	0.026	0.508 (0.059)	19.504 (2.270)
Conserved + 500bp	0.333	0.545 (0.068)	1.640 (0.205)
CTCF	0.024	-0.027 (0.049)	-1.135 (2.051)
CTCF + 500bp	0.071	0.025 (0.045)	0.358 (0.640)
DGF	0.138	0.034 (0.124)	0.249 (0.899)
DGF + 500bp	0.542	0.674 (0.068)	1.244 (0.125)
DHS peaks	0.112	0.125 (0.100)	1.123 (0.894)
DHS	0.168	0.093 (0.123)	0.554 (0.733)
DHS + 500bp	0.499	0.890 (0.123)	1.785 (0.246)
FANTOM5 Enhancer	0.004	0.003 (0.018)	0.792 (4.139)
FANTOM5 Enhancer + 500bp	0.019	-0.004 (0.026)	-0.218 (1.364)
Enhancer	0.063	0.259 (0.052)	4.083 (0.829)
Enhancer + 500bp	0.154	0.305 (0.052)	1.980 (0.337)
Fetal DHS	0.085	0.112 (0.089)	1.320 (1.045)
Fetal DHS + 500bp	0.285	0.572 (0.081)	2.008 (0.284)
H3K27ac[19]	0.391	0.514 (0.037)	1.315 (0.096)
H3K27ac[19] + 500bp	0.423	0.564 (0.039)	1.334 (0.093)
H3K27ac[18]	0.269	0.447 (0.059)	1.660 (0.221)
H3K27ac[18] + 500bp	0.336	0.557 (0.067)	1.657 (0.199)
H3K4me1 peaks	0.171	0.394 (0.102)	2.298 (0.595)
H3K4me1	0.427	0.668 (0.092)	1.565 (0.216)
H3K4me1 + 500bp	0.609	0.880 (0.052)	1.445 (0.086)
H3K4me3 peaks	0.042	0.150 (0.054)	3.583 (1.295)
H3K4me3	0.133	0.219 (0.057)	1.646 (0.429)
H3K4me3 + 500bp	0.255	0.405 (0.054)	1.585 (0.212)
H3K9ac peaks	0.039	0.279 (0.056)	7.206 (1.452)
H3K9ac	0.126	0.214 (0.066)	1.699 (0.520)
H3K9ac + 500bp	0.231	0.450 (0.051)	1.952 (0.222)
Intron	0.387	0.424 (0.032)	1.094 (0.083)
Intron + 500bp	0.397	0.490 (0.030)	1.233 (0.076)
PromoterFlanking	0.008	0.004 (0.023)	0.477 (2.702)
PromoterFlanking + 500bp	0.033	0.042 (0.035)	1.262 (1.035)
Promoter	0.031	0.080 (0.031)	2.559 (0.989)
Promoter + 500bp	0.039	0.060 (0.024)	1.565 (0.615)
Repressed	0.461	0.321 (0.105)	0.696 (0.227)
Repressed + 500bp	0.719	0.619 (0.032)	0.860 (0.045)
Super Enhancer	0.168	0.217 (0.019)	1.289 (0.114)
Super Enhancer + 500bp	0.172	0.251 (0.022)	1.464 (0.129)
TFBS	0.132	0.357 (0.087)	2.692 (0.659)
TFBS + 500bp	0.343	0.438 (0.071)	1.275 (0.207)
Transcribed	0.345	0.442 (0.088)	1.280 (0.256)
Transcribed + 500bp	0.763	0.775 (0.051)	1.015 (0.067)
TSS	0.018	0.059 (0.030)	3.239 (1.670)
TSS + 500bp	0.035	0.097 (0.030)	2.792 (0.874)
3-prime UTR	0.011	0.059 (0.022)	5.352 (2.007)
3-prime UTR + 500bp	0.027	0.054 (0.021)	2.013 (0.796)
5-prime UTR	0.005	0.035 (0.018)	6.541 (3.287)
5-prime UTR + 500bp	0.028	0.055 (0.022)	1.984 (0.794)
Weak Enhancer	0.021	0.119 (0.039)	5.640 (1.837)
Weak Enhancer + 500bp	0.089	0.236 (0.044)	2.658 (0.495)

(S4.B) Proportion of heritability and enrichment for different functional categories for BMI.

bioRxiv preprint doi: https://doi.org/10.1101/014241; this version posted January 23, 2015. The copyright holder for this preprint (which was not certified by peer review) is the author/funder, who has granted bioRxiv a license to display the preprint in perpetuity. It is made available under aCC-BY-ND 4.0 International license.

Annotation	Prop. SNPs	Prop. h^2	Enrichment
Coding	0.015	0.123 (0.030)	8.413 (2.059)
Coding + 500bp	0.065	0.094 (0.035)	1.453 (0.537)
Conserved	0.026	0.462 (0.063)	17.725 (2.414)
Conserved + 500bp	0.333	0.616 (0.090)	1.853 (0.271)
CTCF	0.024	0.022 (0.051)	0.935 (2.150)
CTCF + 500bp	0.071	0.049 (0.053)	0.689 (0.749)
DGF	0.138	0.207 (0.113)	1.508 (0.823)
DGF + 500bp	0.542	0.429 (0.084)	0.793 (0.155)
DHS peaks	0.112	0.008 (0.120)	0.071 (1.071)
DHS	0.168	0.052 (0.135)	0.311 (0.806)
DHS + 500bp	0.499	0.631 (0.096)	1.265 (0.193)
FANTOM5 Enhancer	0.004	-0.000 (0.022)	-0.028 (5.150)
FANTOM5 Enhancer + 500bp	0.019	0.006 (0.025)	0.321 (1.315)
Enhancer	0.063	0.137 (0.061)	2.163 (0.960)
Enhancer + 500bp	0.154	0.215 (0.059)	1.397 (0.384)
Fetal DHS	0.085	0.108 (0.093)	1.272 (1.100)
Fetal DHS + 500bp	0.285	0.291 (0.101)	1.020 (0.356)
H3K27ac[19]	0.391	0.455 (0.037)	1.164 (0.094)
H3K27ac[19] + 500bp	0.423	0.489 (0.052)	1.158 (0.123)
H3K27ac[18]	0.269	0.409 (0.071)	1.517 (0.264)
H3K27ac[18] + 500bp	0.336	0.486 (0.070)	1.446 (0.207)
H3K4me1 peaks	0.171	0.471 (0.116)	2.747 (0.678)
H3K4me1	0.427	0.621 (0.085)	1.455 (0.200)
H3K4me1 + 500bp	0.609	0.847 (0.057)	1.391 (0.094)
H3K4me3 peaks	0.042	0.211 (0.071)	5.042 (1.695)
H3K4me3	0.133	0.237 (0.067)	1.779 (0.502)
H3K4me3 + 500bp	0.255	0.308 (0.064)	1.207 (0.249)
H3K9ac peaks	0.039	0.220 (0.062)	5.671 (1.596)
H3K9ac	0.126	0.345 (0.066)	2.736 (0.520)
H3K9ac + 500bp	0.231	0.460 (0.055)	1.996 (0.240)
Intron	0.387	0.437 (0.035)	1.129 (0.090)
Intron + 500bp	0.397	0.537 (0.031)	1.353 (0.078)
PromoterFlanking	0.008	0.020 (0.031)	2.394 (3.660)
PromoterFlanking + 500bp	0.033	0.056 (0.033)	1.684 (0.992)
Promoter	0.031	0.123 (0.033)	3.945 (1.051)
Promoter + 500bp	0.039	0.116 (0.025)	2.995 (0.660)
Repressed	0.461	0.385 (0.100)	0.835 (0.216)
Repressed + 500bp	0.719	0.513 (0.038)	0.714 (0.053)
Super Enhancer	0.168	0.213 (0.030)	1.264 (0.176)
Super Enhancer + 500bp	0.172	0.233 (0.029)	1.357 (0.171)
TFBS	0.132	0.437 (0.098)	3.301 (0.737)
TFBS + 500bp	0.343	0.427 (0.092)	1.244 (0.268)
Transcribed	0.345	0.436 (0.086)	1.263 (0.250)
Transcribed + 500bp	0.763	0.681 (0.057)	0.893 (0.075)
TSS	0.018	0.165 (0.043)	9.064 (2.354)
TSS + 500bp	0.035	0.167 (0.036)	4.786 (1.040)
3-prime UTR	0.011	0.034 (0.022)	3.053 (1.948)
3-prime UTR + 500bp	0.027	0.047 (0.020)	1.762 (0.761)
5-prime UTR	0.005	0.042 (0.021)	7.792 (3.826)
5-prime UTR + 500bp	0.028	0.059 (0.031)	2.129 (1.101)
Weak Enhancer	0.021	0.011 (0.045)	0.542 (2.148)
Weak Enhancer + 500bp	0.089	0.113 (0.054)	1.274 (0.602)

(S4.C) Proportion of heritability and enrichment for different functional categories for Age at menarche.

bioRxiv preprint doi: https://doi.org/10.1101/014241; this version posted January 23, 2015. The copyright holder for this preprint (which was not certified by peer review) is the author/funder, who has granted bioRxiv a license to display the preprint in perpetuity. It is made available under aCC-BY-ND 4.0 International license.

Annotation	Prop. SNPs	Prop. h^2	Enrichment
Coding	0.015	0.128 (0.093)	8.740 (6.337)
Coding + 500bp	0.065	0.502 (0.089)	7.782 (1.380)
Conserved	0.026	0.264 (0.124)	10.111 (4.756)
Conserved + 500bp	0.333	0.811 (0.143)	2.438 (0.429)
CTCF	0.024	0.179 (0.109)	7.506 (4.590)
CTCF + 500bp	0.071	0.079 (0.106)	1.109 (1.493)
DGF	0.138	0.542 (0.192)	3.938 (1.398)
DGF + 500bp	0.542	0.806 (0.149)	1.489 (0.276)
DHS peaks	0.112	0.417 (0.189)	3.730 (1.691)
DHS	0.168	0.505 (0.247)	3.008 (1.473)
DHS + 500bp	0.499	0.810 (0.162)	1.623 (0.325)
FANTOM5 Enhancer	0.004	-0.050 (0.047)	-11.493 (10.749)
FANTOM5 Enhancer + 500bp	0.019	-0.006 (0.047)	-0.323 (2.442)
Enhancer	0.063	0.500 (0.157)	7.895 (2.477)
Enhancer + 500bp	0.154	0.524 (0.121)	3.406 (0.783)
Fetal DHS	0.085	0.370 (0.194)	4.370 (2.290)
Fetal DHS + 500bp	0.285	0.783 (0.133)	2.746 (0.466)
H3K27ac[19]	0.391	0.776 (0.093)	1.984 (0.237)
H3K27ac[19] + 500bp	0.423	0.962 (0.075)	2.277 (0.177)
H3K27ac[18]	0.269	0.829 (0.155)	3.075 (0.575)
H3K27ac[18] + 500bp	0.336	0.772 (0.100)	2.298 (0.298)
H3K4me1 peaks	0.171	0.430 (0.264)	2.512 (1.539)
H3K4me1	0.427	1.179 (0.151)	2.765 (0.354)
H3K4me1 + 500bp	0.609	1.056 (0.094)	1.733 (0.154)
H3K4me3 peaks	0.042	0.069 (0.186)	1.658 (4.459)
H3K4me3	0.133	0.628 (0.173)	4.715 (1.296)
H3K4me3 + 500bp	0.255	0.933 (0.181)	3.652 (0.710)
H3K9ac peaks	0.039	-0.028 (0.165)	-0.712 (4.249)
H3K9ac	0.126	0.751 (0.167)	5.951 (1.324)
H3K9ac + 500bp	0.231	0.832 (0.187)	3.607 (0.812)
Intron	0.387	0.472 (0.082)	1.218 (0.212)
Intron + 500bp	0.397	0.657 (0.050)	1.654 (0.126)
PromoterFlanking	0.008	0.055 (0.073)	6.544 (8.609)
PromoterFlanking + 500bp	0.033	0.264 (0.087)	7.895 (2.605)
Promoter	0.031	0.140 (0.073)	4.499 (2.352)
Promoter + 500bp	0.039	0.173 (0.048)	4.475 (1.248)
Repressed	0.461	-0.077 (0.140)	-0.167 (0.304)
Repressed + 500bp	0.719	0.168 (0.077)	0.234 (0.107)
Super Enhancer	0.168	0.439 (0.059)	2.608 (0.351)
Super Enhancer + 500bp	0.172	0.467 (0.059)	2.721 (0.345)
TFBS	0.132	0.871 (0.231)	6.576 (1.747)
TFBS + 500bp	0.343	0.787 (0.152)	2.291 (0.443)
Transcribed	0.345	0.573 (0.139)	1.659 (0.403)
Transcribed + 500bp	0.763	0.627 (0.106)	0.821 (0.139)
TSS	0.018	0.086 (0.097)	4.746 (5.306)
TSS + 500bp	0.035	0.452 (0.083)	12.976 (2.387)
3-prime UTR	0.011	0.035 (0.045)	3.190 (4.086)
3-prime UTR + 500bp	0.027	0.109 (0.041)	4.044 (1.528)
5-prime UTR	0.005	0.015 (0.041)	2.768 (7.486)
5-prime UTR + 500bp	0.028	0.088 (0.069)	3.154 (2.471)
Weak Enhancer	0.021	0.145 (0.096)	6.876 (4.532)
Weak Enhancer + 500bp	0.089	0.257 (0.109)	2.890 (1.221)

(S4.D) Proportion of heritability and enrichment for different functional categories for LDL.

bioRxiv preprint doi: https://doi.org/10.1101/014241; this version posted January 23, 2015. The copyright holder for this preprint (which was not certified by peer review) is the author/funder, who has granted bioRxiv a license to display the preprint in perpetuity. It is made available under aCC-BY-ND 4.0 International license.

Annotation	Prop. SNPs	Prop. h^2	Enrichment
Coding	0.015	0.058 (0.058)	3.986 (3.937)
Coding + 500bp	0.065	0.309 (0.064)	4.788 (0.993)
Conserved	0.026	0.269 (0.075)	10.339 (2.870)
Conserved + 500bp	0.333	0.582 (0.121)	1.749 (0.364)
CTCF	0.024	-0.049 (0.068)	-2.077 (2.851)
CTCF + 500bp	0.071	0.032 (0.084)	0.453 (1.178)
DGF	0.138	0.093 (0.195)	0.676 (1.420)
DGF + 500bp	0.542	0.735 (0.149)	1.358 (0.275)
DHS peaks	0.112	0.219 (0.193)	1.960 (1.727)
DHS	0.168	0.289 (0.190)	1.721 (1.132)
DHS + 500bp	0.499	0.921 (0.214)	1.846 (0.428)
FANTOM5 Enhancer	0.004	0.001 (0.049)	0.162 (11.325)
FANTOM5 Enhancer + 500bp	0.019	-0.004 (0.051)	-0.213 (2.700)
Enhancer	0.063	0.211 (0.125)	3.332 (1.971)
Enhancer + 500bp	0.154	0.512 (0.101)	3.327 (0.658)
Fetal DHS	0.085	0.091 (0.137)	1.079 (1.620)
Fetal DHS + 500bp	0.285	0.736 (0.116)	2.583 (0.407)
H3K27ac[19]	0.391	0.802 (0.067)	2.051 (0.172)
H3K27ac[19] + 500bp	0.423	0.828 (0.072)	1.960 (0.171)
H3K27ac[18]	0.269	0.904 (0.190)	3.353 (0.705)
H3K27ac[18] + 500bp	0.336	0.839 (0.082)	2.495 (0.244)
H3K4me1 peaks	0.171	0.602 (0.221)	3.515 (1.291)
H3K4me1	0.427	1.055 (0.165)	2.474 (0.388)
H3K4me1 + 500bp	0.609	1.035 (0.093)	1.699 (0.153)
H3K4me3 peaks	0.042	0.019 (0.129)	0.451 (3.082)
H3K4me3	0.133	0.530 (0.129)	3.975 (0.970)
H3K4me3 + 500bp	0.255	0.690 (0.111)	2.702 (0.435)
H3K9ac peaks	0.039	0.240 (0.121)	6.195 (3.118)
H3K9ac	0.126	0.632 (0.106)	5.015 (0.842)
H3K9ac + 500bp	0.231	0.856 (0.110)	3.714 (0.477)
Intron	0.387	0.523 (0.070)	1.349 (0.180)
Intron + 500bp	0.397	0.603 (0.048)	1.518 (0.120)
PromoterFlanking	0.008	-0.039 (0.038)	-4.590 (4.512)
PromoterFlanking + 500bp	0.033	0.071 (0.058)	2.111 (1.727)
Promoter	0.031	0.180 (0.073)	5.785 (2.340)
Promoter + 500bp	0.039	0.162 (0.046)	4.197 (1.182)
Repressed	0.461	0.143 (0.114)	0.310 (0.246)
Repressed + 500bp	0.719	0.312 (0.072)	0.434 (0.100)
Super Enhancer	0.168	0.531 (0.051)	3.151 (0.305)
Super Enhancer + 500bp	0.172	0.535 (0.048)	3.120 (0.281)
TFBS	0.132	0.358 (0.189)	2.706 (1.428)
TFBS + 500bp	0.343	0.601 (0.142)	1.749 (0.413)
Transcribed	0.345	0.445 (0.108)	1.289 (0.314)
Transcribed + 500bp	0.763	0.839 (0.070)	1.100 (0.091)
TSS	0.018	0.066 (0.057)	3.601 (3.136)
TSS + 500bp	0.035	0.306 (0.072)	8.782 (2.072)
3-prime UTR	0.011	-0.014 (0.036)	-1.224 (3.289)
3-prime UTR + 500bp	0.027	0.071 (0.040)	2.623 (1.498)
5-prime UTR	0.005	0.082 (0.041)	15.172 (7.520)
5-prime UTR + 500bp	0.028	0.086 (0.039)	3.076 (1.410)
Weak Enhancer	0.021	0.081 (0.077)	3.859 (3.629)
Weak Enhancer + 500bp	0.089	0.321 (0.105)	3.605 (1.181)

(S4.E) Proportion of heritability and enrichment for different functional categories for HDL.

bioRxiv preprint doi: https://doi.org/10.1101/014241; this version posted January 23, 2015. The copyright holder for this preprint (which was not certified by peer review) is the author/funder, who has granted bioRxiv a license to display the preprint in perpetuity. It is made available under aCC-BY-ND 4.0 International license.

Annotation	Prop. SNPs	Prop. h^2	Enrichment
Coding	0.015	0.052 (0.049)	3.542 (3.318)
Coding + 500bp	0.065	0.252 (0.051)	3.899 (0.786)
Conserved	0.026	0.269 (0.080)	10.309 (3.077)
Conserved + 500bp	0.333	0.664 (0.090)	1.997 (0.271)
CTCF	0.024	-0.019 (0.078)	-0.814 (3.294)
CTCF + 500bp	0.071	0.010 (0.077)	0.137 (1.078)
DGF	0.138	0.237 (0.150)	1.724 (1.092)
DGF + 500bp	0.542	0.690 (0.108)	1.275 (0.199)
DHS peaks	0.112	0.145 (0.162)	1.293 (1.447)
DHS	0.168	0.249 (0.166)	1.484 (0.989)
DHS + 500bp	0.499	0.941 (0.125)	1.886 (0.250)
FANTOM5 Enhancer	0.004	-0.047 (0.030)	-10.766 (6.886)
FANTOM5 Enhancer + 500bp	0.019	0.030 (0.052)	1.551 (2.737)
Enhancer	0.063	0.232 (0.115)	3.657 (1.815)
Enhancer + 500bp	0.154	0.559 (0.105)	3.630 (0.685)
Fetal DHS	0.085	0.333 (0.128)	3.929 (1.512)
Fetal DHS + 500bp	0.285	0.649 (0.119)	2.276 (0.419)
H3K27ac[19]	0.391	0.768 (0.060)	1.964 (0.152)
H3K27ac[19] + 500bp	0.423	0.759 (0.054)	1.797 (0.127)
H3K27ac[18]	0.269	0.750 (0.149)	2.783 (0.551)
H3K27ac[18] + 500bp	0.336	0.797 (0.091)	2.373 (0.272)
H3K4me1 peaks	0.171	0.132 (0.163)	0.772 (0.951)
H3K4me1	0.427	0.823 (0.144)	1.929 (0.337)
H3K4me1 + 500bp	0.609	1.181 (0.072)	1.939 (0.119)
H3K4me3 peaks	0.042	0.121 (0.112)	2.907 (2.685)
H3K4me3	0.133	0.452 (0.083)	3.394 (0.622)
H3K4me3 + 500bp	0.255	0.736 (0.104)	2.881 (0.406)
H3K9ac peaks	0.039	0.172 (0.095)	4.441 (2.449)
H3K9ac	0.126	0.502 (0.088)	3.978 (0.699)
H3K9ac + 500bp	0.231	0.751 (0.108)	3.259 (0.469)
Intron	0.387	0.475 (0.055)	1.225 (0.141)
Intron + 500bp	0.397	0.550 (0.037)	1.385 (0.094)
PromoterFlanking	0.008	0.050 (0.043)	5.945 (5.067)
PromoterFlanking + 500bp	0.033	0.112 (0.060)	3.356 (1.806)
Promoter	0.031	0.162 (0.052)	5.203 (1.657)
Promoter + 500bp	0.039	0.153 (0.045)	3.962 (1.160)
Repressed	0.461	0.081 (0.102)	0.176 (0.222)
Repressed + 500bp	0.719	0.400 (0.066)	0.556 (0.091)
Super Enhancer	0.168	0.395 (0.038)	2.346 (0.224)
Super Enhancer + 500bp	0.172	0.425 (0.035)	2.477 (0.203)
TFBS	0.132	0.435 (0.159)	3.284 (1.204)
TFBS + 500bp	0.343	0.545 (0.121)	1.586 (0.353)
Transcribed	0.345	0.512 (0.097)	1.483 (0.281)
Transcribed + 500bp	0.763	0.582 (0.097)	0.763 (0.128)
TSS	0.018	0.065 (0.051)	3.562 (2.801)
TSS + 500bp	0.035	0.290 (0.058)	8.341 (1.661)
3-prime UTR	0.011	0.003 (0.037)	0.253 (3.372)
3-prime UTR + 500bp	0.027	0.057 (0.031)	2.101 (1.152)
5-prime UTR	0.005	-0.012 (0.025)	-2.291 (4.617)
5-prime UTR + 500bp	0.028	0.046 (0.035)	1.652 (1.244)
Weak Enhancer	0.021	0.047 (0.069)	2.237 (3.266)
Weak Enhancer + 500bp	0.089	0.265 (0.093)	2.982 (1.042)

(S4.F) Proportion of heritability and enrichment for different functional categories for Triglycerides.

bioRxiv preprint doi: https://doi.org/10.1101/014241; this version posted January 23, 2015. The copyright holder for this preprint (which was not certified by peer review) is the author/funder, who has granted bioRxiv a license to display the preprint in perpetuity. It is made available under aCC-BY-ND 4.0 International license.

Annotation	Prop. SNPs	Prop. h^2	Enrichment
Coding	0.015	0.074 (0.057)	5.050 (3.886)
Coding + 500bp	0.065	0.261 (0.068)	4.043 (1.049)
Conserved	0.026	0.203 (0.096)	7.808 (3.677)
Conserved + 500bp	0.333	0.568 (0.144)	1.708 (0.433)
CTCF	0.024	-0.040 (0.105)	-1.659 (4.397)
CTCF + 500bp	0.071	-0.070 (0.122)	-0.980 (1.713)
DGF	0.138	0.743 (0.256)	5.402 (1.858)
DGF + 500bp	0.542	0.860 (0.143)	1.587 (0.265)
DHS peaks	0.112	0.361 (0.254)	3.229 (2.271)
DHS	0.168	0.514 (0.264)	3.063 (1.575)
DHS + 500bp	0.499	0.943 (0.164)	1.891 (0.330)
FANTOM5 Enhancer	0.004	-0.040 (0.053)	-9.331 (12.124)
FANTOM5 Enhancer + 500bp	0.019	0.045 (0.063)	2.359 (3.329)
Enhancer	0.063	0.394 (0.130)	6.217 (2.046)
Enhancer + 500bp	0.154	0.406 (0.120)	2.635 (0.777)
Fetal DHS	0.085	0.282 (0.200)	3.324 (2.364)
Fetal DHS + 500bp	0.285	0.746 (0.164)	2.618 (0.575)
H3K27ac[19]	0.391	0.727 (0.087)	1.859 (0.221)
H3K27ac[19] + 500bp	0.423	0.801 (0.084)	1.895 (0.198)
H3K27ac[18]	0.269	0.639 (0.141)	2.370 (0.523)
H3K27ac[18] + 500bp	0.336	0.837 (0.129)	2.490 (0.384)
H3K4me1 peaks	0.171	0.497 (0.197)	2.901 (1.148)
H3K4me1	0.427	0.783 (0.164)	1.835 (0.384)
H3K4me1 + 500bp	0.609	1.137 (0.086)	1.866 (0.141)
H3K4me3 peaks	0.042	0.266 (0.156)	6.363 (3.724)
H3K4me3	0.133	0.288 (0.126)	2.161 (0.949)
H3K4me3 + 500bp	0.255	0.890 (0.146)	3.482 (0.571)
H3K9ac peaks	0.039	0.381 (0.141)	9.820 (3.633)
H3K9ac	0.126	0.686 (0.139)	5.439 (1.105)
H3K9ac + 500bp	0.231	0.788 (0.123)	3.418 (0.535)
Intron	0.387	0.483 (0.065)	1.248 (0.167)
Intron + 500bp	0.397	0.525 (0.049)	1.323 (0.124)
PromoterFlanking	0.008	0.001 (0.057)	0.071 (6.744)
PromoterFlanking + 500bp	0.033	0.108 (0.071)	3.237 (2.115)
Promoter	0.031	0.104 (0.071)	3.344 (2.270)
Promoter + 500bp	0.039	0.068 (0.047)	1.765 (1.220)
Repressed	0.461	0.395 (0.168)	0.856 (0.365)
Repressed + 500bp	0.719	0.359 (0.074)	0.499 (0.103)
Super Enhancer	0.168	0.414 (0.053)	2.459 (0.317)
Super Enhancer + 500bp	0.172	0.415 (0.058)	2.418 (0.337)
TFBS	0.132	0.364 (0.211)	2.751 (1.595)
TFBS + 500bp	0.343	0.487 (0.156)	1.418 (0.454)
Transcribed	0.345	0.302 (0.142)	0.874 (0.410)
Transcribed + 500bp	0.763	0.677 (0.113)	0.887 (0.148)
TSS	0.018	0.185 (0.077)	10.152 (4.239)
TSS + 500bp	0.035	0.141 (0.080)	4.061 (2.291)
3-prime UTR	0.011	0.055 (0.045)	5.018 (4.040)
3-prime UTR + 500bp	0.027	0.151 (0.064)	5.624 (2.358)
5-prime UTR	0.005	-0.003 (0.037)	-0.542 (6.731)
5-prime UTR + 500bp	0.028	0.029 (0.054)	1.036 (1.958)
Weak Enhancer	0.021	0.128 (0.091)	6.055 (4.326)
Weak Enhancer + 500bp	0.089	0.285 (0.113)	3.200 (1.266)

(S4.G) Proportion of heritability and enrichment for different functional categories for Coronary artery disease.

bioRxiv preprint doi: https://doi.org/10.1101/014241; this version posted January 23, 2015. The copyright holder for this preprint (which was not certified by peer review) is the author/funder, who has granted bioRxiv a license to display the preprint in perpetuity. It is made available under aCC-BY-ND 4.0 International license.

Annotation	Prop. SNPs	Prop. h^2	Enrichment
Coding	0.015	0.026 (0.071)	1.784 (4.820)
Coding + 500bp	0.065	0.104 (0.089)	1.614 (1.378)
Conserved	0.026	0.347 (0.130)	13.300 (4.990)
Conserved + 500bp	0.333	0.688 (0.178)	2.068 (0.536)
CTCF	0.024	-0.080 (0.120)	-3.350 (5.048)
CTCF + 500bp	0.071	0.013 (0.112)	0.182 (1.580)
DGF	0.138	0.014 (0.330)	0.099 (2.402)
DGF + 500bp	0.542	1.011 (0.184)	1.867 (0.340)
DHS peaks	0.112	0.130 (0.303)	1.167 (2.710)
DHS	0.168	0.385 (0.329)	2.296 (1.963)
DHS + 500bp	0.499	1.009 (0.173)	2.022 (0.346)
FANTOM5 Enhancer	0.004	-0.004 (0.055)	-0.922 (12.664)
FANTOM5 Enhancer + 500bp	0.019	-0.050 (0.070)	-2.628 (3.653)
Enhancer	0.063	0.258 (0.147)	4.068 (2.315)
Enhancer + 500bp	0.154	0.503 (0.141)	3.270 (0.916)
Fetal DHS	0.085	0.208 (0.271)	2.458 (3.193)
Fetal DHS + 500bp	0.285	0.577 (0.180)	2.025 (0.631)
H3K27ac[19]	0.391	0.581 (0.110)	1.485 (0.280)
H3K27ac[19] + 500bp	0.423	0.748 (0.107)	1.771 (0.253)
H3K27ac[18]	0.269	0.699 (0.189)	2.593 (0.703)
H3K27ac[18] + 500bp	0.336	0.760 (0.135)	2.263 (0.403)
H3K4me1 peaks	0.171	0.586 (0.242)	3.419 (1.413)
H3K4me1	0.427	0.799 (0.232)	1.873 (0.544)
H3K4me1 + 500bp	0.609	1.006 (0.102)	1.652 (0.168)
H3K4me3 peaks	0.042	0.186 (0.152)	4.460 (3.639)
H3K4me3	0.133	0.517 (0.159)	3.879 (1.195)
H3K4me3 + 500bp	0.255	0.651 (0.142)	2.549 (0.557)
H3K9ac peaks	0.039	0.043 (0.174)	1.120 (4.494)
H3K9ac	0.126	0.632 (0.186)	5.012 (1.472)
H3K9ac + 500bp	0.231	0.746 (0.147)	3.237 (0.638)
Intron	0.387	0.526 (0.071)	1.357 (0.184)
Intron + 500bp	0.397	0.510 (0.056)	1.283 (0.140)
PromoterFlanking	0.008	0.064 (0.081)	7.616 (9.630)
PromoterFlanking + 500bp	0.033	0.122 (0.110)	3.631 (3.298)
Promoter	0.031	0.098 (0.086)	3.132 (2.762)
Promoter + 500bp	0.039	0.059 (0.053)	1.522 (1.381)
Repressed	0.461	0.122 (0.230)	0.264 (0.500)
Repressed + 500bp	0.719	0.380 (0.084)	0.528 (0.117)
Super Enhancer	0.168	0.307 (0.068)	1.824 (0.405)
Super Enhancer + 500bp	0.172	0.317 (0.062)	1.850 (0.364)
TFBS	0.132	0.242 (0.248)	1.827 (1.876)
TFBS + 500bp	0.343	0.628 (0.184)	1.829 (0.535)
Transcribed	0.345	0.695 (0.219)	2.013 (0.634)
Transcribed + 500bp	0.763	0.557 (0.124)	0.730 (0.162)
TSS	0.018	0.140 (0.087)	7.668 (4.788)
TSS + 500bp	0.035	0.044 (0.090)	1.276 (2.595)
3-prime UTR	0.011	-0.021 (0.048)	-1.927 (4.355)
3-prime UTR + 500bp	0.027	0.020 (0.057)	0.751 (2.105)
5-prime UTR	0.005	0.077 (0.116)	14.223 (21.390)
5-prime UTR + 500bp	0.028	0.097 (0.072)	3.480 (2.576)
Weak Enhancer	0.021	0.143 (0.140)	6.792 (6.655)
Weak Enhancer + 500bp	0.089	0.280 (0.127)	3.152 (1.423)

(S4.H) Proportion of heritability and enrichment for different functional categories for Type 2 Diabetes.

bioRxiv preprint doi: https://doi.org/10.1101/014241; this version posted January 23, 2015. The copyright holder for this preprint (which was not certified by peer review) is the author/funder, who has granted bioRxiv a license to display the preprint in perpetuity. It is made available under aCC-BY-ND 4.0 International license.

Annotation	Prop. SNPs	Prop. h^2	Enrichment
Coding	0.015	-0.014 (0.085)	-0.960 (5.787)
Coding + 500bp	0.065	0.206 (0.087)	3.184 (1.342)
Conserved	0.026	0.286 (0.120)	10.982 (4.588)
Conserved + 500bp	0.333	0.874 (0.153)	2.629 (0.460)
CTCF	0.024	-0.044 (0.117)	-1.842 (4.905)
CTCF + 500bp	0.071	-0.036 (0.132)	-0.501 (1.862)
DGF	0.138	0.394 (0.297)	2.861 (2.156)
DGF + 500bp	0.542	0.723 (0.173)	1.335 (0.319)
DHS peaks	0.112	0.170 (0.291)	1.523 (2.607)
DHS	0.168	0.711 (0.307)	4.238 (1.829)
DHS + 500bp	0.499	0.564 (0.204)	1.132 (0.410)
FANTOM5 Enhancer	0.004	-0.001 (0.057)	-0.176 (13.183)
FANTOM5 Enhancer + 500bp	0.019	0.057 (0.072)	2.975 (3.775)
Enhancer	0.063	0.358 (0.172)	5.658 (2.710)
Enhancer + 500bp	0.154	0.519 (0.139)	3.370 (0.900)
Fetal DHS	0.085	0.375 (0.215)	4.424 (2.537)
Fetal DHS + 500bp	0.285	0.763 (0.206)	2.677 (0.722)
H3K27ac[19]	0.391	0.679 (0.097)	1.737 (0.248)
H3K27ac[19] + 500bp	0.423	0.734 (0.096)	1.737 (0.227)
H3K27ac[18]	0.269	0.734 (0.175)	2.723 (0.649)
H3K27ac[18] + 500bp	0.336	0.952 (0.158)	2.833 (0.471)
H3K4me1 peaks	0.171	0.865 (0.281)	5.049 (1.641)
H3K4me1	0.427	0.743 (0.179)	1.742 (0.420)
H3K4me1 + 500bp	0.609	1.017 (0.117)	1.670 (0.193)
H3K4me3 peaks	0.042	-0.014 (0.157)	-0.323 (3.750)
H3K4me3	0.133	0.583 (0.154)	4.372 (1.156)
H3K4me3 + 500bp	0.255	0.638 (0.141)	2.496 (0.553)
H3K9ac peaks	0.039	0.297 (0.153)	7.658 (3.941)
H3K9ac	0.126	0.753 (0.173)	5.973 (1.370)
H3K9ac + 500bp	0.231	0.542 (0.151)	2.350 (0.654)
Intron	0.387	0.596 (0.086)	1.539 (0.223)
Intron + 500bp	0.397	0.593 (0.064)	1.492 (0.162)
PromoterFlanking	0.008	-0.075 (0.071)	-8.868 (8.458)
PromoterFlanking + 500bp	0.033	0.126 (0.084)	3.750 (2.512)
Promoter	0.031	0.087 (0.080)	2.795 (2.576)
Promoter + 500bp	0.039	0.163 (0.067)	4.214 (1.722)
Repressed	0.461	0.326 (0.195)	0.707 (0.423)
Repressed + 500bp	0.719	0.308 (0.096)	0.429 (0.133)
Super Enhancer	0.168	0.311 (0.064)	1.848 (0.381)
Super Enhancer + 500bp	0.172	0.436 (0.064)	2.541 (0.371)
TFBS	0.132	0.420 (0.230)	3.173 (1.733)
TFBS + 500bp	0.343	0.497 (0.179)	1.446 (0.523)
Transcribed	0.345	0.502 (0.186)	1.454 (0.539)
Transcribed + 500bp	0.763	0.511 (0.139)	0.670 (0.182)
TSS	0.018	-0.066 (0.085)	-3.643 (4.645)
TSS + 500bp	0.035	0.113 (0.093)	3.243 (2.678)
3-prime UTR	0.011	-0.019 (0.053)	-1.722 (4.823)
3-prime UTR + 500bp	0.027	-0.010 (0.063)	-0.367 (2.325)
5-prime UTR	0.005	0.041 (0.084)	7.573 (15.417)
5-prime UTR + 500bp	0.028	0.120 (0.066)	4.312 (2.389)
Weak Enhancer	0.021	0.210 (0.117)	9.946 (5.568)
Weak Enhancer + 500bp	0.089	0.313 (0.131)	3.523 (1.472)

(S4.I) Proportion of heritability and enrichment for different functional categories for Fasting Glucose.

bioRxiv preprint doi: https://doi.org/10.1101/014241; this version posted January 23, 2015. The copyright holder for this preprint (which was not certified by peer review) is the author/funder, who has granted bioRxiv a license to display the preprint in perpetuity. It is made available under aCC-BY-ND 4.0 International license.

Annotation	Prop. SNPs	Prop. h^2	Enrichment
Coding	0.015	0.085 (0.022)	5.823 (1.489)
Coding + 500bp	0.065	0.127 (0.026)	1.970 (0.398)
Conserved	0.026	0.287 (0.044)	11.028 (1.677)
Conserved + 500bp	0.333	0.658 (0.047)	1.979 (0.141)
CTCF	0.024	-0.041 (0.032)	-1.716 (1.344)
CTCF + 500bp	0.071	0.079 (0.033)	1.118 (0.460)
DGF	0.138	0.168 (0.083)	1.222 (0.604)
DGF + 500bp	0.542	0.667 (0.057)	1.232 (0.106)
DHS peaks	0.112	0.066 (0.070)	0.587 (0.625)
DHS	0.168	0.175 (0.083)	1.045 (0.493)
DHS + 500bp	0.499	0.687 (0.058)	1.377 (0.115)
FANTOM5 Enhancer	0.004	-0.024 (0.015)	-5.438 (3.564)
FANTOM5 Enhancer + 500bp	0.019	-0.001 (0.020)	-0.068 (1.033)
Enhancer	0.063	0.029 (0.043)	0.465 (0.675)
Enhancer + 500bp	0.154	0.238 (0.040)	1.544 (0.263)
Fetal DHS	0.085	0.216 (0.070)	2.547 (0.825)
Fetal DHS + 500bp	0.285	0.486 (0.060)	1.705 (0.211)
H3K27ac[19]	0.391	0.503 (0.027)	1.287 (0.070)
H3K27ac[19] + 500bp	0.423	0.552 (0.036)	1.306 (0.085)
H3K27ac[18]	0.269	0.372 (0.045)	1.381 (0.168)
H3K27ac[18] + 500bp	0.336	0.544 (0.042)	1.618 (0.125)
H3K4me1 peaks	0.171	0.412 (0.072)	2.407 (0.420)
H3K4me1	0.427	0.646 (0.053)	1.514 (0.124)
H3K4me1 + 500bp	0.609	0.794 (0.034)	1.304 (0.056)
H3K4me3 peaks	0.042	0.188 (0.048)	4.511 (1.144)
H3K4me3	0.133	0.292 (0.046)	2.192 (0.342)
H3K4me3 + 500bp	0.255	0.353 (0.040)	1.383 (0.156)
H3K9ac peaks	0.039	0.239 (0.042)	6.163 (1.085)
H3K9ac	0.126	0.287 (0.051)	2.278 (0.404)
H3K9ac + 500bp	0.231	0.457 (0.037)	1.981 (0.161)
Intron	0.387	0.513 (0.024)	1.323 (0.063)
Intron + 500bp	0.397	0.524 (0.019)	1.321 (0.047)
PromoterFlanking	0.008	0.029 (0.021)	3.397 (2.545)
PromoterFlanking + 500bp	0.033	0.070 (0.025)	2.099 (0.754)
Promoter	0.031	0.068 (0.028)	2.192 (0.887)
Promoter + 500bp	0.039	0.037 (0.021)	0.952 (0.531)
Repressed	0.461	0.450 (0.070)	0.975 (0.152)
Repressed + 500bp	0.719	0.627 (0.027)	0.873 (0.038)
Super Enhancer	0.168	0.247 (0.022)	1.467 (0.130)
Super Enhancer + 500bp	0.172	0.253 (0.019)	1.475 (0.113)
TFBS	0.132	0.217 (0.059)	1.639 (0.447)
TFBS + 500bp	0.343	0.372 (0.059)	1.083 (0.171)
Transcribed	0.345	0.391 (0.062)	1.133 (0.180)
Transcribed + 500bp	0.763	0.812 (0.035)	1.064 (0.046)
TSS	0.018	0.053 (0.027)	2.918 (1.467)
TSS + 500bp	0.035	0.107 (0.023)	3.081 (0.662)
3-prime UTR	0.011	0.062 (0.019)	5.583 (1.693)
3-prime UTR + 500bp	0.027	0.085 (0.020)	3.140 (0.758)
5-prime UTR	0.005	0.020 (0.012)	3.656 (2.215)
5-prime UTR + 500bp	0.028	0.055 (0.020)	1.975 (0.710)
Weak Enhancer	0.021	0.016 (0.032)	0.759 (1.537)
Weak Enhancer + 500bp	0.089	0.146 (0.040)	1.643 (0.447)

(S4.J) Proportion of heritability and enrichment for different functional categories for Schizophrenia. For many annotations there is heritability in the 500bp flanking regions, as cautioned by Gusev et al.[13] We believe, as hypothesized by Gusev et al., that this flanking heritability inflates the estimates of DHS heritability in Gusev et al. However, our work confirms the main message of Gusev et al. that much of the heritability of many traits, including schizophrenia, is located in regulatory regions.

bioRxiv preprint doi: https://doi.org/10.1101/014241; this version posted January 23, 2015. The copyright holder for this preprint (which was not certified by peer review) is the author/funder, who has granted bioRxiv a license to display the preprint in perpetuity. It is made available under aCC-BY-ND 4.0 International license.

Annotation	Prop. SNPs	Prop. h^2	Enrichment
Coding	0.015	0.186 (0.090)	12.671 (6.108)
Coding + 500bp	0.065	0.200 (0.086)	3.098 (1.336)
Conserved	0.026	0.302 (0.115)	11.588 (4.413)
Conserved + 500bp	0.333	0.527 (0.115)	1.586 (0.345)
CTCF	0.024	0.013 (0.111)	0.556 (4.672)
CTCF + 500bp	0.071	0.138 (0.104)	1.944 (1.466)
DGF	0.138	0.723 (0.241)	5.251 (1.754)
DGF + 500bp	0.542	0.854 (0.169)	1.578 (0.313)
DHS peaks	0.112	0.447 (0.211)	4.001 (1.890)
DHS	0.168	0.670 (0.251)	3.993 (1.495)
DHS + 500bp	0.499	0.735 (0.170)	1.474 (0.340)
FANTOM5 Enhancer	0.004	0.013 (0.046)	2.987 (10.718)
FANTOM5 Enhancer + 500bp	0.019	-0.106 (0.053)	-5.564 (2.793)
Enhancer	0.063	0.317 (0.130)	4.999 (2.059)
Enhancer + 500bp	0.154	0.299 (0.123)	1.940 (0.797)
Fetal DHS	0.085	0.264 (0.186)	3.120 (2.199)
Fetal DHS + 500bp	0.285	0.555 (0.169)	1.947 (0.595)
H3K27ac[19]	0.391	0.456 (0.089)	1.166 (0.226)
H3K27ac[19] + 500bp	0.423	0.564 (0.085)	1.335 (0.202)
H3K27ac[18]	0.269	0.574 (0.136)	2.132 (0.505)
H3K27ac[18] + 500bp	0.336	0.727 (0.116)	2.162 (0.346)
H3K4me1 peaks	0.171	0.719 (0.215)	4.196 (1.256)
H3K4me1	0.427	0.970 (0.166)	2.274 (0.389)
H3K4me1 + 500bp	0.609	0.754 (0.099)	1.238 (0.162)
H3K4me3 peaks	0.042	0.038 (0.124)	0.905 (2.967)
H3K4me3	0.133	0.573 (0.147)	4.295 (1.101)
H3K4me3 + 500bp	0.255	0.220 (0.121)	0.861 (0.473)
H3K9ac peaks	0.039	0.160 (0.125)	4.124 (3.225)
H3K9ac	0.126	0.450 (0.153)	3.572 (1.214)
H3K9ac + 500bp	0.231	0.502 (0.117)	2.176 (0.508)
Intron	0.387	0.509 (0.092)	1.313 (0.237)
Intron + 500bp	0.397	0.608 (0.066)	1.531 (0.166)
PromoterFlanking	0.008	0.051 (0.063)	6.090 (7.507)
PromoterFlanking + 500bp	0.033	0.081 (0.085)	2.429 (2.541)
Promoter	0.031	0.140 (0.085)	4.500 (2.711)
Promoter + 500bp	0.039	0.128 (0.065)	3.317 (1.671)
Repressed	0.461	0.402 (0.184)	0.871 (0.400)
Repressed + 500bp	0.719	0.460 (0.068)	0.640 (0.094)
Super Enhancer	0.168	0.288 (0.047)	1.712 (0.278)
Super Enhancer + 500bp	0.172	0.252 (0.043)	1.469 (0.250)
TFBS	0.132	0.459 (0.218)	3.462 (1.645)
TFBS + 500bp	0.343	0.507 (0.153)	1.477 (0.444)
Transcribed	0.345	0.311 (0.179)	0.900 (0.518)
Transcribed + 500bp	0.763	0.773 (0.107)	1.013 (0.140)
TSS	0.018	0.081 (0.070)	4.435 (3.863)
TSS + 500bp	0.035	0.244 (0.074)	7.016 (2.135)
3-prime UTR	0.011	0.094 (0.062)	8.508 (5.598)
3-prime UTR + 500bp	0.027	0.072 (0.052)	2.664 (1.921)
5-prime UTR	0.005	0.122 (0.052)	22.400 (9.543)
5-prime UTR + 500bp	0.028	0.129 (0.052)	4.656 (1.873)
Weak Enhancer	0.021	0.168 (0.103)	7.988 (4.864)
Weak Enhancer + 500bp	0.089	0.217 (0.098)	2.435 (1.107)

(S4.K) Proportion of heritability and enrichment for different functional categories for Bipolar disorder.

bioRxiv preprint doi: https://doi.org/10.1101/014241; this version posted January 23, 2015. The copyright holder for this preprint (which was not certified by peer review) is the author/funder, who has granted bioRxiv a license to display the preprint in perpetuity. It is made available under aCC-BY-ND 4.0 International license.

Annotation	Prop. SNPs	Prop. h^2	Enrichment
Coding	0.015	0.017 (0.068)	1.145 (4.645)
Coding + 500bp	0.065	0.140 (0.059)	2.169 (0.915)
Conserved	0.026	0.186 (0.110)	7.128 (4.214)
Conserved + 500bp	0.333	0.635 (0.124)	1.910 (0.373)
CTCF	0.024	0.019 (0.098)	0.802 (4.130)
CTCF + 500bp	0.071	0.012 (0.107)	0.162 (1.499)
DGF	0.138	0.257 (0.240)	1.865 (1.743)
DGF + 500bp	0.542	0.573 (0.144)	1.058 (0.266)
DHS peaks	0.112	0.041 (0.212)	0.367 (1.894)
DHS	0.168	-0.021 (0.272)	-0.126 (1.623)
DHS + 500bp	0.499	0.780 (0.173)	1.564 (0.346)
FANTOM5 Enhancer	0.004	-0.118 (0.044)	-27.161 (10.087)
FANTOM5 Enhancer + 500bp	0.019	0.037 (0.050)	1.915 (2.600)
Enhancer	0.063	0.117 (0.117)	1.852 (1.845)
Enhancer + 500bp	0.154	0.237 (0.112)	1.537 (0.731)
Fetal DHS	0.085	0.222 (0.199)	2.618 (2.343)
Fetal DHS + 500bp	0.285	0.458 (0.169)	1.606 (0.595)
H3K27ac[19]	0.391	0.528 (0.077)	1.350 (0.197)
H3K27ac[19] + 500bp	0.423	0.435 (0.089)	1.030 (0.211)
H3K27ac[18]	0.269	0.362 (0.136)	1.343 (0.503)
H3K27ac[18] + 500bp	0.336	0.467 (0.116)	1.391 (0.344)
H3K4me1 peaks	0.171	0.481 (0.215)	2.806 (1.253)
H3K4me1	0.427	0.867 (0.153)	2.033 (0.358)
H3K4me1 + 500bp	0.609	0.798 (0.107)	1.309 (0.175)
H3K4me3 peaks	0.042	0.101 (0.116)	2.424 (2.770)
H3K4me3	0.133	0.205 (0.124)	1.538 (0.929)
H3K4me3 + 500bp	0.255	0.277 (0.121)	1.086 (0.472)
H3K9ac peaks	0.039	-0.025 (0.138)	-0.656 (3.572)
H3K9ac	0.126	0.244 (0.129)	1.935 (1.019)
H3K9ac + 500bp	0.231	0.178 (0.122)	0.771 (0.528)
Intron	0.387	0.417 (0.066)	1.076 (0.170)
Intron + 500bp	0.397	0.429 (0.054)	1.081 (0.137)
PromoterFlanking	0.008	0.041 (0.060)	4.904 (7.124)
PromoterFlanking + 500bp	0.033	0.114 (0.077)	3.412 (2.313)
Promoter	0.031	0.022 (0.069)	0.692 (2.223)
Promoter + 500bp	0.039	-0.027 (0.043)	-0.694 (1.116)
Repressed	0.461	0.402 (0.179)	0.871 (0.389)
Repressed + 500bp	0.719	0.724 (0.063)	1.006 (0.088)
Super Enhancer	0.168	0.171 (0.048)	1.017 (0.284)
Super Enhancer + 500bp	0.172	0.238 (0.045)	1.387 (0.263)
TFBS	0.132	0.309 (0.177)	2.330 (1.340)
TFBS + 500bp	0.343	0.386 (0.159)	1.125 (0.462)
Transcribed	0.345	0.397 (0.158)	1.150 (0.456)
Transcribed + 500bp	0.763	0.685 (0.113)	0.897 (0.147)
TSS	0.018	0.078 (0.074)	4.287 (4.044)
TSS + 500bp	0.035	0.081 (0.062)	2.336 (1.767)
3-prime UTR	0.011	0.005 (0.040)	0.477 (3.639)
3-prime UTR + 500bp	0.027	0.052 (0.047)	1.935 (1.737)
5-prime UTR	0.005	0.001 (0.039)	0.261 (7.157)
5-prime UTR + 500bp	0.028	0.029 (0.053)	1.041 (1.900)
Weak Enhancer	0.021	0.126 (0.085)	5.969 (4.039)
Weak Enhancer + 500bp	0.089	0.139 (0.094)	1.564 (1.058)

(S4.L) Proportion of heritability and enrichment for different functional categories for Anorexia.

bioRxiv preprint doi: https://doi.org/10.1101/014241; this version posted January 23, 2015. The copyright holder for this preprint (which was not certified by peer review) is the author/funder, who has granted bioRxiv a license to display the preprint in perpetuity. It is made available under aCC-BY-ND 4.0 International license.

Annotation	Prop. SNPs	Prop. h^2	Enrichment
Coding	0.015	0.103 (0.045)	7.009 (3.040)
Coding + 500bp	0.065	0.154 (0.053)	2.383 (0.821)
Conserved	0.026	0.398 (0.074)	15.273 (2.853)
Conserved + 500bp	0.333	0.785 (0.092)	2.362 (0.277)
CTCF	0.024	-0.040 (0.062)	-1.658 (2.610)
CTCF + 500bp	0.071	0.063 (0.076)	0.888 (1.071)
DGF	0.138	0.065 (0.163)	0.474 (1.183)
DGF + 500bp	0.542	0.644 (0.111)	1.189 (0.205)
DHS peaks	0.112	0.346 (0.155)	3.093 (1.391)
DHS	0.168	0.333 (0.184)	1.985 (1.099)
DHS + 500bp	0.499	0.995 (0.133)	1.994 (0.266)
FANTOM5 Enhancer	0.004	0.002 (0.030)	0.406 (7.007)
FANTOM5 Enhancer + 500bp	0.019	0.074 (0.042)	3.860 (2.194)
Enhancer	0.063	0.307 (0.085)	4.851 (1.342)
Enhancer + 500bp	0.154	0.390 (0.087)	2.537 (0.568)
Fetal DHS	0.085	0.355 (0.146)	4.190 (1.728)
Fetal DHS + 500bp	0.285	0.870 (0.128)	3.052 (0.450)
H3K27ac[19]	0.391	0.530 (0.060)	1.354 (0.154)
H3K27ac[19] + 500bp	0.423	0.468 (0.077)	1.107 (0.182)
H3K27ac[18]	0.269	0.312 (0.099)	1.157 (0.369)
H3K27ac[18] + 500bp	0.336	0.480 (0.083)	1.429 (0.248)
H3K4me1 peaks	0.171	0.602 (0.140)	3.511 (0.818)
H3K4me1	0.427	0.678 (0.145)	1.589 (0.341)
H3K4me1 + 500bp	0.609	0.781 (0.076)	1.282 (0.125)
H3K4me3 peaks	0.042	0.147 (0.095)	3.510 (2.275)
H3K4me3	0.133	0.358 (0.093)	2.685 (0.699)
H3K4me3 + 500bp	0.255	0.401 (0.087)	1.569 (0.340)
H3K9ac peaks	0.039	0.299 (0.084)	7.717 (2.178)
H3K9ac	0.126	0.442 (0.088)	3.509 (0.697)
H3K9ac + 500bp	0.231	0.500 (0.076)	2.170 (0.329)
Intron	0.387	0.471 (0.047)	1.215 (0.121)
Intron + 500bp	0.397	0.464 (0.038)	1.169 (0.095)
PromoterFlanking	0.008	0.001 (0.045)	0.073 (5.314)
PromoterFlanking + 500bp	0.033	0.055 (0.050)	1.636 (1.493)
Promoter	0.031	0.030 (0.047)	0.973 (1.521)
Promoter + 500bp	0.039	0.041 (0.036)	1.070 (0.922)
Repressed	0.461	0.511 (0.139)	1.107 (0.302)
Repressed + 500bp	0.719	0.498 (0.050)	0.693 (0.070)
Super Enhancer	0.168	0.188 (0.035)	1.113 (0.206)
Super Enhancer + 500bp	0.172	0.216 (0.033)	1.259 (0.190)
TFBS	0.132	0.453 (0.135)	3.420 (1.020)
TFBS + 500bp	0.343	0.457 (0.129)	1.330 (0.376)
Transcribed	0.345	0.205 (0.110)	0.594 (0.320)
Transcribed + 500bp	0.763	0.731 (0.077)	0.958 (0.101)
TSS	0.018	0.052 (0.049)	2.840 (2.673)
TSS + 500bp	0.035	0.159 (0.050)	4.558 (1.428)
3-prime UTR	0.011	0.038 (0.028)	3.478 (2.503)
3-prime UTR + 500bp	0.027	0.068 (0.033)	2.543 (1.240)
5-prime UTR	0.005	0.056 (0.033)	10.371 (6.120)
5-prime UTR + 500bp	0.028	0.132 (0.040)	4.754 (1.436)
Weak Enhancer	0.021	0.138 (0.069)	6.540 (3.277)
Weak Enhancer + 500bp	0.089	0.276 (0.072)	3.105 (0.804)

(S4.M) Proportion of heritability and enrichment for different functional categories for Years of education.

bioRxiv preprint doi: https://doi.org/10.1101/014241; this version posted January 23, 2015. The copyright holder for this preprint (which was not certified by peer review) is the author/funder, who has granted bioRxiv a license to display the preprint in perpetuity. It is made available under aCC-BY-ND 4.0 International license.

Annotation	Prop. SNPs	Prop. h^2	Enrichment
Coding	0.015	0.116 (0.077)	7.929 (5.258)
Coding + 500bp	0.065	0.114 (0.077)	1.759 (1.188)
Conserved	0.026	0.402 (0.125)	15.414 (4.811)
Conserved + 500bp	0.333	0.750 (0.134)	2.256 (0.403)
CTCF	0.024	0.095 (0.128)	3.973 (5.371)
CTCF + 500bp	0.071	0.215 (0.132)	3.029 (1.862)
DGF	0.138	0.419 (0.287)	3.048 (2.088)
DGF + 500bp	0.542	0.896 (0.208)	1.655 (0.384)
DHS peaks	0.112	0.352 (0.268)	3.153 (2.396)
DHS	0.168	0.433 (0.286)	2.581 (1.706)
DHS + 500bp	0.499	0.958 (0.206)	1.921 (0.413)
FANTOM5 Enhancer	0.004	0.006 (0.050)	1.319 (11.432)
FANTOM5 Enhancer + 500bp	0.019	-0.109 (0.072)	-5.736 (3.778)
Enhancer	0.063	0.326 (0.152)	5.141 (2.408)
Enhancer + 500bp	0.154	0.387 (0.166)	2.513 (1.078)
Fetal DHS	0.085	0.538 (0.241)	6.346 (2.845)
Fetal DHS + 500bp	0.285	0.808 (0.180)	2.834 (0.630)
H3K27ac[19]	0.391	0.494 (0.093)	1.263 (0.237)
H3K27ac[19] + 500bp	0.423	0.379 (0.131)	0.897 (0.309)
H3K27ac[18]	0.269	0.192 (0.178)	0.713 (0.661)
H3K27ac[18] + 500bp	0.336	0.549 (0.153)	1.634 (0.455)
H3K4me1 peaks	0.171	0.643 (0.257)	3.751 (1.501)
H3K4me1	0.427	0.946 (0.224)	2.218 (0.525)
H3K4me1 + 500bp	0.609	0.750 (0.136)	1.231 (0.223)
H3K4me3 peaks	0.042	0.176 (0.180)	4.210 (4.313)
H3K4me3	0.133	0.275 (0.154)	2.066 (1.154)
H3K4me3 + 500bp	0.255	0.259 (0.148)	1.016 (0.581)
H3K9ac peaks	0.039	0.233 (0.153)	6.009 (3.951)
H3K9ac	0.126	0.252 (0.151)	2.002 (1.194)
H3K9ac + 500bp	0.231	0.162 (0.147)	0.702 (0.635)
Intron	0.387	0.372 (0.081)	0.960 (0.210)
Intron + 500bp	0.397	0.443 (0.068)	1.115 (0.171)
PromoterFlanking	0.008	-0.017 (0.061)	-1.974 (7.269)
PromoterFlanking + 500bp	0.033	-0.001 (0.094)	-0.032 (2.795)
Promoter	0.031	-0.010 (0.070)	-0.334 (2.245)
Promoter + 500bp	0.039	-0.019 (0.055)	-0.483 (1.420)
Repressed	0.461	0.192 (0.218)	0.417 (0.473)
Repressed + 500bp	0.719	0.504 (0.094)	0.701 (0.131)
Super Enhancer	0.168	0.135 (0.061)	0.800 (0.365)
Super Enhancer + 500bp	0.172	0.071 (0.062)	0.414 (0.359)
TFBS	0.132	0.743 (0.245)	5.613 (1.849)
TFBS + 500bp	0.343	0.385 (0.217)	1.121 (0.630)
Transcribed	0.345	0.276 (0.197)	0.798 (0.570)
Transcribed + 500bp	0.763	0.739 (0.113)	0.969 (0.148)
TSS	0.018	0.065 (0.087)	3.591 (4.777)
TSS + 500bp	0.035	0.046 (0.081)	1.309 (2.315)
3-prime UTR	0.011	0.009 (0.053)	0.839 (4.758)
3-prime UTR + 500bp	0.027	-0.005 (0.054)	-0.171 (2.012)
5-prime UTR	0.005	-0.009 (0.046)	-1.695 (8.473)
5-prime UTR + 500bp	0.028	0.029 (0.059)	1.048 (2.126)
Weak Enhancer	0.021	0.136 (0.116)	6.438 (5.507)
Weak Enhancer + 500bp	0.089	0.212 (0.129)	2.387 (1.450)

(S4.N) Proportion of heritability and enrichment for different functional categories for Ever smoked.

bioRxiv preprint doi: https://doi.org/10.1101/014241; this version posted January 23, 2015. The copyright holder for this preprint (which was not certified by peer review) is the author/funder, who has granted bioRxiv a license to display the preprint in perpetuity. It is made available under aCC-BY-ND 4.0 International license.

Annotation	Prop. SNPs	Prop. h^2	Enrichment
Coding	0.015	0.174 (0.090)	11.891 (6.155)
Coding + 500bp	0.065	0.365 (0.081)	5.659 (1.262)
Conserved	0.026	0.109 (0.115)	4.195 (4.402)
Conserved + 500bp	0.333	0.771 (0.122)	2.319 (0.368)
CTCF	0.024	-0.006 (0.113)	-0.261 (4.762)
CTCF + 500bp	0.071	-0.152 (0.114)	-2.140 (1.610)
DGF	0.138	0.871 (0.251)	6.331 (1.826)
DGF + 500bp	0.542	1.065 (0.147)	1.966 (0.271)
DHS peaks	0.112	0.357 (0.255)	3.195 (2.283)
DHS	0.168	0.523 (0.272)	3.121 (1.619)
DHS + 500bp	0.499	0.858 (0.145)	1.719 (0.290)
FANTOM5 Enhancer	0.004	0.158 (0.071)	36.410 (16.488)
FANTOM5 Enhancer + 500bp	0.019	0.283 (0.084)	14.848 (4.407)
Enhancer	0.063	0.379 (0.154)	5.984 (2.437)
Enhancer + 500bp	0.154	0.668 (0.120)	4.342 (0.778)
Fetal DHS	0.085	0.567 (0.199)	6.690 (2.345)
Fetal DHS + 500bp	0.285	0.537 (0.157)	1.882 (0.551)
H3K27ac[19]	0.391	0.980 (0.086)	2.506 (0.219)
H3K27ac[19] + 500bp	0.423	0.957 (0.083)	2.263 (0.195)
H3K27ac[18]	0.269	0.951 (0.161)	3.530 (0.597)
H3K27ac[18] + 500bp	0.336	0.792 (0.112)	2.358 (0.333)
H3K4me1 peaks	0.171	0.502 (0.201)	2.931 (1.173)
H3K4me1	0.427	0.884 (0.191)	2.072 (0.448)
H3K4me1 + 500bp	0.609	1.041 (0.085)	1.709 (0.140)
H3K4me3 peaks	0.042	0.313 (0.144)	7.501 (3.435)
H3K4me3	0.133	0.750 (0.149)	5.628 (1.119)
H3K4me3 + 500bp	0.255	0.610 (0.124)	2.387 (0.484)
H3K9ac peaks	0.039	0.146 (0.139)	3.770 (3.580)
H3K9ac	0.126	0.335 (0.149)	2.655 (1.178)
H3K9ac + 500bp	0.231	0.434 (0.130)	1.883 (0.562)
Intron	0.387	0.416 (0.071)	1.073 (0.184)
Intron + 500bp	0.397	0.513 (0.052)	1.291 (0.132)
PromoterFlanking	0.008	0.017 (0.073)	2.049 (8.639)
PromoterFlanking + 500bp	0.033	0.228 (0.095)	6.818 (2.846)
Promoter	0.031	0.251 (0.079)	8.046 (2.526)
Promoter + 500bp	0.039	0.169 (0.056)	4.364 (1.442)
Repressed	0.461	0.179 (0.145)	0.388 (0.315)
Repressed + 500bp	0.719	0.260 (0.078)	0.362 (0.109)
Super Enhancer	0.168	0.563 (0.061)	3.341 (0.362)
Super Enhancer + 500bp	0.172	0.615 (0.059)	3.582 (0.346)
TFBS	0.132	0.791 (0.221)	5.970 (1.666)
TFBS + 500bp	0.343	0.552 (0.182)	1.607 (0.531)
Transcribed	0.345	0.302 (0.144)	0.875 (0.418)
Transcribed + 500bp	0.763	0.596 (0.104)	0.781 (0.136)
TSS	0.018	0.341 (0.091)	18.703 (4.996)
TSS + 500bp	0.035	0.372 (0.080)	10.679 (2.290)
3-prime UTR	0.011	0.073 (0.047)	6.588 (4.219)
3-prime UTR + 500bp	0.027	0.107 (0.055)	3.958 (2.056)
5-prime UTR	0.005	0.019 (0.044)	3.562 (8.104)
5-prime UTR + 500bp	0.028	0.150 (0.063)	5.381 (2.248)
Weak Enhancer	0.021	0.230 (0.116)	10.914 (5.510)
Weak Enhancer + 500bp	0.089	0.424 (0.108)	4.762 (1.214)

(S4.O) Proportion of heritability and enrichment for different functional categories for Rheumatoid arthritis.

bioRxiv preprint doi: https://doi.org/10.1101/014241; this version posted January 23, 2015. The copyright holder for this preprint (which was not certified by peer review) is the author/funder, who has granted bioRxiv a license to display the preprint in perpetuity. It is made available under aCC-BY-ND 4.0 International license.

Annotation	Prop. SNPs	Prop. h^2	Enrichment
Coding	0.015	0.125 (0.071)	8.551 (4.851)
Coding + 500bp	0.065	0.352 (0.065)	5.453 (1.007)
Conserved	0.026	0.069 (0.072)	2.640 (2.766)
Conserved + 500bp	0.333	0.919 (0.098)	2.765 (0.296)
CTCF	0.024	-0.050 (0.087)	-2.081 (3.645)
CTCF + 500bp	0.071	-0.127 (0.083)	-1.781 (1.174)
DGF	0.138	0.770 (0.182)	5.600 (1.324)
DGF + 500bp	0.542	1.088 (0.090)	2.009 (0.166)
DHS peaks	0.112	0.303 (0.136)	2.713 (1.220)
DHS	0.168	0.154 (0.177)	0.915 (1.057)
DHS + 500bp	0.499	0.713 (0.126)	1.430 (0.253)
FANTOM5 Enhancer	0.004	0.169 (0.042)	39.042 (9.623)
FANTOM5 Enhancer + 500bp	0.019	0.428 (0.073)	22.468 (3.853)
Enhancer	0.063	0.237 (0.096)	3.740 (1.519)
Enhancer + 500bp	0.154	0.554 (0.106)	3.600 (0.691)
Fetal DHS	0.085	0.398 (0.133)	4.693 (1.570)
Fetal DHS + 500bp	0.285	0.686 (0.131)	2.406 (0.461)
H3K27ac[19]	0.391	0.838 (0.049)	2.143 (0.126)
H3K27ac[19] + 500bp	0.423	0.840 (0.060)	1.987 (0.141)
H3K27ac[18]	0.269	0.768 (0.121)	2.849 (0.450)
H3K27ac[18] + 500bp	0.336	0.748 (0.074)	2.227 (0.221)
H3K4me1 peaks	0.171	0.506 (0.169)	2.953 (0.987)
H3K4me1	0.427	0.742 (0.132)	1.739 (0.310)
H3K4me1 + 500bp	0.609	1.004 (0.068)	1.648 (0.111)
H3K4me3 peaks	0.042	0.318 (0.157)	7.621 (3.765)
H3K4me3	0.133	0.675 (0.147)	5.064 (1.100)
H3K4me3 + 500bp	0.255	0.669 (0.126)	2.618 (0.492)
H3K9ac peaks	0.039	0.082 (0.113)	2.109 (2.926)
H3K9ac	0.126	0.231 (0.122)	1.834 (0.964)
H3K9ac + 500bp	0.231	0.565 (0.101)	2.450 (0.438)
Intron	0.387	0.400 (0.068)	1.032 (0.176)
Intron + 500bp	0.397	0.504 (0.054)	1.268 (0.135)
PromoterFlanking	0.008	-0.054 (0.045)	-6.361 (5.315)
PromoterFlanking + 500bp	0.033	0.018 (0.066)	0.535 (1.959)
Promoter	0.031	0.146 (0.065)	4.685 (2.075)
Promoter + 500bp	0.039	0.137 (0.047)	3.553 (1.223)
Repressed	0.461	0.102 (0.114)	0.222 (0.248)
Repressed + 500bp	0.719	0.392 (0.052)	0.545 (0.072)
Super Enhancer	0.168	0.554 (0.050)	3.289 (0.297)
Super Enhancer + 500bp	0.172	0.594 (0.046)	3.462 (0.270)
TFBS	0.132	0.614 (0.195)	4.635 (1.474)
TFBS + 500bp	0.343	0.730 (0.133)	2.126 (0.386)
Transcribed	0.345	0.402 (0.124)	1.163 (0.359)
Transcribed + 500bp	0.763	0.747 (0.081)	0.978 (0.106)
TSS	0.018	0.248 (0.073)	13.613 (4.019)
TSS + 500bp	0.035	0.398 (0.070)	11.424 (2.013)
3-prime UTR	0.011	0.021 (0.035)	1.909 (3.148)
3-prime UTR + 500bp	0.027	0.171 (0.076)	6.347 (2.827)
5-prime UTR	0.005	0.040 (0.045)	7.436 (8.298)
5-prime UTR + 500bp	0.028	0.151 (0.047)	5.413 (1.703)
Weak Enhancer	0.021	0.101 (0.069)	4.797 (3.258)
Weak Enhancer + 500bp	0.089	0.258 (0.084)	2.903 (0.940)

(S4.P) Proportion of heritability and enrichment for different functional categories for Crohn's disease.

bioRxiv preprint doi: https://doi.org/10.1101/014241; this version posted January 23, 2015. The copyright holder for this preprint (which was not certified by peer review) is the author/funder, who has granted bioRxiv a license to display the preprint in perpetuity. It is made available under aCC-BY-ND 4.0 International license.

Annotation	Prop. SNPs	Prop. h^2	Enrichment
Coding	0.015	0.172 (0.088)	11.727 (6.022)
Coding + 500bp	0.065	0.421 (0.079)	6.529 (1.218)
Conserved	0.026	0.203 (0.091)	7.786 (3.478)
Conserved + 500bp	0.333	0.878 (0.123)	2.639 (0.369)
CTCF	0.024	-0.101 (0.106)	-4.218 (4.430)
CTCF + 500bp	0.071	-0.077 (0.111)	-1.087 (1.559)
DGF	0.138	0.901 (0.247)	6.546 (1.795)
DGF + 500bp	0.542	1.117 (0.134)	2.063 (0.248)
DHS peaks	0.112	0.706 (0.218)	6.319 (1.950)
DHS	0.168	0.416 (0.236)	2.481 (1.409)
DHS + 500bp	0.499	0.815 (0.165)	1.635 (0.330)
FANTOM5 Enhancer	0.004	0.181 (0.049)	41.783 (11.190)
FANTOM5 Enhancer + 500bp	0.019	0.285 (0.076)	14.939 (3.999)
Enhancer	0.063	0.348 (0.135)	5.490 (2.133)
Enhancer + 500bp	0.154	0.699 (0.138)	4.544 (0.897)
Fetal DHS	0.085	0.360 (0.186)	4.243 (2.200)
Fetal DHS + 500bp	0.285	0.550 (0.170)	1.929 (0.596)
H3K27ac[19]	0.391	0.989 (0.084)	2.527 (0.214)
H3K27ac[19] + 500bp	0.423	1.031 (0.088)	2.440 (0.209)
H3K27ac[18]	0.269	0.848 (0.163)	3.148 (0.603)
H3K27ac[18] + 500bp	0.336	0.813 (0.132)	2.420 (0.394)
H3K4me1 peaks	0.171	0.710 (0.243)	4.142 (1.418)
H3K4me1	0.427	0.774 (0.173)	1.814 (0.406)
H3K4me1 + 500bp	0.609	0.911 (0.078)	1.495 (0.128)
H3K4me3 peaks	0.042	0.264 (0.174)	6.318 (4.161)
H3K4me3	0.133	0.709 (0.179)	5.321 (1.345)
H3K4me3 + 500bp	0.255	0.707 (0.137)	2.767 (0.536)
H3K9ac peaks	0.039	0.276 (0.144)	7.125 (3.713)
H3K9ac	0.126	0.584 (0.172)	4.634 (1.367)
H3K9ac + 500bp	0.231	0.692 (0.122)	3.002 (0.531)
Intron	0.387	0.364 (0.082)	0.941 (0.210)
Intron + 500bp	0.397	0.506 (0.055)	1.275 (0.138)
PromoterFlanking	0.008	0.030 (0.055)	3.586 (6.532)
PromoterFlanking + 500bp	0.033	0.049 (0.080)	1.464 (2.381)
Promoter	0.031	0.150 (0.072)	4.799 (2.296)
Promoter + 500bp	0.039	0.185 (0.054)	4.797 (1.392)
Repressed	0.461	0.065 (0.160)	0.140 (0.347)
Repressed + 500bp	0.719	0.275 (0.072)	0.383 (0.100)
Super Enhancer	0.168	0.567 (0.062)	3.365 (0.367)
Super Enhancer + 500bp	0.172	0.616 (0.057)	3.593 (0.331)
TFBS	0.132	1.144 (0.283)	8.637 (2.134)
TFBS + 500bp	0.343	0.660 (0.173)	1.921 (0.503)
Transcribed	0.345	0.446 (0.162)	1.291 (0.470)
Transcribed + 500bp	0.763	0.677 (0.107)	0.888 (0.140)
TSS	0.018	0.209 (0.065)	11.447 (3.569)
TSS + 500bp	0.035	0.307 (0.076)	8.827 (2.188)
3-prime UTR	0.011	0.034 (0.053)	3.111 (4.792)
3-prime UTR + 500bp	0.027	0.176 (0.065)	6.524 (2.425)
5-prime UTR	0.005	0.097 (0.043)	17.831 (7.949)
5-prime UTR + 500bp	0.028	0.204 (0.073)	7.325 (2.612)
Weak Enhancer	0.021	0.057 (0.099)	2.723 (4.693)
Weak Enhancer + 500bp	0.089	0.328 (0.106)	3.690 (1.190)

(S4.Q) Proportion of heritability and enrichment for different functional categories for Ulcerative colitis.

bioRxiv preprint doi: https://doi.org/10.1101/014241; this version posted January 23, 2015. The copyright holder for this preprint (which was not certified by peer review) is the author/funder, who has granted bioRxiv a license to display the preprint in perpetuity. It is made available under aCC-BY-ND 4.0 International license.

Annotation	Prop. SNPs	Prop. h^2	Enrichment
Coding	0.015	0.108 (0.013)	7.357 (0.859)
Coding + 500bp	0.065	0.192 (0.030)	2.979 (0.469)
Conserved	0.026	0.359 (0.042)	13.762 (1.603)
Conserved + 500bp	0.333	0.656 (0.026)	1.972 (0.080)
CTCF	0.024	-0.014 (0.019)	-0.578 (0.807)
CTCF + 500bp	0.071	0.043 (0.020)	0.601 (0.278)
DGF	0.138	0.367 (0.097)	2.669 (0.702)
DGF + 500bp	0.542	0.747 (0.071)	1.380 (0.132)
DHS peaks	0.112	0.221 (0.065)	1.978 (0.584)
DHS	0.168	0.280 (0.071)	1.666 (0.420)
DHS + 500bp	0.499	0.756 (0.040)	1.516 (0.081)
FANTOM5 Enhancer	0.004	-0.004 (0.009)	-0.853 (2.162)
FANTOM5 Enhancer + 500bp	0.019	0.016 (0.018)	0.815 (0.921)
Enhancer	0.063	0.242 (0.051)	3.825 (0.811)
Enhancer + 500bp	0.154	0.349 (0.043)	2.266 (0.280)
Fetal DHS	0.085	0.236 (0.044)	2.787 (0.517)
Fetal DHS + 500bp	0.285	0.559 (0.059)	1.960 (0.207)
H3K27ac[19]	0.391	0.628 (0.055)	1.605 (0.141)
H3K27ac[19] + 500bp	0.423	0.664 (0.060)	1.571 (0.142)
H3K27ac[18]	0.269	0.485 (0.056)	1.798 (0.207)
H3K27ac[18] + 500bp	0.336	0.607 (0.042)	1.806 (0.124)
H3K4me1 peaks	0.171	0.464 (0.041)	2.711 (0.241)
H3K4me1	0.427	0.807 (0.066)	1.891 (0.156)
H3K4me1 + 500bp	0.609	0.899 (0.041)	1.476 (0.067)
H3K4me3 peaks	0.042	0.166 (0.026)	3.966 (0.616)
H3K4me3	0.133	0.345 (0.045)	2.587 (0.335)
H3K4me3 + 500bp	0.255	0.488 (0.058)	1.909 (0.227)
H3K9ac peaks	0.039	0.259 (0.025)	6.674 (0.635)
H3K9ac	0.126	0.409 (0.057)	3.240 (0.452)
H3K9ac + 500bp	0.231	0.502 (0.041)	2.178 (0.178)
Intron	0.387	0.467 (0.014)	1.206 (0.035)
Intron + 500bp	0.397	0.528 (0.015)	1.329 (0.037)
PromoterFlanking	0.008	0.010 (0.011)	1.137 (1.346)
PromoterFlanking + 500bp	0.033	0.083 (0.018)	2.488 (0.543)
Promoter	0.031	0.091 (0.016)	2.923 (0.521)
Promoter + 500bp	0.039	0.079 (0.017)	2.045 (0.441)
Repressed	0.461	0.268 (0.065)	0.581 (0.141)
Repressed + 500bp	0.719	0.443 (0.049)	0.616 (0.068)
Super Enhancer	0.168	0.303 (0.036)	1.797 (0.214)
Super Enhancer + 500bp	0.172	0.316 (0.038)	1.843 (0.221)
TFBS	0.132	0.440 (0.065)	3.321 (0.492)
TFBS + 500bp	0.343	0.481 (0.054)	1.399 (0.156)
Transcribed	0.345	0.430 (0.039)	1.244 (0.112)
Transcribed + 500bp	0.763	0.726 (0.028)	0.951 (0.037)
TSS	0.018	0.105 (0.024)	5.768 (1.303)
TSS + 500bp	0.035	0.171 (0.029)	4.907 (0.839)
3-prime UTR	0.011	0.053 (0.010)	4.781 (0.872)
3-prime UTR + 500bp	0.027	0.075 (0.011)	2.792 (0.422)
5-prime UTR	0.005	0.029 (0.008)	5.309 (1.402)
5-prime UTR + 500bp	0.028	0.067 (0.011)	2.395 (0.384)
Weak Enhancer	0.021	0.070 (0.024)	3.326 (1.141)
Weak Enhancer + 500bp	0.089	0.190 (0.031)	2.138 (0.343)

Table S5: Proportion of heritability and enrichment for different functional categories, meta-analyzed over nine traits, including derived allele frequency bins in the model (Methods).

bioRxiv preprint doi: https://doi.org/10.1101/014241; this version posted January 23, 2015. The copyright holder for this preprint (which was not certified by peer review) is the author/funder, who has granted bioRxiv a license to display the preprint in perpetuity. It is made available under aCC-BY-ND 4.0 International license.

Cell type	Cell-type group	Mark
Fetal adrenal	H3K4me1	Adrenal/Pancreas
Fetal adrenal	H3K4me3	Adrenal/Pancreas
Pancreas	H3K4me1	Adrenal/Pancreas
Pancreas	H3K4me3	Adrenal/Pancreas
Pancreatic islets	H3K27ac	Adrenal/Pancreas
Pancreatic islets	H3K4me1	Adrenal/Pancreas
Pancreatic islets	H3K4me1	Adrenal/Pancreas
Pancreatic islets	H3K4me3	Adrenal/Pancreas
Pancreatic islets	H3K4me3	Adrenal/Pancreas
Pancreatic islets	H3K9ac	Adrenal/Pancreas
Angular gyrus	H3K27ac	CNS
Angular gyrus	H3K4me1	CNS
Angular gyrus	H3K4me3	CNS
Angular gyrus	H3K9ac	CNS
Anterior caudate	H3K27ac	CNS
Anterior caudate	H3K4me1	CNS
Anterior caudate	H3K4me3	CNS
Anterior caudate	H3K9ac	CNS
Cingulate gyrus	H3K27ac	CNS
Cingulate gyrus	H3K4me1	CNS
Cingulate gyrus	H3K4me3	CNS
Cingulate gyrus	H3K9ac	CNS
Fetal brain	H3K4me1	CNS
Fetal brain	H3K4me3	CNS
Fetal brain	H3K4me3	CNS
Fetal brain	H3K9ac	CNS
Germinal matrix	H3K4me3	CNS
Hippocampus middle	H3K27ac	CNS
Hippocampus middle	H3K4me1	CNS
Hippocampus middle	H3K4me3	CNS
Hippocampus middle	H3K9ac	CNS
Inferior temporal lobe	H3K27ac	CNS
Inferior temporal lobe	H3K4me1	CNS
Inferior temporal lobe	H3K4me3	CNS
Inferior temporal lobe	H3K9ac	CNS
Mid frontal lobe	H3K27ac	CNS
Mid frontal lobe	H3K4me1	CNS
Mid frontal lobe	H3K4me3	CNS
Mid frontal lobe	H3K9ac	CNS

bioRxiv preprint doi: https://doi.org/10.1101/014241; this version posted January 23, 2015. The copyright holder for this preprint (which was not certified by peer review) is the author/funder, who has granted bioRxiv a license to display the preprint in perpetuity. It is made available under aCC-BY-ND 4.0 International license.

Neurosphere	H3K27ac	CNS
Substantia nigra	H3K27ac	CNS
Substantia nigra	H3K4me1	CNS
Substantia nigra	H3K4me3	CNS
Substantia nigra	H3K9ac	CNS
Aorta	H3K4me3	Cardiovascular
Fetal heart	H3K4me1	Cardiovascular
Fetal heart	H3K4me3	Cardiovascular
Fetal heart	H3K9ac	Cardiovascular
Fetal lung	H3K4me1	Cardiovascular
Fetal lung	H3K4me3	Cardiovascular
Fetal lung	H3K9ac	Cardiovascular
Left Ventricle	H3K4me1	Cardiovascular
Left Ventricle	H3K4me3	Cardiovascular
Lung	H3K4me1	Cardiovascular
Lung	H3K4me3	Cardiovascular
Right atrium	H3K4me1	Cardiovascular
Right atrium	H3K4me3	Cardiovascular
Right ventricle	H3K4me1	Cardiovascular
Right ventricle	H3K4me3	Cardiovascular
Breast fibroblast primary	H3K4me1	Connective/Bone
Breast fibroblast primary	H3K4me3	Connective/Bone
Chondrogenic dif	H3K27ac	Connective/Bone
Osteoblast	H3K27ac	Connective/Bone
Penis foreskin fibroblast primary	H3K4me1	Connective/Bone
Penis foreskin fibroblast primary	H3K4me3	Connective/Bone
Colon smooth muscle	H3K27ac	Gastrointestinal
Colon smooth muscle	H3K4me1	Gastrointestinal
Colon smooth muscle	H3K4me3	Gastrointestinal
Colon smooth muscle	H3K9ac	Gastrointestinal
Colonic mucosa	H3K27ac	Gastrointestinal
Colonic mucosa	H3K4me1	Gastrointestinal
Colonic mucosa	H3K4me3	Gastrointestinal
Colonic mucosa	H3K9ac	Gastrointestinal
Duodenum Mucosa	H3K4me1	Gastrointestinal
Duodenum Mucosa	H3K4me3	Gastrointestinal
Duodenum Mucosa	H3K9ac	Gastrointestinal
Duodenum mucosa	H3K27ac	Gastrointestinal
Duodenum smooth muscle	H3K27ac	Gastrointestinal
Duodenum smooth muscle	H3K4me1	Gastrointestinal

bioRxiv preprint doi: https://doi.org/10.1101/014241; this version posted January 23, 2015. The copyright holder for this preprint (which was not certified by peer review) is the author/funder, who has granted bioRxiv a license to display the preprint in perpetuity. It is made available under aCC-BY-ND 4.0 International license.

Duodenum smooth muscle	H3K4me3	Gastrointestinal
Esophagus	H3K4me1	Gastrointestinal
Esophagus	H3K4me3	Gastrointestinal
Fetal large intestine	H3K4me1	Gastrointestinal
Fetal large intestine	H3K4me3	Gastrointestinal
Fetal small intestine	H3K4me1	Gastrointestinal
Fetal small intestine	H3K4me3	Gastrointestinal
Fetal stomach	H3K4me1	Gastrointestinal
Fetal stomach	H3K4me3	Gastrointestinal
Gastric	H3K4me1	Gastrointestinal
Gastric	H3K4me3	Gastrointestinal
Rectal mucosa	H3K27ac	Gastrointestinal
Rectal mucosa	H3K4me1	Gastrointestinal
Rectal mucosa	H3K4me3	Gastrointestinal
Rectal mucosa	H3K9ac	Gastrointestinal
Rectal smooth muscle	H3K27ac	Gastrointestinal
Rectal smooth muscle	H3K4me1	Gastrointestinal
Rectal smooth muscle	H3K4me3	Gastrointestinal
Rectal smooth muscle	H3K9ac	Gastrointestinal
Sigmoid colon	H3K4me1	Gastrointestinal
Sigmoid colon	H3K4me3	Gastrointestinal
Small intestine	H3K4me1	Gastrointestinal
Small intestine	H3K4me3	Gastrointestinal
Stomach mucosa	H3K4me1	Gastrointestinal
Stomach mucosa	H3K4me3	Gastrointestinal
Stomach mucosa	H3K9ac	Gastrointestinal
Stomach smooth muscle	H3K27ac	Gastrointestinal
Stomach smooth muscle	H3K4me1	Gastrointestinal
Stomach smooth muscle	H3K4me3	Gastrointestinal
Stomach smooth muscle	H3K9ac	Gastrointestinal
CD14	H3K27ac	Immune
CD14 primary	H3K4me1	Immune
CD14 primary	H3K4me3	Immune
CD15 primary	H3K4me1	Immune
CD15 primary	H3K4me3	Immune
CD19	H3K27ac	Immune
CD19 primary (BI)	H3K4me1	Immune
CD19 primary (BI)	H3K4me3	Immune
CD19 primary (UW)	H3K4me1	Immune
CD19 primary (UW)	H3K4me3	Immune

bioRxiv preprint doi: https://doi.org/10.1101/014241; this version posted January 23, 2015. The copyright holder for this preprint (which was not certified by peer review) is the author/funder, who has granted bioRxiv a license to display the preprint in perpetuity. It is made available under aCC-BY-ND 4.0 International license.

CD20	H3K27ac	Immune
CD25+ CD127- Treg	H3K27ac	Immune
CD25- CD45RA+ naive	H3K27ac	Immune
CD25- IL17+ Th17 stim	H3K27ac	Immune
CD25- IL17- Th stim MACS	H3K27ac	Immune
CD25int CD127+ Tmem	H3K27ac	Immune
CD3 primary	H3K27ac	Immune
CD3 primary (BI)	H3K4me1	Immune
CD3 primary (BI)	H3K4me3	Immune
CD3 primary (UW)	H3K4me1	Immune
CD3 primary (UW)	H3K4me3	Immune
CD34 primary	H3K4me1	Immune
CD34 primary	H3K4me3	Immune
CD4 memory primary	H3K4me1	Immune
CD4 memory primary	H3K4me3	Immune
CD4 naive primary	H3K4me1	Immune
CD4 naive primary	H3K4me3	Immune
CD4 primary	H3K4me3	Immune
CD4+ CD25+ CD127- Treg primary	H3K4me1	Immune
CD4+ CD25+ CD127- Treg primary	H3K4me3	Immune
CD4+ CD25- CD45R0+ memory primary	H3K4me1	Immune
CD4+ CD25- CD45R0+ memory primary	H3K4me3	Immune
CD4+ CD25- CD45RA+ naive primary	H3K4me1	Immune
CD4+ CD25- CD45RA+ naive primary	H3K4me3	Immune
CD4+ CD25- IL17+ PMA Ionomycin stim Th17 primary	H3K4me1	Immune
CD4+ CD25- IL17+ PMA Ionomycin stim Th17 primary	H3K4me3	Immune
CD4+ CD25- IL17- PMA Ionomycin stim MACS Th primary	H3K4me1	Immune
CD4+ CD25- IL17- PMA Ionomycin stim MACS Th primary	H3K4me3	Immune
CD4+ CD25- Th primary	H3K4me1	Immune
CD4+ CD25- Th primary	H3K4me3	Immune
CD4+ CD25int CD127+ Tmem primary	H3K4me1	Immune
CD4+ CD25int CD127+ Tmem primary	H3K4me3	Immune
CD56 primary	H3K4me1	Immune
CD56 primary	H3K4me3	Immune
CD8 memory primary	H3K4me1	Immune
CD8 memory primary	H3K4me3	Immune
CD8 naive primary (BI)	H3K4me1	Immune
CD8 naive primary (BI)	H3K4me3	Immune
CD8 naive primary (UCSF-UBC)	H3K4me1	Immune
CD8 naive primary (UCSF-UBC)	H3K4me3	Immune

bioRxiv preprint doi: https://doi.org/10.1101/014241; this version posted January 23, 2015. The copyright holder for this preprint (which was not certified by peer review) is the author/funder, who has granted bioRxiv a license to display the preprint in perpetuity. It is made available under aCC-BY-ND 4.0 International license.

CD8 naive primary (UCSF-UBC)	H3K9ac	Immune
CD8 primary	H3K4me3	Immune
Fetal thymus	H3K4me1	Immune
Fetal thymus	H3K4me3	Immune
Mobilized CD34	H3K27ac	Immune
Mobilized CD34 primary	H3K4me1	Immune
Mobilized CD34 primary	H3K4me3	Immune
Peripheralblood mononuclear primary	H3K4me1	Immune
Peripheralblood mononuclear primary	H3K4me3	Immune
Peripheralblood mononuclear primary	H3K9ac	Immune
Spleen	H3K4me1	Immune
Spleen	H3K4me3	Immune
Th0	H3K27ac	Immune
Th1	H3K27ac	Immune
Th2	H3K27ac	Immune
Thymus	H3K4me1	Immune
Treg primary	H3K4me3	Immune
Fetal kidney	H3K9ac	Kidney
Kidney	H3K27ac	Kidney
Kidney	H3K4me1	Kidney
Kidney	H3K4me3	Kidney
Kidney	H3K9ac	Kidney
Liver	H3K27ac	Liver
Liver (BI)	H3K4me1	Liver
Liver (BI)	H3K4me3	Liver
Liver (BI)	H3K9ac	Liver
Liver (UCSD)	H3K4me1	Liver
Liver (UCSD)	H3K4me3	Liver
Adipose nuclei	H3K27ac	Other
Adipose nuclei	H3K4me1	Other
Adipose nuclei	H3K4me3	Other
Adipose nuclei	H3K9ac	Other
Breast luminal epithelial	H3K4me1	Other
Breast myoepithelial	H3K4me1	Other
Breast myoepithelial	H3K4me3	Other
Breast myoepithelial	H3K9ac	Other
Breast vHMEC	H3K4me1	Other
Breast vHMEC	H3K4me3	Other
Fetal placenta	H3K4me1	Other
Fetal placenta	H3K4me3	Other

bioRxiv preprint doi: https://doi.org/10.1101/014241; this version posted January 23, 2015. The copyright holder for this preprint (which was not certified by peer review) is the author/funder, who has granted bioRxiv a license to display the preprint in perpetuity. It is made available under aCC-BY-ND 4.0 International license.

Ovary	H3K4me1	Other
Ovary	H3K4me3	Other
Penis foreskin keratinocyte primary	H3K4me1	Other
Penis foreskin keratinocyte primary	H3K4me3	Other
Penis foreskin keratinocyte primary	H3K9ac	Other
Penis foreskin melanocyte primary	H3K4me1	Other
Penis foreskin melanocyte primary	H3K4me3	Other
Placenta amnion	H3K4me1	Other
Placenta amnion	H3K4me3	Other
Placenta chorion	H3K4me1	Other
Placenta chorion	H3K4me3	Other
Fetal leg muscle	H3K4me1	Skeletal muscle
Fetal leg muscle	H3K4me3	Skeletal muscle
Fetal trunk muscle	H3K4me1	Skeletal muscle
Fetal trunk muscle	H3K4me3	Skeletal muscle
Psoas muscle	H3K4me1	Skeletal muscle
Psoas muscle	H3K4me3	Skeletal muscle
Skeletal muscle	H3K27ac	Skeletal muscle
Skeletal muscle	H3K4me1	Skeletal muscle
Skeletal muscle	H3K4me3	Skeletal muscle
Skeletal muscle	H3K9ac	Skeletal muscle

Table S6: Cell types used in the cell-type-specific analysis. When the same cell type in the same histone mark from more than one institution was used, the institution is given in parentheses.

bioRxiv preprint doi: https://doi.org/10.1101/014241; this version posted January 23, 2015. The copyright holder for this preprint (which was not certified by peer review) is the author/funder, who has granted bioRxiv a license to display the preprint in perpetuity. It is made available under aCC-BY-ND 4.0 International license.

Cell type	Cell type group	Mark	$-log_{10}(p)$
Chondrogenic dif**	Connective/Bone	H3K27ac	6.81
Penis foreskin fibroblast primary**	Connective/Bone	H3K4me1	6.43
Fetal lung**	Cardiovascular	H3K4me1	6.34
Fetal stomach**	GI	H3K4me1	5.48
Colon smooth muscle*	GI	H3K4me1	4.64
Aorta*	Cardiovascular	H3K4me3	4.64
Fetal lung*	Cardiovascular	H3K9ac	4.31
Stomach smooth muscle*	GI	H3K4me3	4.26
Osteoblast*	Connective/Bone	H3K27ac	4.04
Penis foreskin fibroblast primary*	Connective/Bone	H3K4me3	3.96
Stomach smooth muscle*	GI	H3K4me1	3.94
Fetal leg muscle*	Skeletal Muscle	H3K4me3	3.91
Fetal trunk muscle*	Skeletal Muscle	H3K4me3	3.72
Rectal smooth muscle*	GI	H3K4me3	3.57
Fetal lung*	Cardiovascular	H3K4me3	3.37
Rectal smooth muscle*	GI	H3K4me1	3.32
Fetal placenta*	Other	H3K4me3	3.26
Adipose nuclei*	Other	H3K4me1	3.1
Ovary*	Other	H3K4me1	3.06
Fetal large intestine*	GI	H3K4me3	3.05
Placenta chorion*	Other	H3K4me3	2.98
CD34 primary*	Immune	H3K4me1	2.96
Penis foreskin melanocyte primary*	Other	H3K4me1	2.95
Skeletal muscle*	Skeletal Muscle	H3K9ac	2.93
Mobilized CD34 primary*	Immune	H3K4me1	2.88
Fetal stomach*	GI	H3K4me3	2.87
Mobilized CD34 primary*	Immune	H3K4me3	2.87
Fetal adrenal*	Adrenal/Pancreas	H3K4me3	2.86
Breast fibroblast primary*	Connective/Bone	H3K4me3	2.85
Duodenum smooth muscle*	GI	H3K4me1	2.81
Colon smooth muscle*	GI	H3K4me3	2.76
Ovary*	Other	H3K4me3	2.7
Fetal brain*	CNS	H3K4me3	2.62
Skeletal muscle*	Skeletal Muscle	H3K4me1	2.6
Fetal small intestine*	GI	H3K4me3	2.6
Colon smooth muscle*	GI	H3K27ac	2.57
Lung*	Cardiovascular	H3K4me3	2.56
Liver (UCSD)*	Liver	H3K4me3	2.53
Esophagus*	GI	H3K4me3	2.53
Placenta amnion*	Other	H3K4me3	2.48
Right ventricle*	Cardiovascular	H3K4me3	2.47
Sigmoid colon*	GI	H3K4me3	2.44
Fetal leg muscle*	Skeletal Muscle	H3K4me1	2.44
Colonic mucosa*	GI	H3K4me3	2.18
Right atrium*	Cardiovascular	H3K4me3	2.14
CD34 primary*	Immune	H3K4me3	2.13
Gastric*	GI	H3K4me3	2.08
Skeletal muscle*	Skeletal Muscle	H3K4me3	2.07
Lung*	Cardiovascular	H3K4me1	2.06
Pancreatic islets*	Adrenal/Pancreas	H3K4me3	2.05
Adipose nuclei*	Other	H3K9ac	2.01
Right atrium*	Cardiovascular	H3K4me1	1.98
Stomach smooth muscle*	GI	H3K27ac	1.96
Rectal smooth muscle*	GI	H3K27ac	1.95
Breast fibroblast primary*	Connective/Bone	H3K4me1	1.93
Germinal matrix*	CNS	H3K4me3	1.92
Small intestine*	GI	H3K4me3	1.91
Fetal placenta*	Other	H3K4me1	1.91

(S7.A) Enrichment of top cell types for Height. * = significant at FDR < 0.05. ** = significant at p < 0.05 after correcting for multiple hypotheses.

bioRxiv preprint doi: https://doi.org/10.1101/014241; this version posted January 23, 2015. The copyright holder for this preprint (which was not certified by peer review) is the author/funder, who has granted bioRxiv a license to display the preprint in perpetuity. It is made available under aCC-BY-ND 4.0 International license.

Cell type	Cell type group	Mark	$-log_{10}(p)$
Fetal brain*	CNS	H3K4me3	4.48
Penis foreskin fibroblast primary*	Connective/Bone	H3K4me3	4.43
Inferior temporal lobe*	CNS	H3K4me1	4.3
Mid frontal lobe*	CNS	H3K9ac	4.25
Anterior caudate*	CNS	H3K4me3	4.25
Mid frontal lobe*	CNS	H3K27ac	3.96
Anterior caudate*	CNS	H3K9ac	3.91
Cingulate gyrus*	CNS	H3K4me1	3.73
Inferior temporal lobe*	CNS	H3K4me3	3.73
Penis foreskin keratinocyte primary*	Other	H3K9ac	3.72
Mid frontal lobe*	CNS	H3K4me3	3.71
Hippocampus middle*	CNS	H3K4me1	3.66
Inferior temporal lobe*	CNS	H3K9ac	3.59
Fetal brain*	CNS	H3K9ac	3.57
Hippocampus middle*	CNS	H3K9ac	3.47
Cingulate gyrus*	CNS	H3K9ac	3.46
Hippocampus middle*	CNS	H3K4me3	3.4
Germinal matrix*	CNS	H3K4me3	3.4
Cingulate gyrus*	CNS	H3K4me3	3.4
Anterior caudate*	CNS	H3K4me1	3.31
Substantia nigra*	CNS	H3K4me3	3.24
Angular gyrus*	CNS	H3K27ac	3.05
Penis foreskin melanocyte primary*	Other	H3K4me3	2.83
Angular gyrus*	CNS	H3K4me3	2.76
Substantia nigra*	CNS	H3K4me1	2.75
Pancreatic islets*	Adrenal/Pancreas	H3K4me3	2.6
Cingulate gyrus*	CNS	H3K27ac	2.57
Fetal adrenal*	Adrenal/Pancreas	H3K4me3	2.57
Angular gyrus*	CNS	H3K9ac	2.51
Inferior temporal lobe*	CNS	H3K27ac	2.39
Breast myoepithelial*	Other	H3K4me3	2.35
Substantia nigra*	CNS	H3K9ac	2.26
Substantia nigra*	CNS	H3K27ac	2.22
Hippocampus middle*	CNS	H3K27ac	2.07

(S7.B) Enrichment of top cell types for BMI. * = significant at FDR < 0.05. ** = significant at p < 0.05 after correcting for multiple hypotheses.

bioRxiv preprint doi: https://doi.org/10.1101/014241; this version posted January 23, 2015. The copyright holder for this preprint (which was not certified by peer review) is the author/funder, who has granted bioRxiv a license to display the preprint in perpetuity. It is made available under aCC-BY-ND 4.0 International license.

Cell type	Cell type group	Mark	$-log_{10}(p)$
Fetal brain**	CNS	H3K4me3	12.25
Pancreatic islets**	Adrenal/Pancreas	H3K4me3	11.73
Angular gyrus**	CNS	H3K4me3	11.22
Germinal matrix**	CNS	H3K4me3	11.18
Fetal adrenal**	Adrenal/Pancreas	H3K4me3	11.12
Mid frontal lobe**	CNS	H3K4me3	11.11
Inferior temporal lobe**	CNS	H3K4me3	10.22
Cingulate gyrus**	CNS	H3K4me3	9.94
Anterior caudate**	CNS	H3K4me3	8.91
Psoas muscle**	Skeletal Muscle	H3K4me3	8.66
Right ventricle**	Cardiovascular	H3K4me3	8.58
Pancreatic islets**	Adrenal/Pancreas	H3K9ac	7.74
Fetal leg muscle**	Skeletal Muscle	H3K4me3	7.71
Pancreas**	Adrenal/Pancreas	H3K4me3	7.26
Hippocampus middle**	CNS	H3K4me3	7.19
Breast myoepithelial**	Other	H3K4me3	6.93
Fetal trunk muscle**	Skeletal Muscle	H3K4me3	6.87
Peripheralblood mononuclear primary**	Immune	H3K4me3	6.66
Penis foreskin melanocyte primary**	Other	H3K4me3	6.53
Fetal stomach**	GI	H3K4me3	6.26
Gastric**	GI	H3K4me3	6.24
Right atrium**	Cardiovascular	H3K4me3	6.24
CD4+ CD25- CD45RA+ naive primary**	Immune	H3K4me3	6.16
CD4+ CD25int CD127+ Tmem primary**	Immune	H3K4me3	5.96
Ovary**	Other	H3K4me3	5.64
Penis foreskin fibroblast primary**	Connective/Bone	H3K4me3	5.57
Substantia nigra**	CNS	H3K4me3	5.41
Esophagus**	GI	H3K4me3	5.35
Colonic mucosa**	GI	H3K4me3	5.3
Fetal large intestine**	GI	H3K4me3	5.14
Fetal placenta**	Other	H3K4me3	5.07
Fetal brain**	CNS	H3K9ac	5.05
Aorta*	Cardiovascular	H3K4me3	4.74
CD8 naive primary (BI)*	Immune	H3K4me3	4.49
CD14 primary*	Immune	H3K4me3	4.49
Fetal small intestine*	GI	H3K4me3	4.43
Breast vHMEC*	Other	H3K4me3	4.39
CD4+ CD25- Th primary*	Immune	H3K4me3	4.38
CD34 primary*	Immune	H3K4me3	4.37
Placenta amnion*	Other	H3K4me3	4.34
Angular gyrus*	CNS	H3K9ac	4.33
Penis foreskin keratinocyte primary*	Other	H3K4me3	4.3
Pancreatic islets*	Adrenal/Pancreas	H3K4me3	4.26
Mid frontal lobe*	CNS	H3K9ac	4.23
CD4+ CD25- CD45R0+ memory primary*	Immune	H3K4me3	4.14
Rectal smooth muscle*	GI	H3K4me3	4.12
Left Ventricle*	Cardiovascular	H3K4me3	4.11
CD8 memory primary*	Immune	H3K4me3	4.06
CD4+ CD25+ CD127- Treg primary*	Immune	H3K4me3	4.05
Placenta chorion*	Other	H3K4me3	4.05
CD8 naive primary (UCSF-UBC)*	Immune	H3K4me3	3.77
Anterior caudate*	CNS	H3K9ac	3.73
Cingulate gyrus*	CNS	H3K9ac	3.69
CD19 primary (UW)*	Immune	H3K4me3	3.63
CD4+ CD25- IL17+ PMA Ionomycin stim Th17 primary*	Immune	H3K4me3	3.58
CD4 naive primary*	Immune	H3K4me3	3.53
Fetal brain*	CNS	H3K4me3	3.53
Lung*	Cardiovascular	H3K4me3	3.5
Mid frontal lobe*	CNS	H3K27ac	3.43
Breast fibroblast primary*	Connective/Bone	H3K4me3	3.41

(S7.C) Enrichment of top cell types for Age at menarche. * = significant at FDR < 0.05. ** = significant at p < 0.05 after correcting for multiple hypotheses.

bioRxiv preprint doi: https://doi.org/10.1101/014241; this version posted January 23, 2015. The copyright holder for this preprint (which was not certified by peer review) is the author/funder, who has granted bioRxiv a license to display the preprint in perpetuity. It is made available under aCC-BY-ND 4.0 International license.

Cell type	Cell type group	Mark	$-log_{10}(p)$
Liver (BI)*	Liver	H3K4me1	4.76
Fetal adrenal*	Adrenal/Pancreas	H3K4me1	3.41
CD14 primary*	Immune	H3K4me1	3.33
Liver*	Liver	H3K27ac	2.97
Adipose nuclei	Other	H3K9ac	2.71

(S7.D) Enrichment of top cell types for LDL. * = significant at FDR < 0.05. ** = significant at p < 0.05 after correcting for multiple hypotheses.

Cell type	Cell type group	Mark	$-log_{10}(p)$
Liver (BI)*	Liver	H3K4me1	4.51
Adipose nuclei*	Other	H3K4me1	4.26
Liver*	Liver	H3K27ac	3.61
Adipose nuclei*	Other	H3K9ac	3.34
Adipose nuclei*	Other	H3K4me3	3.08
CD14 primary*	Immune	H3K4me1	2.86
Adipose nuclei*	Other	H3K27ac	2.84
Liver (BI)*	Liver	H3K9ac	2.74
Liver (BI)*	Liver	H3K4me3	2.66

(S7.E) Enrichment of top cell types for HDL. * = significant at FDR < 0.05. ** = significant at p < 0.05 after correcting for multiple hypotheses.

Cell type	Cell type group	Mark	$-log_{10}(p)$
Liver (BI)*	Liver	H3K4me1	3.99
Liver*	Liver	H3K27ac	3.66
Liver (BI)*	Liver	H3K9ac	3.02
Duodenum Mucosa	GI	H3K4me3	2.71
Liver (UCSD)	Liver	H3K4me3	2.68

(S7.F) Enrichment of top cell types for Triglycerides. * = significant at FDR < 0.05. ** = significant at p < 0.05 after correcting for multiple hypotheses.

Cell type	Cell type group	Mark	$-log_{10}(p)$
Adipose nuclei*	Other	H3K4me1	4.21
Duodenum Mucosa*	GI	H3K4me1	3.43
Colonic mucosa*	GI	H3K9ac	3.01
Duodenum Mucosa	GI	H3K9ac	2.78
Rectal mucosa	GI	H3K9ac	2.68

(S7.G) Enrichment of top cell types for Coronary artery disease. * = significant at FDR < 0.05. ** = significant at p < 0.05 after correcting for multiple hypotheses.

Cell type	Cell type group	Mark	$-log_{10}(p)$
Pancreatic islets	Adrenal/Pancreas	H3K4me3	2.87
Pancreatic islets	Adrenal/Pancreas	H3K27ac	2.73
Fetal large intestine	GI	H3K4me1	2.49
Fetal small intestine	GI	H3K4me1	2.31
Adipose nuclei	Other	H3K9ac	2.27

(S7.H) Enrichment of top cell types for Type 2 Diabetes. * = significant at FDR < 0.05. ** = significant at p < 0.05 after correcting for multiple hypotheses.

Cell type	Cell type group	Mark	$-log_{10}(p)$
Pancreatic islets*	Adrenal/Pancreas	H3K27ac	3.93
Pancreatic islets*	Adrenal/Pancreas	H3K4me1	3.1
Pancreatic islets	Adrenal/Pancreas	H3K4me3	2.93
Pancreatic islets	Adrenal/Pancreas	H3K4me3	2.25
Fetal small intestine	GI	H3K4me1	2.18

(S7.I) Enrichment of top cell types for Fasting Glucose. * = significant at FDR < 0.05. ** = significant at p < 0.05 after correcting for multiple hypotheses.

bioRxiv preprint doi: https://doi.org/10.1101/014241; this version posted January 23, 2015. The copyright holder for this preprint (which was not certified by peer review) is the author/funder, who has granted bioRxiv a license to display the preprint in perpetuity. It is made available under aCC-BY-ND 4.0 International license.

Cell type	Cell type group	Mark	$-log_{10}(p)$
Fetal brain**	CNS	H3K4me3	18.51
Mid frontal lobe**	CNS	H3K4me3	14.44
Germinal matrix**	CNS	H3K4me3	12.68
Mid frontal lobe**	CNS	H3K9ac	11.27
Angular gyrus**	CNS	H3K4me3	10.89
Inferior temporal lobe**	CNS	H3K4me3	10.77
Cingulate gyrus**	CNS	H3K9ac	10.27
Fetal brain**	CNS	H3K9ac	10.24
Anterior caudate**	CNS	H3K4me3	9.66
Cingulate gyrus**	CNS	H3K4me3	9.34
Pancreatic islets**	Adrenal/Pancreas	H3K4me3	8.65
Anterior caudate**	CNS	H3K9ac	8.5
Angular gyrus**	CNS	H3K9ac	8.33
Mid frontal lobe**	CNS	H3K27ac	8.1
Anterior caudate**	CNS	H3K4me1	7.92
Inferior temporal lobe**	CNS	H3K4me1	7.43
Psoas muscle**	Skeletal Muscle	H3K4me3	7.38
Fetal brain**	CNS	H3K4me1	7.21
Inferior temporal lobe**	CNS	H3K9ac	7.03
Hippocampus middle**	CNS	H3K9ac	6.03
Pancreatic islets**	Adrenal/Pancreas	H3K9ac	5.79
Penis foreskin melanocyte primary**	Other	H3K4me3	5.68
Angular gyrus**	CNS	H3K27ac	5.63
Cingulate gyrus**	CNS	H3K4me1	5.55
Hippocampus middle**	CNS	H3K4me3	5.55
CD34 primary**	Immune	H3K4me3	5.33
Sigmoid colon**	GI	H3K4me3	5.3
Fetal adrenal**	Adrenal/Pancreas	H3K4me3	5.2
Inferior temporal lobe**	CNS	H3K27ac	5.08
Peripheralblood mononuclear primary**	Immune	H3K4me3	5.03
Gastric**	GI	H3K4me3	4.93
Substantia nigra*	CNS	H3K4me3	4.71
Fetal brain*	CNS	H3K4me3	4.58
Hippocampus middle*	CNS	H3K4me1	4.48
Ovary*	Other	H3K4me3	4.19
CD19 primary (UW)*	Immune	H3K4me3	4.15
Small intestine*	GI	H3K4me3	4.07
Lung*	Cardiovascular	H3K4me3	3.93
Fetal stomach*	GI	H3K4me3	3.89
Fetal leg muscle*	Skeletal Muscle	H3K4me3	3.82
Spleen*	Immune	H3K4me3	3.77
Breast fibroblast primary*	Connective/Bone	H3K4me3	3.69
Right ventricle*	Cardiovascular	H3K4me3	3.67
CD4+ CD25- Th primary*	Immune	H3K4me3	3.66
CD4+ CD25- IL17- PMA Ionomycin stim MACS Th primary*	Immune	H3K4me1	3.66
CD8 naive primary (UCSF-UBC)*	Immune	H3K4me3	3.65
Pancreas*	Adrenal/Pancreas	H3K4me3	3.63
CD4+ CD25- Th primary*	Immune	H3K4me1	3.56
CD4+ CD25- CD45RA+ naive primary*	Immune	H3K4me1	3.56
Colonic mucosa*	GI	H3K4me3	3.49
Right atrium*	Cardiovascular	H3K4me3	3.48
Fetal trunk muscle*	Skeletal Muscle	H3K4me3	3.47
CD4+ CD25int CD127+ Tmem primary*	Immune	H3K4me3	3.46
Substantia nigra*	CNS	H3K9ac	3.44
Placenta amnion*	Other	H3K4me3	3.38
Breast myoepithelial*	Other	H3K9ac	3.26
CD8 naive primary (BI)*	Immune	H3K4me1	3.24
Substantia nigra*	CNS	H3K4me1	3.18
Cingulate gyrus*	CNS	H3K27ac	3.1
CD4+ CD25- CD45RA+ naive primary*	Immune	H3K4me3	3.06

(S7.J) Enrichment of top cell types for Schizophrenia. * = significant at FDR < 0.05. ** = significant at p < 0.05 after correcting for multiple hypotheses.

bioRxiv preprint doi: https://doi.org/10.1101/014241; this version posted January 23, 2015. The copyright holder for this preprint (which was not certified by peer review) is the author/funder, who has granted bioRxiv a license to display the preprint in perpetuity. It is made available under aCC-BY-ND 4.0 International license.

Cell type	Cell type group	Mark	$-log_{10}(p)$
Mid frontal lobe*	CNS	H3K27ac	4.42
Penis foreskin keratinocyte primary	Other	H3K9ac	3.05
Fetal brain	CNS	H3K9ac	2.92
Fetal brain	CNS	H3K4me3	2.9
Mid frontal lobe	CNS	H3K4me3	2.78

(S7.K) Enrichment of top cell types for Bipolar disorder. * = significant at FDR < 0.05. ** = significant at p $<$ 0.05 after correcting for multiple hypotheses.

Cell type	Cell type group	Mark	$-log_{10}(p)$
Angular gyrus	CNS	H3K9ac	2.61
Mid frontal lobe	CNS	H3K9ac	2.38
Mid frontal lobe	CNS	H3K4me1	2.36
Anterior caudate	CNS	H3K9ac	2.28
Cingulate gyrus	CNS	H3K9ac	2.22

(S7.L) Enrichment of top cell types for Anorexia. * = significant at FDR < 0.05. ** = significant at p < 0.05 after correcting for multiple hypotheses.

bioRxiv preprint doi: https://doi.org/10.1101/014241; this version posted January 23, 2015. The copyright holder for this preprint (which was not certified by peer review) is the author/funder, who has granted bioRxiv a license to display the preprint in perpetuity. It is made available under aCC-BY-ND 4.0 International license.

Cell type	Cell type group	Mark	$-log_{10}(p)$
Angular gyrus**	CNS	H3K4me3	6.63
Fetal brain**	CNS	H3K4me3	6.05
Mid frontal lobe**	CNS	H3K4me3	5.99
Anterior caudate**	CNS	H3K4me3	5.73
Inferior temporal lobe**	CNS	H3K4me3	5.63
CD56 primary**	Immune	H3K4me3	5.32
Germinal matrix**	CNS	H3K4me3	5.29
Mid frontal lobe**	CNS	H3K9ac	5.26
Cingulate gyrus**	CNS	H3K9ac	4.98
Cingulate gyrus**	CNS	H3K4me3	4.94
CD8 naive primary (UCSF-UBC)*	Immune	H3K4me3	4.88
Penis foreskin melanocyte primary*	Other	H3K4me3	4.73
Mid frontal lobe*	CNS	H3K27ac	4.43
Peripheralblood mononuclear primary*	Immune	H3K4me3	4.39
CD34 primary*	Immune	H3K4me3	4.12
Fetal brain*	CNS	H3K9ac	4.03
CD14 primary*	Immune	H3K4me3	4.01
Inferior temporal lobe*	CNS	H3K9ac	3.98
Angular gyrus*	CNS	H3K9ac	3.96
Sigmoid colon*	GI	H3K4me3	3.83
Pancreatic islets*	Adrenal/Pancreas	H3K9ac	3.83
CD4+ CD25int CD127+ Tmem primary*	Immune	H3K4me3	3.72
Anterior caudate*	CNS	H3K9ac	3.65
Hippocampus middle*	CNS	H3K4me3	3.65
CD19 primary (UW)*	Immune	H3K4me3	3.63
Small intestine*	GI	H3K4me3	3.52
CD4+ CD25- Th primary*	Immune	H3K4me3	3.45
Lung*	Cardiovascular	H3K4me3	3.19
CD4+ CD25- CD45R0+ memory primary*	Immune	H3K4me3	3.19
Hippocampus middle*	CNS	H3K9ac	3.17
Liver (UCSD)*	Liver	H3K4me3	3.08
Fetal placenta*	Other	H3K4me3	3.08
Fetal adrenal*	Adrenal/Pancreas	H3K4me3	3.04
Right atrium*	Cardiovascular	H3K4me3	2.99
Pancreatic islets*	Adrenal/Pancreas	H3K4me3	2.96
CD8 naive primary (UCSF-UBC)*	Immune	H3K9ac	2.95
CD3 primary (BI)*	Immune	H3K4me3	2.94
Angular gyrus*	CNS	H3K27ac	2.93
CD4+ CD25- CD45RA+ naive primary*	Immune	H3K4me3	2.93
Gastric*	GI	H3K4me3	2.92
CD4 naive primary*	Immune	H3K4me3	2.89
CD8 memory primary*	Immune	H3K4me3	2.78
CD3 primary (UW)*	Immune	H3K4me3	2.76
Rectal smooth muscle*	GI	H3K4me3	2.73
Fetal brain*	CNS	H3K4me3	2.67
Esophagus*	GI	H3K4me3	2.66
CD8 naive primary (BI)*	Immune	H3K4me3	2.58
Left Ventricle*	Cardiovascular	H3K4me3	2.56
CD19 primary (BI)*	Immune	H3K4me3	2.56
Fetal thymus*	Immune	H3K4me3	2.52
Breast vHMEC*	Other	H3K4me3	2.51
CD8 primary*	Immune	H3K4me3	2.51
Psoas muscle*	Skeletal Muscle	H3K4me3	2.51
Peripheralblood mononuclear primary*	Immune	H3K9ac	2.5
Ovary*	Other	H3K4me3	2.47
Pancreas*	Adrenal/Pancreas	H3K4me3	2.46
Breast fibroblast primary*	Connective/Bone	H3K4me3	2.45
CD4+ CD25+ CD127- Treg primary*	Immune	H3K4me3	2.36
Placenta amnion*	Other	H3K4me3	2.34
Right ventricle*	Cardiovascular	H3K4me3	2.33

(S7.M) Enrichment of top cell types for Years of education. * = significant at FDR < 0.05. ** = significant at p $<$ 0.05 after correcting for multiple hypotheses.

bioRxiv preprint doi: https://doi.org/10.1101/014241; this version posted January 23, 2015. The copyright holder for this preprint (which was not certified by peer review) is the author/funder, who has granted bioRxiv a license to display the preprint in perpetuity. It is made available under aCC-BY-ND 4.0 International license.

Cell type	Cell type group	Mark	$-log_{10}(p)$
Inferior temporal lobe*	CNS	H3K4me3	3.21
Cingulate gyrus*	CNS	H3K27ac	3.2
Substantia nigra*	CNS	H3K27ac	3.16
Hippocampus middle*	CNS	H3K27ac	3.13
Breast myoepithelial*	Other	H3K9ac	3.06
Inferior temporal lobe*	CNS	H3K4me1	2.93
Anterior caudate*	CNS	H3K27ac	2.81
Inferior temporal lobe*	CNS	H3K27ac	2.81
Angular gyrus*	CNS	H3K27ac	2.77
Pancreatic islets*	Adrenal/Pancreas	H3K4me1	2.55

(S7.N) Enrichment of top cell types for Ever smoked. * = significant at FDR < 0.05. ** = significant at p < 0.05 after correcting for multiple hypotheses.

Cell type	Cell type group	Mark	$-log_{10}(p)$
CD4+ CD25- IL17+ PMA Ionomycin stim Th17 primary**	Immune	H3K4me1	6.76
CD4+ CD25- IL17- PMA Ionomycin stim MACS Th primary**	Immune	H3K4me1	6.11
CD4+ CD25- CD45R0+ memory primary**	Immune	H3K4me1	5.92
CD4 memory primary**	Immune	H3K4me1	5.88
CD4+ CD25+ CD127- Treg primary**	Immune	H3K4me1	5.83
CD25- IL17- Th stim MACS**	Immune	H3K27ac	5.7
Th2**	Immune	H3K27ac	5.5
CD8 memory primary**	Immune	H3K4me1	5.38
CD4 naive primary**	Immune	H3K4me1	5.26
CD4+ CD25- Th primary**	Immune	H3K4me1	5.25
CD19 primary (UW)**	Immune	H3K4me1	5.25
CD4+ CD25int CD127+ Tmem primary*	Immune	H3K4me1	4.88
CD4+ CD25- CD45RA+ naive primary*	Immune	H3K4me1	4.75
CD3 primary (BI)*	Immune	H3K4me1	4.64
CD3 primary (UW)*	Immune	H3K4me1	4.63
CD25- IL17+ Th17 stim*	Immune	H3K27ac	4.55
CD8 naive primary (UCSF-UBC)*	Immune	H3K4me1	4.49
CD8 naive primary (BI)*	Immune	H3K4me1	4.45
Th0*	Immune	H3K27ac	4.09
CD25+ CD127- Treg*	Immune	H3K27ac	4.09
Th1*	Immune	H3K27ac	3.96
CD19 primary (BI)*	Immune	H3K4me1	3.91
CD56 primary*	Immune	H3K4me1	3.77
Treg primary*	Immune	H3K4me3	3.63
CD3 primary*	Immune	H3K27ac	3.62
CD20*	Immune	H3K27ac	3.45
CD4+ CD25- IL17- PMA Ionomycin stim MACS Th primary*	Immune	H3K4me3	3.45
CD4+ CD25- IL17+ PMA Ionomycin stim Th17 primary*	Immune	H3K4me3	3.17
CD4+ CD25+ CD127- Treg primary*	Immune	H3K4me3	3.1
CD4+ CD25int CD127+ Tmem primary*	Immune	H3K4me3	2.76
Peripheralblood mononuclear primary*	Immune	H3K9ac	2.58
CD25int CD127+ Tmem*	Immune	H3K27ac	2.27
CD4+ CD25- CD45R0+ memory primary*	Immune	H3K4me3	2.24
CD4+ CD25- CD45RA+ naive primary*	Immune	H3K4me3	2.2
CD8 memory primary*	Immune	H3K4me3	2.17
CD19*	Immune	H3K27ac	2.13
CD4 memory primary*	Immune	H3K4me3	2.12
Peripheralblood mononuclear primary*	Immune	H3K4me1	2.12
CD4+ CD25- Th primary*	Immune	H3K4me3	1.98

(S7.O) Enrichment of top cell types for Rheumatoid arthritis. * = significant at FDR < 0.05. ** = significant at p < 0.05 after correcting for multiple hypotheses.

bioRxiv preprint doi: https://doi.org/10.1101/014241; this version posted January 23, 2015. The copyright holder for this preprint (which was not certified by peer review) is the author/funder, who has granted bioRxiv a license to display the preprint in perpetuity. It is made available under aCC-BY-ND 4.0 International license.

Cell type	Cell type group	Mark	$-log_{10}(p)$
CD4+ CD25- IL17+ PMA Ionomycin stim Th17 primary**	Immune	H3K4me1	7.59
Th1**	Immune	H3K27ac	6.54
CD25- IL17+ Th17 stim**	Immune	H3K27ac	6.5
CD4+ CD25- IL17- PMA Ionomycin stim MACS Th primary**	Immune	H3K4me1	6.24
CD4 memory primary**	Immune	H3K4me1	5.88
Th2**	Immune	H3K27ac	5.87
CD4+ CD25- Th primary**	Immune	H3K4me1	5.59
CD8 memory primary**	Immune	H3K4me1	5.13
CD14 primary**	Immune	H3K4me1	5.03
CD3 primary (UW)**	Immune	H3K4me1	4.96
Th0*	Immune	H3K27ac	4.8
CD56 primary*	Immune	H3K4me1	4.8
CD25- IL17- Th stim MACS*	Immune	H3K27ac	4.72
CD4+ CD25- CD45R0+ memory primary*	Immune	H3K4me1	4.7
CD4 naive primary*	Immune	H3K4me1	4.51
CD4+ CD25int CD127+ Tmem primary*	Immune	H3K4me1	4.44
CD4+ CD25- CD45RA+ naive primary*	Immune	H3K4me1	4.36
CD8 naive primary (BI)*	Immune	H3K4me1	4.31
CD19 primary (UW)*	Immune	H3K4me1	4.26
CD8 naive primary (UCSF-UBC)*	Immune	H3K4me1	4.2
CD4+ CD25- IL17+ PMA Ionomycin stim Th17 primary*	Immune	H3K4me3	4.18
CD19 primary (BI)*	Immune	H3K4me1	4.17
CD3 primary (BI)*	Immune	H3K4me1	3.73
CD4+ CD25+ CD127- Treg primary*	Immune	H3K4me1	3.62
CD3 primary*	Immune	H3K27ac	3.25
CD4+ CD25- IL17- PMA Ionomycin stim MACS Th primary*	Immune	H3K4me3	3.16
CD34 primary*	Immune	H3K4me1	2.87
Peripheralblood mononuclear primary*	Immune	H3K9ac	2.87
CD15 primary*	Immune	H3K4me1	2.85
Spleen*	Immune	H3K4me1	2.7
CD4 primary*	Immune	H3K4me3	2.49
Peripheralblood mononuclear primary*	Immune	H3K4me1	2.46
CD8 primary*	Immune	H3K4me3	2.44
CD14*	Immune	H3K27ac	2.18
CD4 memory primary*	Immune	H3K4me3	2.12
Colonic mucosa*	GI	H3K4me1	2.11
CD19 primary (BI)*	Immune	H3K4me3	2.1
CD4 naive primary*	Immune	H3K4me3	2.09
Mobilized CD34 primary*	Immune	H3K4me1	2.08
CD25int CD127+ Tmem*	Immune	H3K27ac	2.04

(S7.P) Enrichment of top cell types for Crohn's disease. * = significant at FDR < 0.05. ** = significant at p < 0.05 after correcting for multiple hypotheses.

bioRxiv preprint doi: https://doi.org/10.1101/014241; this version posted January 23, 2015. The copyright holder for this preprint (which was not certified by peer review) is the author/funder, who has granted bioRxiv a license to display the preprint in perpetuity. It is made available under aCC-BY-ND 4.0 International license.

Cell type	Cell type group	Mark	$-log_{10}(p)$
CD4+ CD25- IL17+ PMA Ionomycin stim Th17 primary**	Immune	H3K4me1	6.37
CD25- IL17+ Th17 stim**	Immune	H3K27ac	5.53
CD4+ CD25- CD45R0+ memory primary**	Immune	H3K4me1	5.48
CD4 memory primary**	Immune	H3K4me1	5.19
CD4+ CD25+ CD127- Treg primary*	Immune	H3K4me1	4.88
CD4+ CD25- IL17- PMA Ionomycin stim MACS Th primary*	Immune	H3K4me1	4.73
CD3 primary*	Immune	H3K27ac	4.72
Th2*	Immune	H3K27ac	4.5
CD25+ CD127- Treg*	Immune	H3K27ac	4.42
Colonic mucosa*	GI	H3K4me1	4.17
Spleen*	Immune	H3K4me1	4.06
CD4+ CD25- IL17+ PMA Ionomycin stim Th17 primary*	Immune	H3K4me3	4.04
CD4+ CD25- Th primary*	Immune	H3K4me1	4.03
Colonic mucosa*	GI	H3K27ac	4.0
Th1*	Immune	H3K27ac	3.96
CD4 naive primary*	Immune	H3K4me1	3.91
CD4+ CD25int CD127+ Tmem primary*	Immune	H3K4me1	3.87
CD8 memory primary*	Immune	H3K4me1	3.84
Rectal mucosa*	GI	H3K4me1	3.74
CD19 primary (UW)*	Immune	H3K4me1	3.72
Colonic mucosa*	GI	H3K9ac	3.63
Rectal mucosa*	GI	H3K9ac	3.57
CD25- IL17- Th stim MACS*	Immune	H3K27ac	3.54
CD25int CD127+ Tmem*	Immune	H3K27ac	3.45
Th0*	Immune	H3K27ac	3.44
CD8 naive primary (UCSF-UBC)*	Immune	H3K4me1	3.43
CD56 primary*	Immune	H3K4me1	3.21
Rectal mucosa*	GI	H3K27ac	3.16
CD19 primary (BI)*	Immune	H3K4me1	2.95
Treg primary*	Immune	H3K4me3	2.93
CD8 naive primary (BI)*	Immune	H3K4me1	2.91
CD3 primary (UW)*	Immune	H3K4me1	2.83
CD4+ CD25- CD45RA+ naive primary*	Immune	H3K4me1	2.7
CD3 primary (BI)*	Immune	H3K4me1	2.44
Rectal mucosa*	GI	H3K4me3	2.29
CD4+ CD25- IL17- PMA Ionomycin stim MACS Th primary*	Immune	H3K4me3	2.24
Duodenum smooth muscle*	GI	H3K27ac	2.17
Duodenum Mucosa*	GI	H3K4me1	2.15
CD34 primary*	Immune	H3K4me1	2.12

(S7.Q) Enrichment of top cell types for Ulcerative colitis. * = significant at FDR < 0.05. ** = significant at p $<$ 0.05 after correcting for multiple hypotheses.

bioRxiv preprint doi: https://doi.org/10.1101/014241; this version posted January 23, 2015. The copyright holder for this preprint (which was not certified by peer review) is the author/funder, who has granted bioRxiv a license to display the preprint in perpetuity. It is made available under aCC-BY-ND 4.0 International license.

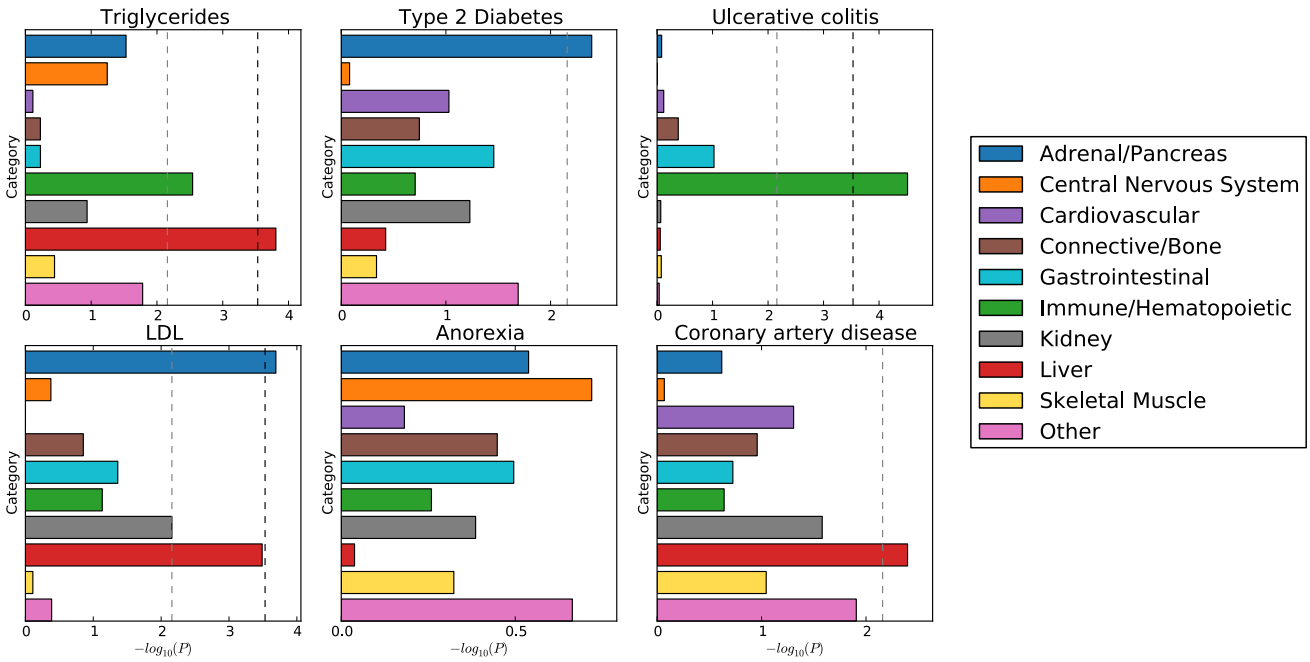

Figure S1: Enrichment of cell type groups for traits not included in Figure 4.The black dotted line at $-\log_{10}(P) = 3.5$ is the cutoff for Bonferroni significance. The grey dotted line at $-\log_{10}(P) = 2.1$ is the cutoff for FDR < 0.05.